EARTH OBSERVATION FOR RICE CROP MONITORING AND YIELD ESTIMATION: APPLICATION OF SATELLITE DATA AND PHYSICALLY BASED MODELS TO THE MEKONG DELTA

Nguyen Thi Thu Ha

Examining committee:

Prof.dr.ir. A. Veldkamp	University of Twente
Prof.dr. V.G. Jetten	University of Twente
Dr. D. van Speybroeck	VITO, Belgium
Prof.dr. M. Herold	University of Wageningen

ITC dissertation number 222
ITC, P.O. Box 217, 7500 AE Enschede, The Netherlands

ISBN 978-90-6164-348-7
Cover designed by Job Duim
Printed by ITC Printing Department

UNIVERSITY OF TWENTE.

FACULTY OF GEO-INFORMATION SCIENCE AND EARTH OBSERVATION

EARTH OBSERVATION FOR RICE CROP MONITORING AND YIELD ESTIMATION: APPLICATION OF SATELLITE DATA AND PHYSICALLY BASED MODELS TO THE MEKONG DELTA

DISSERTATION

to obtain
the degree of doctor at the University of Twente,
on the authority of the Rector Magnificus,
prof.dr. H. Brinksma,
on account of the decision of the graduation committee,
to be publicly defended
on Friday 25 January, 2013 at 16.45 hrs

by

Nguyen Thi Thu Ha

born on November 23 1977

in Hanoi, Vietnam

This thesis is approved by

Prof.dr.ir. E.M.A. Smaling, promoter
Faculty of Geoinformation Science and Earth Observation (ITC), University of Twente, the Netherlands

Prof.dr. W. Verhoef, promoter
Faculty of Geoinformation Science and Earth Observation (ITC), University of Twente, the Netherlands

Dr. Kees de Bie, assistant promoter
Faculty of Geoinformation Science and Earth Observation (ITC), University of Twente, the Netherlands

To my parents

Acknowledgements

The completion of this thesis has come through the great support and help of many people over the past five and a half years. I wish to express my sincerely gratitude to everyone who offered their help and guidance throughout my PhD time at ITC.

I would like to thank the Netherlands Organization for International Cooperation in Higher Education (NUFFIC) for awarding me a PhD Fellowship to carry out my PhD study at ITC. I thank to ITC and Hanoi University of Agriculture for their support and facilitation during my PhD period. This journey would have never been completed without their great support.

I convey my thanks and gratitude to my promoters; Prof. Eric M.A Smaling and Prof. Wouter Verhoef for their encouragement, advice and guidance that made me to achieve this task. I've learnt a lot from them.

My special thanks go to the co-promoter, Dr. Kees de Bie who has been always understanding, standing by and supporting me throughout my study. I highly appreciate his significant criticisms and expertise during the period of this work. It's been really enjoyable to share my thoughts and discussions with him. Kees, it was the moment that I joined you and the 2003-2005 NRM MSc group for the fieldwork in Mozambique back in 2004 that I came to know that if I was going to ITC for my PhD, you will be the person I would like to have as my supervisor. Fortunately, this became true. Thank you again for accepting me as your student.

I also thank to Prof. Herman van Keulen at Wageningen University for his advice and help during the first year of my PhD, especially for his critical comments on my research proposal. I'm very thankful for that and would like to wish him well.

My utmost thanks also go to all ITC NRS staff and PhD students for their support and friendship. I'm going to miss our PhD tutorials and the department Monday coffee and cakes. My thank goes to Prof. Andrew Skidmore and his wife for their hospitality and organizing PhD summer BBQ every year at their wonderful farm.

My sincere thanks to Willem Nieuwenhuis for his help in MATLAB and Java programming without which my SLC and ORYZA2000 running would have been more difficult.

My thanks also go to Prof. Clement Atzberger at University of Natural Resources and Life Sciences, Vienna for his advice on LAI sampling and measurement.

My special thanks to Loes for providing me with relevant information and for assisting me from the beginning to the end of my PhD. My thank also go to my office-mate Khan, Ajay, Wamu, Amjad, Abel and John for the nice time we shared with each other, our thoughts on life and hobby on football. I also thank Mariela and Rafael, Sisi, Maitreyi, Claudia, Filiz, Armindo, Tho and Bart, Quang, Ha, Anas, Atkilt, Sabrina, Tyas, Nicky and many other friends for their care, support and friendship. It's been wonderful to know you guys and to share my time at ITC with all of you.

I am deeply indebted to my parents, their love and support has inspired and helped me to achieve this level. Mom and Dad, I'm really proud to be your daughter.

Last but not least, my sincere thanks also go to my sister and brother in-law for their kindness and hospitality during my time in the Netherlands.

Finally my sincere thanks and regards to all those of you who have supported and helped me one way or the other during my entire PhD period.

Table of Contents

List of figures

List of tables

List of abbreviations

AVHRR	Advanced Very High Resolution Radiometer
CGSM	Crop Growth Simulation Model
DAS	Days after sowing
EVI	Enhanced Vegetation Index
FPAR	Fraction of Photosynthesis Active Radiation
ISODATA	Iterative Self-Organizing Data Analysis Technique Algorithm
LAI	Leaf Area Index
LCGP	Length of growing period
LULC	Land use Land cover
LUT	Look-up table
MERIS	MEdium Resolution Imaging Spectrometer
MODIS	Moderate Resolution Imaging Spectroradiometer
MVC	Maximum Value Composite
NDVI	Normalized Difference Vegetation Index
NOAA	National Oceanic and Atmospheric Administration
PCA	Principal Component Analysis
RMSE	Root Mean Square Error
RTM	Radiative Transfer Model
SLC	Soil-Leaf-Canopy
SPOT	Système Pour l'Observation de la Terre
VGT	Vegetation
VND	Vietnamese dong

Chapter 1
General Introduction

1.1 Justification and need to estimate irrigated rice yield using earth observation

It has been addressed in a prior conference, to the World Summit on Food Security (Rome 16-18 November 2009), on How to Feed the World 2050 *High-level Expert Forum* (Rome 12-13 October 2009), that agriculture in the 21st Century faces multiple challenges. These are i) the demand to produce more food to feed over 2.3 billion more people, ii) the demand for more feed stocks for a potentially huge bio-fuel market, iii) the need to adopt more efficiently and sustainable production methods, and iv) to adapt to climatic change (http://www.fao.org/wsfs/forum2050/wsfs-background-documents/hlef-issues-briefs/en/). The Food and Agriculture Organization of the United Nations (FAO) has projected that feeding a world population of 9.1 billion people in 2050 would require raising overall food production by 70 percent (between 2005/07 and 2050). Production in the developing countries would need to almost double. Annual cereal production would have to grow by almost 1 billion tons with a projected cereal yield of 4.3 tons/ha by 2050 (up from 3.2 tons/ha at present).

Rice, along with wheat and maize, is one of three leading food crops in the world; together they supply more than 50 percent of all calories consumed by the entire human population (Farina, 2006). Global milled rice consumption is projected to reach around 474 million tons in 2012/2013 (Trade and Markets Division-Food and Agriculture Organization of the United Nation, 2012). Over 87 percent of the world rice is produced and consumed in the Asian continent (Papademetriou et al., 2000).

The global rapid population growth and the demand of staple food have put more pressure on the major rice producers. Although the global rice (milled rice) production has tripled in the last five decades from 120 million tons in 1960 to 456 million tons in 2009 (FAO, 2012), thanks in large part to the rice Green Revolution in Asia, there was a period when global rice production had dropped sharply at the beginning of the 21st Century, from 399 million tons in 2000 to 380 tons in 2002, due to severe droughts in parts of Asia. Since then, with more introductions of high-yielding varieties by the International Rice Research Institute (IRRI), a rapid recovery of global rice production was seen by growing 65 million tons between 2003 and 2009. Figure 1.1 shows

the milled rice equivalent that was imported, exported, and produced by region in 2009.

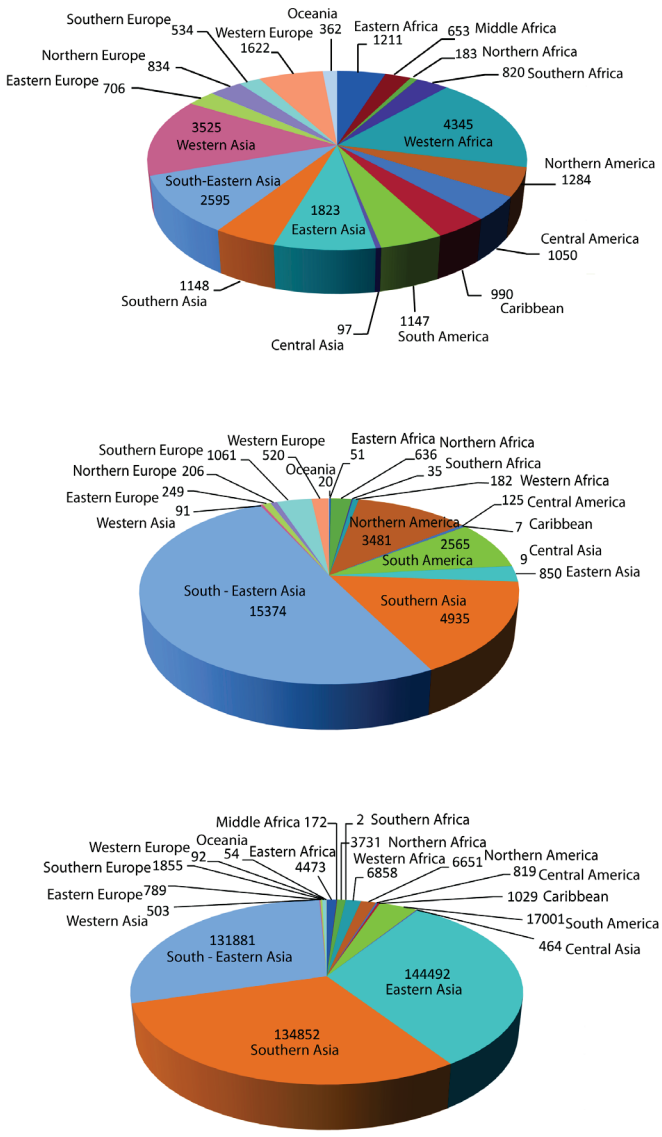

Figure 1.1: Import, export, and production of rice in 2009 (milled rice equivalent – '000 tons) (FAO, 2012)

Moreover, as rice demand is anticipated to be highly inelastic (Mohanty et al., 2010), and rice is a staple food accounting for a large share of income for almost a half of the world population that are poor, production, stock and utilization trends in rice markets will have significant implications for alleviating poverty, achieving food security, and elevating economic development in most of developing countries, especially those in Asia. The key to achieve these goals is to maximize rice production while lowering production costs and harmonizing rice crop management practices on the basis of its demands with reducing negative environmental effects. In order to maximize rice production, taking into account that the global cultivated rice area has only increased by about 12.5 million hectares (ha) between 1990 and 2010 (FAO, 2012), there is a must to increase rice yields. Because the genetic yield potential of inbred rice has not increased much since the late 1960s, the challenges is to reduce the yield gaps in farmers' fields (Peng et al., 1999). These yield gaps exist because the most advantage production technologies are not fully adopted in farmers' fields (Laborte et al., 2012). Because farmers' field yields are critical driving forces of food prices, food security, and cropland expansion, yield gaps must be further quantified and understood (de Bie, 2000). As for the diagnosis of rice yield gaps, this would ask for guidelines on methods, that include identification, quantification, year-to-year variability assessment, and environmental impact of available management technologies that matter in adding value to the present and conventional ways of rice-cultivation.

In agro-ecological research on e.g. to soils, water use, radiation, and crop growth, complex ecological and physiological processes are studied to identify environmental side effects and positive crop responses to crop management options. The use of crop growth simulation models (CGSM) enables timely and quantitative estimation of the dynamic requirements of crop growth and development (ten Berge et al., 1997). Better crop-management practices can further be improved by considering the spatial variation of crop-growth environmental conditions. This concept can be applied at either field-plot or regional level if required information can be generated through *in situ* measurement (with interpolation) or remote sensing (RS) observation.

Availability of RS data provides powerful access to the spatial and temporal information of the earth surface. Real-time earth observation data acquired during a cropping season can assist in assessing crop growth and

development performance, and provide information for crop management practices considering when/if nutrient or water deficits may occur, or the crop is likely to be infested by pests and diseases. As RS data is generally available at large scale, rather than at field-plot level, use of this information would improve crop management through farming activities at large scale. Consequently, it would help to minimize crop production failure risks and to lower farming investment.

Linking dynamic CGSMs to spatio-temporal RS information provides a possibility to extend the use of an advanced research and advisory tool, originally developed for point-specific analyses, to larger areas. RS data can be used to calibrate CGSMs in data-scarce environments, and/or to increase simulation accuracy for rice yield estimating or even forecasting, by forcing observed values on the model during the simulation period. This generates questions on how this can be technically achieved, what would be the spatio-temporal requirements for RS information taking account of CGSMs' operation, and what would be the potential fields for RS application.

1.2 Opportunities and challenges of using RS for crop yield estimation

To collect information on crops and agro-ecosystems, many new remote sensing techniques have been developed in recent years in various domains from optical to microwave sensing systems. Radar is an active microwave sensor which has been a major focus in many agro-ecological studies (Bouman et al., 1999; Wigneron et al., 1999; Wood et al., 2002; Baghdadi et al., 2009; McNairn et al., 2009). Up till now, most successes of using radar data retrieved from satellites (e.g. ERS, ENVISAT, JERS, ALOS, RADARSAT) have been achieved in mapping crops (Panigrahy et al., 1999; Smith et al., 2006; McNairn et al., 2009; Bouvet and Le Toan, 2011) and assessing crop production (Wigneron et al., 1999; Shao et al., 2001; Hadria et al., 2010). These techniques were mostly developed based on empirical relationships between radar backscatter and crop canopy characteristics. Although radar can penetrate clouds and thick canopies, its application to agro-ecological research is still less expanded compared to that of optical RS. This is due to the high cost of using continuous radar imagery in research, making it unsuitable for seasonal crop monitoring. Moreover, since the interaction of microwaves with vegetation canopy is very complex, radar backscatter from

crops often fails to relate to measureable physical quantities once used in physical interaction models (i.e., the radar response to leaf-area-index(LAI) saturates soon around an LAI value of 2) (Bouman and Hoekman, 1993). In the other domain, optical RS techniques have been developed toward multitemporal and multispectral measurements in order to overcome these problems. With the multitude of on-board satellite sensors like LANDSAT, NOAA-AVHRR, SPOT VEGETATION, MODIS, MERIS, etc., the probability of obtaining multitemporal reflectance data of croplands is now relatively high. This information can be used directly to map agricultural land or to derive time-series profiles of vegetation indices (i.e. NDVI, EVI, etc.) to delineate croplands (Lobell and Asner, 2004; Xiao et al., 2005; Lucas et al., 2007; Khan et al., 2010; Peng et al., 2011; Vintrou et al., 2012).

At landscape level, high spatial and temporal heterogeneity of vegetation may be present, but in most dynamic vegetation models this variation has not been accounted for yet (Doherty et al., 2010). For such a challenge, one-time RS observations are hard to interpret without additional information on vegetation phenological events. Improvement can only achieved with continuous observations from multitemporal optical RS which allows distinguishing vegetation patterns in time and space. Daily RS observations now can be obtained with satellite sensors such as MODIS and SPOT-VEGETATION, but atmospheric effects (i.e. water vapour, aerosols) or cloud contaminations may reduce the quality of these data. To minimize these effects, while still being able to monitor the dynamic change in vegetation patterns, a new RS technique is needed. This technique should be developed toward an improvement of clustering algorithms based on the use vegetation indices (e.g. NDVI).

The parallel development of remote sensing techniques and agro-ecosystem models has led to a new combination of these two fields in the development of synergistic applications (Dorigo et al., 2007). An example is the focus on retrieving biophysical parameters (i.e. LAI, fraction of absorbed photosynthetically active radiation (fAPAR), fraction of ground cover (fCOVER), etc.) (Bouman, 1995; Moulin et al., 2003; Doraiswamy et al., 2004; Duveiller et al., 2011; Verger et al., 2011). Of these parameters, LAI is the most important biophysical state variable used to estimate either biomass production or yield in agro-ecosystem models because it presents the leaf area that is available for the exchange of energy and mass between the

vegetation canopy and the atmosphere. RS LAI can be estimated based on either empirical statistical or radiative transfer models (Weiss et al., 2001; Koetz et al., 2005).

Linking of RS data with crop production has been studied for many years (Delécolle et al., 1992; Moulin et al., 1998; Dorigo et al., 2007). There are two well-known approaches of using RS data to estimate crop yield: the statistical approach and the physically-based modelling approach (also known as CGSM).

The statistical approach was developed based on the strong correlation between the time-accumulated vegetation index (VI) and crop production over the growing season. This relationship was first found by Tucker et al. (1981) when he studied the biomass production of winter wheat. Similar results were found when assessing winter wheat yield (Benedetti and Rossini, 1993), maize and rice yield (Quarmby et al., 1993), and millet yield (Rasmussen, 1998). However, simple regression techniques as used in statistical approaches have been criticized for their lack of generalization since the correlation between VI and biomass production depends very much on crop growing stages and the environmental conditions under which this correlation is obtained. Moreover, crop biomass is not always a good indicator of final yield (Delécolle et al., 1992).

The physically-based model (Delécolle et al., 1992; Casa et al., 2012) is an approach that relies on the coupling of RS-derived biophysical parameters to process-based dynamic CGSM. Various methods have been developed to integrate RS-derived biophysical parameters, more in particular LAI, to CGSM (Dorigo et al., 2007). In the calibration method (Maas, 1988a; Bouman, 1995), model parameters (initial states) are adjusted to obtain an optimal agreement between simulated and observed state variables. In the forcing method, a state variable of the CGSM is replaced by the observed RS data (Casa et al., 2012). For that purpose, LAI should be provided at the same time step of the model. In this type of application the other parameters and driving variables of the model are not affected by LAI adjustment. As an alternative, in data assimilation schemes, model parameters are updated and recalibrated in such a way that simulated LAI matches with the observations (Casa et al., 2012). In the updating method, observed RS data continuously update model state variables whenever an observation is available. This is referred as sequential data assimilation (McLaughlin, 2002).

1.3 Objectives of the thesis

Investigating the use of earth observation for irrigated rice yield estimation as discussed in this thesis has led to the following objectives:

- To identify and map a regional rice cropping patterns using hyper-temporal SPOT NDVI data with support from field observation
- To develop a methodology to map the landscape heterogeneity from various hyper-temporal remote sensing datasets
- To investigate the application of a radiative transfer model to remotely sensed surface reflectance data to derive the seasonal variation of LAI for irrigated rice
- To couple a RTM with a crop growth simulation model (CGSM) through LAI for field-based estimation of irrigated rice yield based on calibration of CGSM model parameters

The Mekong delta, Vietnam was used as a study site for this thesis.

1.4 Study area

The Mekong delta is the southernmost region of Vietnam. It is located between 8°30' to 11°00′ N and 104°30' to 106°50' E and is bounded by the South China Sea in the east, the Gulf of Thailand in the southwest and Cambodia in the northwest (see Figure 1.2(a)). The delta covers an area of 39,000 km^2. Mekong is well-known for its rice production, fruits and fisheries due to favourable climatic conditions characterized as savanna type according to the Köppen classification (Sakamoto et al., 2006). It is one of the largest rice producing regions of the world. Rice produced in the delta is mostly exported, providing about 90% of the total annual export revenues of the country (Ministry of Agriculture and Rural Development, 2009). The delta also caters for about 50% of the total domestic rice consumption.

In the delta, the major systems practiced in the irrigated lowlands are double and triple sequential mono-cropping of rice (Nguyen et al., 2012a) . Single rice cropping occurs only in some coastal areas where soil salinity is a problem. Soils are mainly alluvial containing sulfates (Le Quang Minh, 2001).

(a)

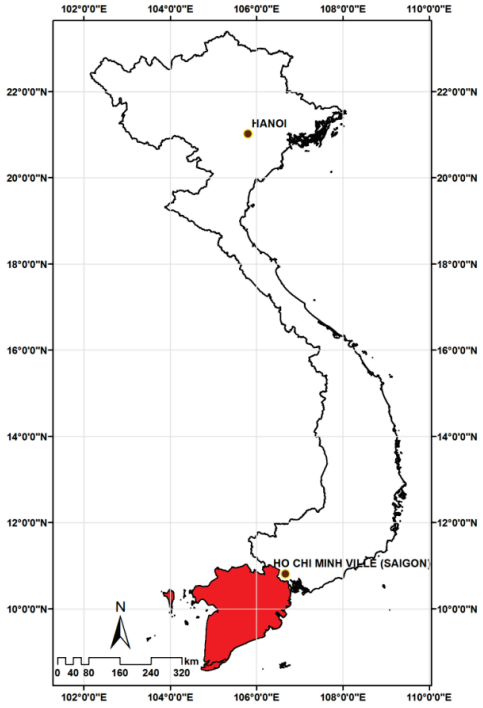

(b)

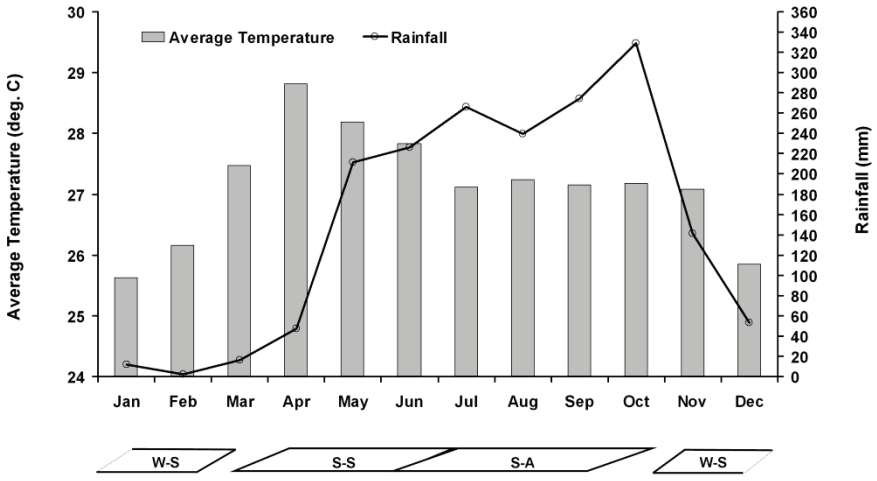

Figure 1.2: Mekong delta: *(a)* its regional location, and *(b)* its rice cropping seasons in association with meteorological data

The delta receives an average annual precipitation of about 1,800 mm, of which 90% occurs during the rainy season (May to November). The average daily temperature is around 27^{o}C, and has never dropped below 10^{0}C (National Institute of Meteorology, 2009). Figure 1.2(b) shows monthly variations in temperature and rainfall, averaged from 11 stations (2003-2008), in association with the rice cropping seasons. Most of the cultivated rice varieties were high-yielding with a growth cycle of around 90-100 days. They were bred and selected by the Cuu Long delta Rice Research Institute (CLRRI).The rice crops are winter-spring (W-S), spring-summer (S-S) and summer-autumn (S-A).

1.5 Thesis outline

This thesis comprises four main technical chapters which are presented as follows:

1.5.1 Chapter 2

This chapter presents a new method to map the irrigated rice cropping patterns in an extraordinary dynamic and extensive farming system. Optical hyper-temporal SPOT VEGETATION data (1998–2008) were used to describe and map variability in the rice cropping patterns of the Mekong delta. The NDVI-based rice classes were first identified using the ISODATA cluster algorithm. Rice class signature separabilities were later evaluated based on the divergence statistics.

1.5.2 Chapter 3

In this chapter, a new quantitative method to map landscape heterogeneity is proposed. The proposed methodology was used to map land cover heterogeneity of the Mekong delta's landscape using hyper-temporal RS data which were 10-year NDVI data obtained from SPOT VGT and MODIS Terra sensors. The method is data-driven, unbiased, and builds on ISODATA clustering and the use of divergence separability indices.

1.5.3 Chapter 4

In this chapter, MODIS 8-day LAI (MOD15A2) data at 1km spatial resolution were compared with field data and with LAI estimates derived from MODIS 8-day surface reflectance data (MOD09A1). The chapter investigates the possibility of estimating rice LAI through the inversion of the Soil-Leaf-

Canopy (SLC) radiative transfer model by the look-up table (LUT) approach for MOD09A1.

1.5.4 Chapter 5

This chapter investigated a method of coupling RS LAI-estimates with a modified ORYZA2000 CGSM to estimate actual irrigated rice yields. RS LAI estimates from SLC model inversion were used to calibrate ORYZA 2000 model's parameters for three most cultivated rice varieties in the Mekong delta in order to estimate the rice yields under sub-optimal growth conditions.

1.5.5 Chapter 6

This chapter provides the major findings and conclusions of the study. Further recommendations on future study and development toward the use of earth observation in rice heterogeneity mapping and yield estimation are discussed.

Chapter 2
Mapping rice cropping patterns[1]

[1] Chapter is based on: Nguyen, T.T.H., de Bie, C.A.J.M., Ali, A., Smaling, E.M.A., & Chu, T.H. (2012). Mapping the irrigated rice cropping patterns of the Mekong delta, Vietnam, through hyper-temporal SPOT NDVI image analysis. *International Journal of Remote Sensing, 33*, 415-434

Abstract

Successful identification and mapping of different cropping patterns under cloudy conditions of a specific crop through remote sensing provides important base line information for planning and monitoring. In Vietnam, this information is either missing or unavailable; several on-going projects studying options with radar to avoid earth observation problem caused by the prevailing cloudy conditions have till date produced only partial successes. In this research, optical hyper-temporal SPOT VEGETATION data (1998-2008) was used to describe and map variability in irrigated rice cropping patterns of the Mekong delta. Divergence statistics were used to evaluate signature separabilities of NDVI classes generated from ISODATA classification of 10-day SPOT NDVI image series. Based on this evaluation the map with 77 classes was selected. Out of these 77 mapped classes, 26 classes with prior knowledge that they represent rice were selected to design the sampling scheme for fieldwork and for crop calendar characterisation. Using the collected information of 112 farmers' fields belonging to the 26 selected classes, the produced map provides highly accurate information on followed rice cropping patterns (94% overall accuracy, 0.93 Kappa coefficient). We found that the spatial distributions of the triple and the double rice cropping systems are highly related to the flooding regime from the Hau and Tien rivers. Areas that are highly vulnerable to flooding in the upper part and those that are saline in the north-western part of the delta mostly have a double rice cropping system, whilst areas in the central and the south-eastern parts mostly have a triple rice cropping system. In turn, the duration of flooding is highly correlated with the decision by farmers to cultivate shorter or longer duration rice varieties. The overall spatial variability mostly coincides with administrative units, indicating that crop pattern choices and water control measures are locally synchronized. Water supply risks, soil acidity and salinity constraints, and the anticipated highly fluctuating rice market prices all strongly influence specific farmers' choices of rice varieties. These choices vary considerably annually, and therefore grown rice varieties are difficult to map. Our study demonstrates high potential of optical hyper-temporal images that were taken on a daily basis to differentiate and map a high variety of irrigated rice cropping patterns and crop calendars at a high level of accuracy in spite of the cloudy conditions.

2.1 Introduction

In 1986, Vietnam launched a political and economic innovation campaign (*Doi Moi*) with the aim of introducing reforms to facilitate the transition from a centralized economy to a so-called socialist-oriented market economy. *Doi Moi* combined government planning with free-market incentives. The programme opened the doors for establishment of private businesses and foreign investment. It also abolished agricultural cooperatives, allocated communal land to individual farm households, removed price controls on agricultural goods and enabled farmers to sell their goods in the open market. *Doi Moi* affected three important areas of the Vietnamese national economy: (i) food production, (ii) investments, and (iii) freedom of business activities. In 1993, the land tenure system was legalized and the transfer of land use rights was allowed by passing a Land Law (Dang *et al.*, 2006). These reforms had a great impact and by 2000 both the area under rice cultivation and the production of rice increased to over 3 million hectares and 32.5 million tons respectively (The Information Center - Ministry of Agriculture and Rural Development, 2009). This led to Vietnam's emergence as the second largest rice exporting country in the world, with almost 5.8 million tons of rice exported annually. With the passage of time, however, the focus of *Doi Moi* changed to industrialization. As a consequence of this shift of interest in policies, many productive rice areas were converted to industrial and urban land uses. Recognizing this problem, in 2001, the Vietnamese government adopted a 20-year plan for the agricultural sector to reach 4 million hectares of irrigated rice area by 2020 and targeting an annual rice production of 33 million tons (Planning Department - Ministry of Agriculture and Rural Development, 2009). To identify progress and prospects in meeting such an ambitious goal, annual assessment of the rice production needs to be carried out across the country. This requires up to date and accurate information on 'where and when' rice is grown in the Mekong delta, the largest rice producing region of the country. Because of the variation of rice cropping patterns by areas, this is proving to be an extremely difficult task. Throughout the year, changes in the rice cropping patterns are driven by the availability of water supply and crop management practices, leading to a variety of land cover patterns across the region. This has created serious problems for the local authorities and MARD, and in particular caused inaccurate information on the area of rice cultivated and production achieved. As a consequence, published statistical data are, unreliable and hence

planning to avoid food security issues suffers accordingly. Although several studies have been carried out in the Mekong delta using MODIS and radar observations, so far the contribution to an improvement of the situation has been marginal. The studies attempted either to look at the distribution of rice phenology in association with cropping systems within a one or two year period (Sakamoto *et al.*, 2006), or to monitor rice production for specific areas of interest (Nguyen et al., 2005; Nguyen et al., 2007; Bouvet et al., 2009; Sakamoto et al., 2009a; Sakamoto et al., 2009b). Our present work, in contrast, examines rice cropping patterns over a longer period for the whole region of the delta.

Land surface information obtained from satellite data is widely used to map land cover/ land use and its change. A common mapping approach is to use long time series of the Normalized Difference Vegetation Index (NDVI) derived from optical satellite sensors (e.g. NOAA AVHRR, SPOT VEGETATION, MODIS and MERIS). This approach assumes that the seasonal NDVI variability is related to the behaviour of vegetation phenology. NDVI is numerically calculated as:

$$NDVI = \frac{(NIR - RED)}{(NIR + RED)} \quad \textbf{(2.1)}$$

where RED and NIR stand for the spectral reflectance measurements acquired in red and near-infrared regions, respectively. NDVI indicates the greenness of vegetation cover (Sellers, 1985) and by using multi-temporal or hyper-temporal imagery, researchers have been able to provide useful information on LCLU and their changes over time (Townshend and Justice, 1986; Townshend et al., 1987; Lenney et al., 1996). However, optical remote sensing methods are sensitive to atmospheric conditions, cloud coverage, and aerosol scattering. To minimize these effects, daily NDVI images are often pre-processed to obtain maximum value composite (MVC) NDVI images that cover a fixed period, normally from 8 to 16 days (Holben, 1986; Townshend et al., 1994). Holben (1986) also showed that the MVC method could reduce the variability associated with changing view and illumination geometry.

Time series data of MVC NDVI have been proven useful for LCLU studies due to their high temporal coverage and easy availability. Several studies on

mapping vegetation types and their phenological patterns were carried out in China with the use of AVHRR MVC NDVI data (Xin et al., 2002; Wang and Tenhunen, 2004; Jiang et al., 2008), and MODIS MVC NDVI images (Xiao *et al.*, 2005). Both AVHRR 10-day and MODIS 8-day NDVI composites have been shown to be capable of differentiating spatial variability in vegetation productivity and greenness over time. Wardlow *et al*. (2008) showed that the time series of MODIS 16-day MVC NDVI can be used to map regional cropping patterns in the central United States with an overall accuracy of 84%. The use of MODIS MVC NDVI was further studied to detect the expansion and intensification of row-crop agriculture in the south-western Brazilian Amazon (Galford *et al.*, 2008), and to derive estimations of the areas of larger cropped fields in Rostov Oblast, Russia (Fritz *et al.*, 2008).

The term hyper-temporal was first introduced by Piwowar and LeDrew (1995) in their study of arctic sea-ice change. It is defined as a multi-temporal image data set involving the acquisition of many images of the same area over a period of time; and for such images to be useful, the image data needs to be consistent from image to image, in the same way as internal image consistency is often assumed in the analysis of single images (Piwowar et al., 1998; McCloy, 2006).

Hyper-temporal SPOT VEGETATION (SPOT VGT) 10-day MVC NDVI imagery acquired from 1998 - 2003 was used successfully by Immerzeel *et al.* (2005). Kamthonkiat *et al.* (2005) analyzed time-lag relationships between the peaks of hyper-temporal SPOT VGT NDVI and rainfall data collected from 1999 - 2001 for discriminating rainfed and irrigated rice in central Thailand. Xiao *et al* (2002a) also found the use of NDVI and Normalised Difference Water Index (NDWI) time series effective for detection of irrigation before rice transplanting in Jiangsu, China. Recently SPOT VGT 10-day MVC NDVI images were used to provide useful information for disaggregation of crop statistics data (de Bie et al., 2008; Verbeiren et al., 2008; Khan et al., 2010).

A number of studies have used optical remote sensing to map irrigated rice areas (Xiao et al., 2002a; Kamthonkiat et al., 2005; Xiao et al., 2005; Sakamoto et al., 2006; Xiao et al., 2006; Sakamoto et al., 2009a; Sakamoto et al., 2009b). However, these studies stopped before detecting and describing all major temporal and spatial details of practised rice cropping patterns. Given the proven high potential of hyper-temporal NDVI image series for monitoring and mapping cropping patterns, our study aimed to

investigate the use of SPOT VGT 10-day MVC NDVI images to describe and map irrigated rice cropping patterns of the Mekong delta. The specific aim was to differentiate and describe the spatial and temporal patterns of rice grown in the region that has around 145 overcast days per year by using, besides the ISODAT clustering routine, also the divergence statistic to evaluate signature separabilities in order to select the best number of classes present in the NDVI-dataset, and the correlation between those classes and interviewed data, to develop an informative and user-friendly legend.

2.2 Data and methods

2.2.1 Rice cultivation in the Mekong delta

The Mekong delta is relatively flat with elevations ranging from 0 to 20 metres above sea level. The soils of the region are mostly alluvial. Every year, the delta is fertilized by approximately 1 billion cubic meters of sediment by the distributaries of the Mekong River. Newly created soils are often saline intrusive (Nguyen, 2007; Yamashita, 2009).

Rice is mostly cultivated as a monoculture using double or triple sequential cropping methods, although in some areas only a single crop of rice is grown in the year. The number of crops per year is strongly related to water availability and water management practices. Water originates from the two largest branches of the Mekong: the Tiền and the Hậu rivers, and is distributed by a dense and well-connected canal system. In some flood-controlled areas, gates of dikes are opened during the flooding season every three or four years to flood the paddy fields. This is done for about a month, usually from September to October before the start of the W-S rice crop. This helps to deposit silt, increase soil fertility and manage pests and diseases without affecting the cropping calendar. Pest and diseases are managed by area-wise synchronization of sowing dates based on forecasts of local agricultural extension offices' and farmers' knowledge. Most of the fields are seeded manually, seven to fifteen days after crosswise and lengthwise wet ploughing and harrowing. This tillage makes the soil well puddled and the land level for uniform distribution of water throughout each field. Fertilizers are applied from three to five times per crop.

2.2.2 Data

2.2.2.1 SPOT VGT 10-day NDVI MVC data

The SPOT VGT sensors onboard the SPOT-4 and SPOT-5 platforms are in orbit with an equator crossing time at 10:30 am. The SPOT 10-day MVC NDVI images comprise a 10-day synthesis (S10) which selects the highest measurement by pixel during an entire period (VEGETATION Programme, 2009). The S10 MVC NDVI product is directly based on the quality of the so-called *P* products which are all corrected for system errors and atmospheric conditions. Users obtaining S10 SPOT MVC NDVI data also receive quality flags per pixel. Only pixels rated "good' or having high radiometric quality for bands 2 (Red: 0.61-0.68µm) and 3 (NIR: 0.78-0.89µm), while also not having "cloud", "shadow" and "uncertain", were retained in this study. Excluded pixels were all labelled as "missing".

SPOT 4 and 5 10-day MVC NDVI 1 km resolution imagery was retrieved for the period from April 1998 to January 2008 (VITO, 2008). These two systems have identical characteristics. Unlike the normal NDVI data ranging from -1 to 1, the SPOT NDVI images used in this study were unsigned-8-bit integers. The digital numbers (DN) were calculated by VITO using Equation 2.2:

$$DN = \frac{NDVI + 0.1}{0.004} \qquad \textbf{(2.2)}$$

All retrieved 354 images were stacked into a single image for subsequent classification.

2.2.2.2 Ground sampling data

Two fieldtrips to the Mekong delta were carried out. The first took place in September 2008 and October 2008. Through stratified clustered random sampling based on the initial map generated from the SPOT NDVI data (see 2.2.3), of 26 preselected NDVI classes, 112 paddy fields were visited. All 26 classes were confirmed as rice, and their crop calendars were characterized based on interviews with farmers in their fields. For each interview, cropping calendar dates, crop management information, crop rice variety and production details were collected for all crops grown over the preceding two years. The second fieldtrip was conducted from December 2008 to May 2009. During this trip, 68 additional fields were surveyed to serve as validation data

for the generated rice cropping pattern map. During both fieldtrips, all paddy field boundaries were digitized in the field using an HP-iPaq running ArcPAD mobile GIS software.

2.2.2.3 Secondary data

Several ancillary data sets were collected and used in this study. These data sets include the official land use map 2005 of the Mekong delta (NIAPP, 2008) (see Figure 2.1), and the official districts, roads, rivers and irrigation works maps. The official land use map of 2005 provides information on where rice is possibly grown, and helped to pre-selection the 26 NDVI classes for the first fieldwork. This map was basically prepared using all possible cloud-free Landsat ETM image quicklooks of the area.

2.2.3 Image classification

2.2.3.1 Unsupervised classification

To classify the image containing all SPOT VGT MVC NDVI data, the Iterative Self-Organizing Data Analysis Technique Algorithm (ISODATA) was used. ISODATA is an unsupervised classification technique, which calculates class means evenly distributed in the data space and iteratively clusters pixels using the minimum distance rule (Tou and Gonzalez, 1974). Each iteration calculates the class means and then reclassifies the pixels with respect to the new means. By providing threshold parameters, iterative class splitting, merging and deleting is done. All pixels are classified to the nearest class unless a standard deviation or distance threshold is specified. This process continues until the number of pixels in each class changes by less than the selected pixel change threshold or maximum number of iterations is reached. ISODATA presents a fairly comprehensive set of analysis on adjustment processes that are incorporated into an interactive scheme.

ISODATA was used to make a series of classification runs of the 10-year stacked NDVI image; the pre-defined number of classes was set from 10 to 100, making a total of 91 classification runs. For each run, the maximum number of iteration and convergence threshold was set to 50 and 1 respectively. Selection of the best classification was based on cluster separability.

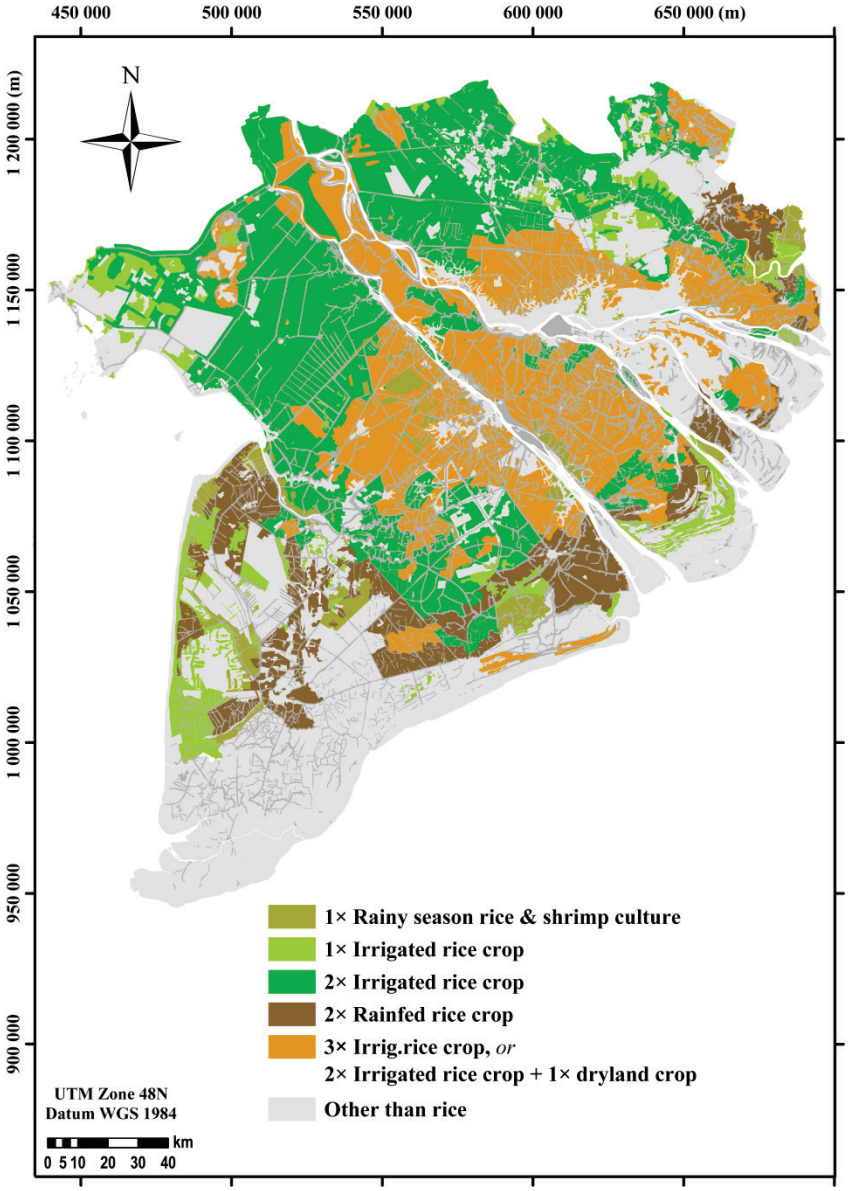

Figure 2.1: Land use map of 2005 of the Mekong delta with focus on rice areas (NIAPP, 2008)

2.2.3.2 Evaluation of cluster separability

The major problem of using ISODATA is the unavailability of prior knowledge on the ideal number of clusters (Boudraa, 1999). In order to obtain an optimal number of clusters, an estimation of the number of clusters from observed data is required and this also must be validated. The corrected

number of clusters for the number of object classes present in the data can be derived by evaluating a cluster validity index also called separability index (Pal and Bezdek, 1995; Boudraa, 1999).

Divergence was one of the first measures of statistical separability of clusters used in pattern recognition. It can be calculated for any combination of image-bands. The divergence index (see Equation 2.3) was developed by Swain (1978):

$$D_{ij} = \frac{1}{2} tr\left[(\Sigma_i - \Sigma_j)(\Sigma_j^{-1} - \Sigma_i^{-1})\right] + \frac{1}{2} tr\left[(\Sigma_i^{-1} + \Sigma_j^{-1})(U_i - U_j)(U_i - U_j)^T\right] \quad \textbf{(2.3)}$$

where, D_{ij} is the divergence statistics between two signatures (classes) *i* and *j;* being compared ; Σ_i & Σ_j are the covariance matrices of signature *i* and *j*; U_i & U_j are the mean vectors of signatures *i* and *j*; *tr* denotes the trace of the matrix; and *T* is the transposition function. In cases where there are more than two classes, Swain (1978) suggested to use the average divergence, which computes the average distance over all pairs of classes. Selection of the classification with the highest value of average divergence is the most reasonable strategy for correct recognition. In addition, in this study, the minimum divergence separability index was also evaluated. The minimum separability values reflect the distance between the most similar classes. By visual inspection of both the average and minimum divergence values, the best number of classes was decided upon (Khan *et al.*, 2010).

2.2.4 Construction of the rice cropping pattern map

Firstly, from the 112 interview data, information on followed crop calendars was extracted. These records were then grouped by NDVI class and on the basis of the number of crops grown sequentially within one year. Combining this with the information from interviews on rice varieties cultivated in specific cropping seasons, the NDVI classes were described in more detail.

Secondly, as rice cropping calendars are very much related to the flooding regime from the main rivers, information on flood duration (full inundation) and extent was added to the map legend. Assumed is that low NDVI values indicate flooding (Xiao et al., 2002a; de Bie et al., 2008). An arbitrary decadal mean NDVI DN value of 50, which is equal to 0.1 of a normal NDVI value (see equation 2), was set as the upper threshold for flooding detection. This value is lower than the value of 75 suggested by Xiao *et al*. (2002a).

This is because, in our research, flooding refers to complete inundation of the area by sometimes up to 5m of water, whilst in the other it refers to irrigation associated with the rice transplanting period. The flood extent was recorded as either partial or extensive. The assessments on timing and extent of flooding were made by evaluating by NDVI class the spatial patterns over time of pixels having NDVI DN values lower than 50. These were based on the original 2004-2007 10-day NDVI images only. Areas with flood duration of less than one month were labelled as controlled, otherwise as uncontrolled.

Finally, all surveyed NDVI classes were described based on tabulated information on cropping patterns, flooding regime and varieties grown. Additional information collected on soil type, soil salinity and soil pH were added to the legend as notes. A suitable colour scheme and hatching patterns was prepared to visualize major and minor map unit differences clearly.

2.2.5 Validation

Validation of the rice cropping pattern map was carried out using the second field dataset. Assessment was based on the performance of the Kappa statistic showing the agreement between the classes assigned to the survey sites according to the map versus its legend. Information on the variety grown was excluded from validation since this proved to be too variable across years.

2.3 Results

2.3.1 Unsupervised classification

Figure 2.2 shows the separability comparison for the 10 to 100 separate NDVI classifications. The separability indices increase slowly until the number of classes reaches 77 where the average separability displays a unique peak; after 77 classes the pattern is erratic. This indicates that 77 is the most reasonable choice for correct pattern recognition while keeping the number of classes relatively low (less than 100).

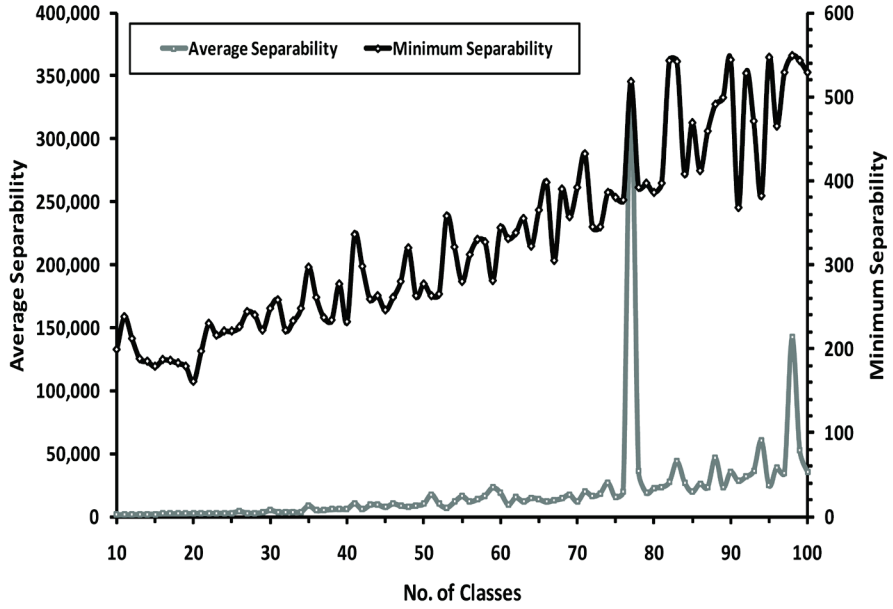

Figure 2.2: Average and minimum separability based on the divergence index for the series of 91 classification runs

Figure 2.3 provides an example of the hyper-temporal NDVI behaviour of classes 53 and 41. The curves represent all pixels belonging to the respective classes. In this figure, one can recognize the change within and differences between the two classes. From 2001 onwards, class 53 suggests a clear shift from a double to a triple rice cropping pattern with severe annual flooding around October when the hyper-temporal NDVI curve shows very low values. Irregularly lower NDVI values are caused by cloudy periods. As for class 41, the hyper-temporal NDVI curve suggests a quite regular double rice cropping pattern for the whole period.

The dips in NDVI between the individual crops grown clearly differentiate when the area is fully inundated (DN<50), and when soggy soil and rice sowing occurs (DN<100). The latter periods tend to be of short duration.

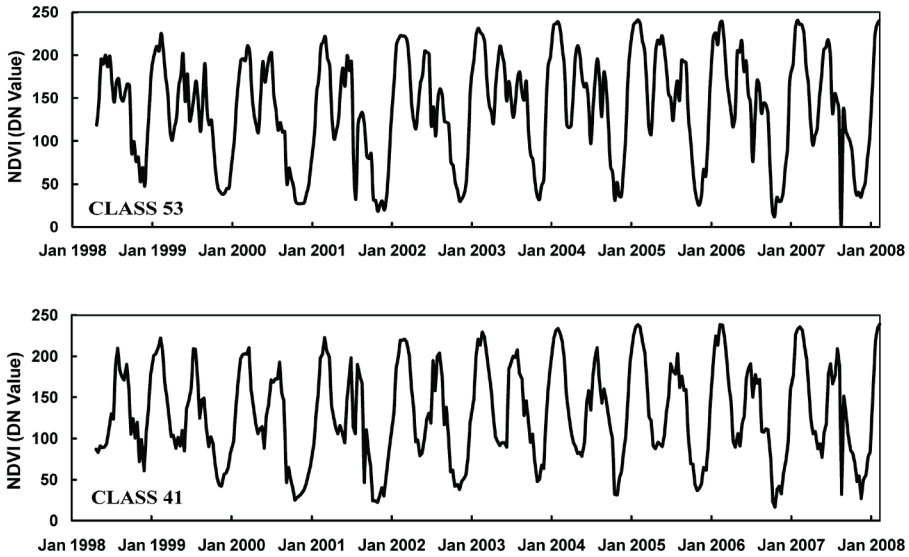

Figure 2.3: Hyper-temporal NDVI curves of classes 53 and 41

2.3.2 Rice cropping pattern map

Figure 2.4 shows the rice cropping pattern map *(a)* and its detailed legend *(b).* The short legend to the rice cropping pattern map is shown in figure 6*(a)*. The legend presents the rice patterns in the delta and provides key information about the types of rice cropping (2 x Rice, 3 x Rice) in association to information about the flooding regime. The map also shows areas of rice that were not surveyed due to time limitations. In all surveyed areas, farmers practise either double rice cropping (2 x Rice) or triple rice cropping (3 x Rice) in a year.

The detailed legend (see figure 2.4 *(b)*) provides detailed information about the variability in cropping patterns. Farmers only started harvesting the second crop in class 41 when the harvesting of the second crop in class 28 was completed. Meanwhile, class 42 reached at that time the middle of its second crop cycle, and class 51 its third. Even within a class, overlap between two crops is found. For instance, in class 53, while the harvesting of the second crop had not totally been completed in some areas, sowing of the third crop already began elsewhere. This clearly indicates a high degree of temporal variability in cropping calendars.

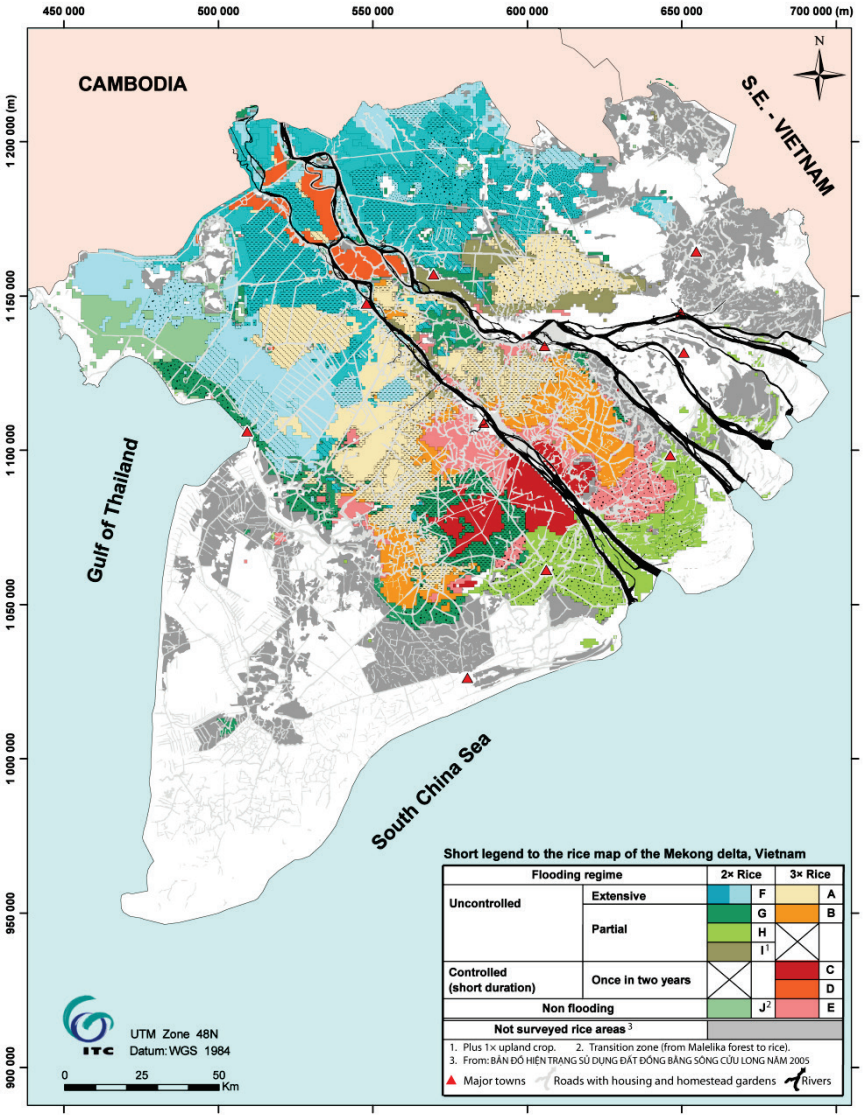

Figure 2.4: *(a)* Rice cropping pattern map of the Mekong delta and *(b)* Detailed legend of the rice cropping pattern map of the Mekong delta. Reported grown rice varieties vary considerably over years, and reflect here only the situation as of 2007 and 2008

The legend also reveals that a variety of flooding conditions exist. Classes that are located in areas that are extensively flooded for long periods, such as classes 22, 31 and 33, only have two rice crops per year. Classes that are located in controlled flooding areas, and that are only flooded for a short period often have three crops.

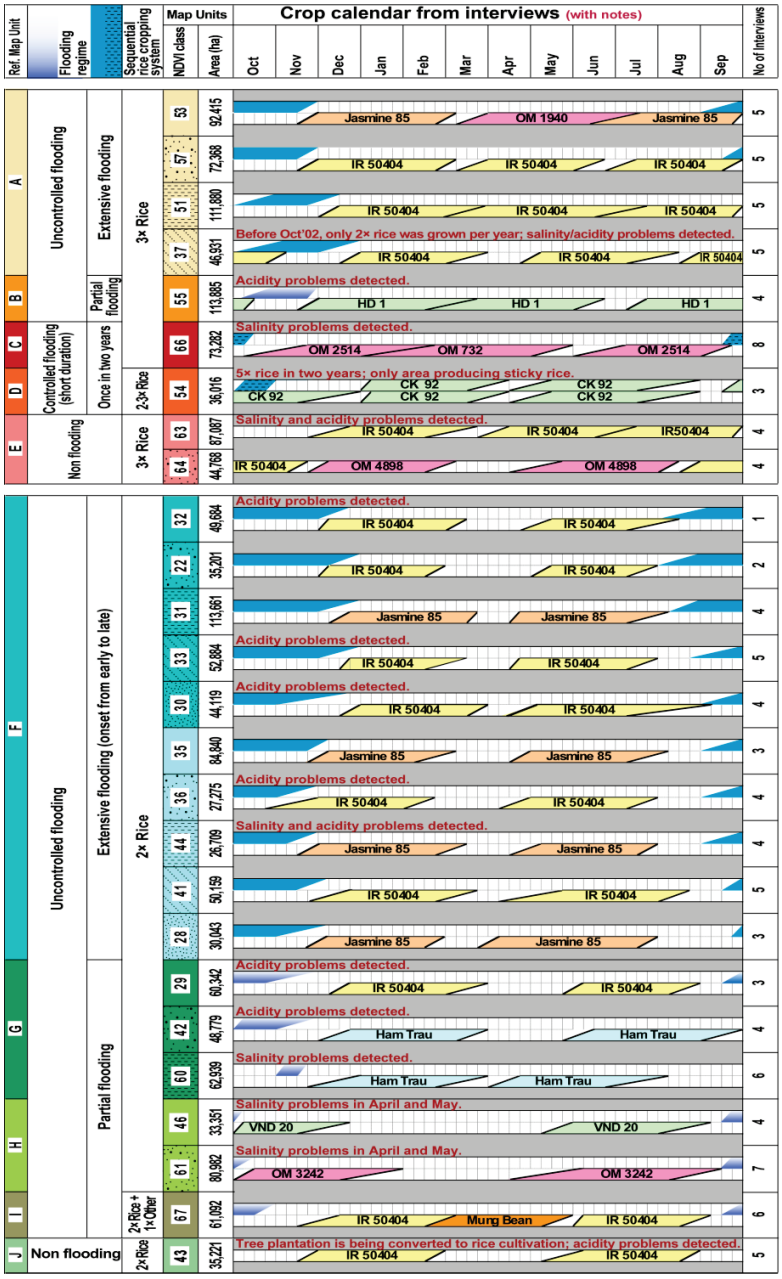

Figure 2.4 (Continued)

Figure 2.4 *(b)* also provides information on rice varieties grown. In 2006-2008, IR 50404 was the most common variety. It has a short growing period, high resistance to pests and diseases, and relatively low fertilizer requirements. Less common were Jasmine 85 and OM 576-18 (Ham trau) varieties, which have longer growing periods. Categorized in the same low quality rice group as IR 50454 is OM 576-18, found to be highly adapted to areas where salinity or acidity is experienced. Jasmine 85 is, in other hand, known as a high quality fragrant variety, and was only grown in areas where farmers have high management skills. This variety is very vulnerable to pests and diseases. It was the dominant rice variety in classes 53 and 31.

Table 2.1: Rice varieties grown in the Mekong delta and their characteristics

Rice variety	Length of crop growing period (LCGP,days)	Cropping season[2]	Market price (VND/dried kg)[3]	
			Early 2008	Late 2008
IR50404	85-90	W-S, S-S & S-A	4,200-4,500	3,600-3,800
OM 576-18 (Hàm trâu)	90-105	W-S & S-A	4,200-4,500	3,600-3,800
Jasmine 85	95-108	W-S & S-A	6,000–6,500	4,800-5,500
OM 1490	85-90	W-S, S-S & S-A	4,600–5,000	4,000-4,200
OM 2517	90-95	W-S & S-A	4,600–5,000	4,000-4,200
OM 2395	90- 100	W-S, S-S & S-A	4,600-5,000	4,000-4,200
OM 4900	100-105	W-S & S-A	4,500-5,000	4,500–5,200
OM 4218	90-95	W-S & S-A	4,500-5,000	4,500–5,200

The flood regime affects the farmers' choices of which rice varieties to grow. To sustain the triple rice cropping pattern, in controlled flooding areas, farmers tend to choose varieties with shorter growing periods (around 90 days), whereas in uncontrolled flooding areas, farmers prefer longer duration rice varieties. Most rice varieties are bred by the Cuu Long Delta Rice Research Institute. Table 2.1 lists the lengths of the crop growing period (LCGPs) of the most common cultivated rice varieties that were encountered during the first fieldwork period. We found that the market price of rice - which reflects the potential use of the variety for export - drives the choice by farmers as well. Since the W-S season of 2008-2009, grown rice varieties

[2] W-S, winter-spring; S-S, spring-summer; S-A, summer-autumn
[3] 1€ = 25,200 VND

have changed considerably. An example is the replacement of IR 50404, for which the price dropped quickly on the market, by higher quality varieties such as OM 4900 and OM 4218.

The legend also shows soil problems reported by farmers. Classes such as 42, 29 and 33 experience acidity problems whereas others including classes 61, 46 and 66, suffer from salinity

2.3.3 Validation

Table 2.2 shows the accuracy indices for the rice cropping pattern map. The accuracy assessment of the map was based on the type of rice cropping pattern, crop calendars, and flood extent. The rice cropping pattern map proved able to provide very accurate information on all tested rice classes with an overall accuracy of 94% and a Kappa of 0.93. Misclassifications based on site location occurred once for NDVI class42, characterized by double rice cropping and 3 times for class 53, mapped as triple cropping.

2.4 Discussion and conclusions

The research has shown that mapping irrigated rice cropping patterns in the Mekong delta using hyper-temporal images was highly successful. The 10-year sequence of decadal images from the SPOT VGT sensor supported a very effective and detailed identification of complex agricultural cropping patterns of irrigated rice. Considering that the official land use map is updated only once every 5 years, the use of hyper-temporal NDVI data allows accurate and up-to-date information to be mapped when required. Since the use SPOT product is originally based on daily imagery, sufficient cloud free information remained to make the mapping possible.

Figure 2.5 shows side-by-side a detailed comparison of the official land use map of 2005 (see figure 2.1) and the rice cropping pattern map produced in this research (see figure 2.4*(a)*). According to the official land use map, farmers in Thoai Son district practised double rice cropping, but according to our derived map, they grow three rice crops (class 37).

Table 2.2: Accuracy of the rice cropping pattern map using the detail legend (excluding information on varieties grown)

		NDVI group and class of the sample sites according to their location on map										Samples	User's accuracy (%)
		A 53	A 51	A 37	B 55	C 66	E 63	F 44	G 29	G 42	G 60		
Class of the sample sites according to the map legend	53	16	0	0	0	0	0	0	0	0	0	16	100
	51	2	5	0	0	0	0	0	0	0	0	7	71
	37	0	0	2	0	0	0	0	0	0	0	2	100
	55	0	0	0	10	0	0	0	0	0	0	10	100
	66	0	0	0	0	2	0	0	0	0	0	2	100
	63	1	0	0	0	0	4	0	0	0	0	5	80
	44	0	0	0	0	0	0	2	0	0	0	2	100
	29	0	0	0	0	0	0	0	4	0	0	4	100
	42	0	0	0	0	0	0	0	0	4	0	4	100
	60	0	0	0	0	0	0	0	0	1	15	16	94
Samples		19	5	2	10	2	4	2	4	5	15	68	
Producer's accuracy (%)		84	100	100	100	100	100	100	100	80	100	Overall accuracy: 94% Kappa: 0.93	

Similarly in Co Do district, our map identified double rice cropping (class 44) whereas the official land use map reported single rice cropping and shrimp culture, which is no longer practised in the area.

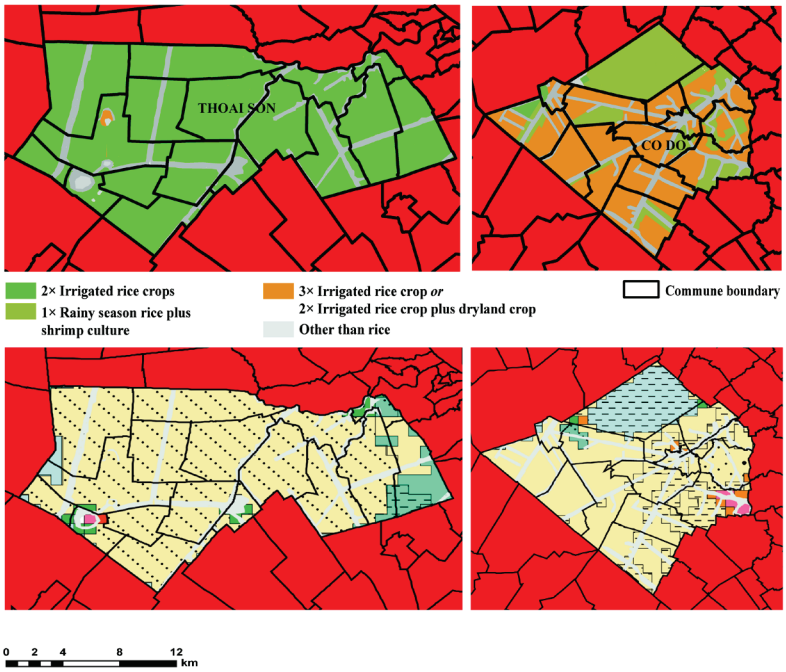

Figure 2.5: Rice maps of Thoai Son and Co Do districts: *(a)* from the official land use map of 2005 and *(b)* from the produced rice cropping pattern map (Figure 2.4)

Figure 7 also shows that our map has limitations due to the coarse resolution of SPOT imagery (1km). This only shows that its inherent scale is smaller than 1:100,000.

Further comparison between our map of rice cropping pattern (see Figure 2.4*(a)*) and the official 2005 land use map (see Figure 2.1) shows that the amount of detail about grown rice crops is much higher in our map legend and, in addition, it reflects that the cropping patterns are highly associated with environmental conditions, especially with prevailing flooding regimes.

At the commune level, the rice cropping patterns proved very homogeneous. By the self–organized seeding and harvesting time synchronization, damages to rice by pests and diseases remain limited, and water management is locally better controlled That is why the borders of our map units often coincide with administrative boundaries (see Figure 2.6). This area-based homogeneity contributed to our mapping success; the map-units that are based on 1km^2 pixels hardly contain a mix of cropping patterns so that in the legend a 1:1 relationship between class and pattern could be reported.

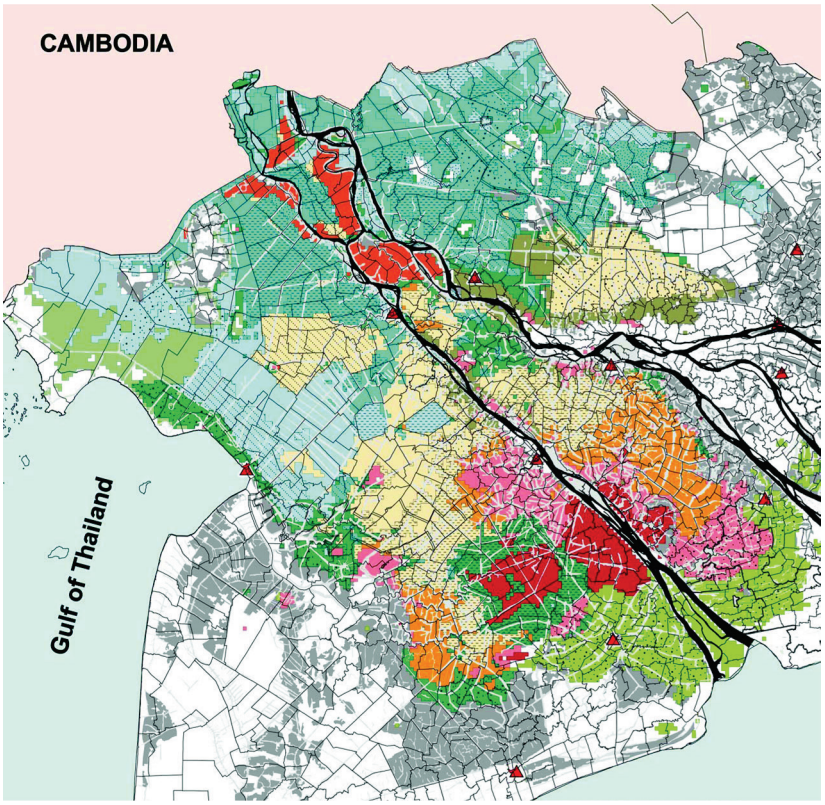

Figure 2.6: Overlay of Mekong Commune boundaries on the normalized difference vegetation index (NDVI) – rice map

In our study we were not, however, able to include in the legend pertinent information on grown rice varieties. This is due to the high annual variability in farmers' choice of varieties.

Our study proved that using hyper-temporal SPOT Vegetation NDVI imagery and ISODATA is able to capture relevant rice cropping differences of all 26 studied NDVI classes. We found that by applying the ISODATA unsupervised classification algorithm and using the divergence separability indices, the prevailing rice cropping patterns could be mapped successfully. The choice made on the number of classes present in the NDVI-dataset though the use of divergence index worked out excellently. We also found that in spite of the cloudy conditions of the Mekong delta, 10-years of decadal SPOT data contained sufficient valid information to overcome this problem. We therefore conclude that hyper-temporal SPOT Vegetation NDVI data is very useful and

suitable to map cropping patterns and we recommend that our approach be applied to the whole Mekong delta region.

Acknowledgment

The authors would like to thank Ms. S. Karibi and Mr. R. Scarrott, MSc students from ITC for their great help during the first fieldwork. Thanks to Dr. Vo Quang Minh, Department of Soil Science and Land Management, School of Agriculture, Can Tho University for sharing data about the delta. Many thanks go to the Cuu Long Delta Rice Research Institute for their support and for their permission to use their facilities and to all the farmers who kindly provided us useful information of their fields. Thanks to the Hanoi University of Agriculture for coordinating fieldwork activities. Especially thanks to Dr. A. Laborte from IRRI, Dr. D. Rossiter and Dr. M. Weir from ITC for their help in editing the manuscript. This study was funded by the Netherlands Organization for International Cooperation in Higher Education (NUFFIC) under the PhD Fellowship Programme.

Chapter 3
LaHMa: a new method to map landscape heterogeneity[4]

[4] This chapter is based on: de Bie, C.A.J.M., Nguyen Thi Thu Ha, Amjad Ali, Scarrot, R., & Skidmore, A.K. (2012). LaHMa: a landscape heterogeneity mapping method using hyper-temporal datasets. *International Journal of Geographical Information Science, 26(11), 2177-2192*

Abstract

A new quantitative method extracts a land cover heterogeneity map (LaHMa) from hyper-temporal remote sensing data. The feature extraction method is data-driven, unbiased, and builds on the commonly used data reduction technique of ISODATA clustering with the support of divergence separability indices. Firstly, the relevant spatial-temporal variation in NDVI is classified through ISODATA clustering. Secondly, a series of prepared cluster maps are overlaid to examine and detect the frequency with which boundaries between clusters occur at the same location. This step identifies the boundary strength between clusters, and detects spatial heterogeneity within them. Results of the method are explored for the typical agriculture-defined landscape of the Mekong delta, Vietnam, using NDVI-imagery time-series from SPOT-Vegetation and MODIS-Terra. The method extracts useful landscape heterogeneity features and can support land cover mapping requiring information on fragmentation and land cover gradients.

3.1 Introduction

3.1.1 Spatial heterogeneity

Global and regional ecosystem patterns have long been studied by biologists and ecologists (Lieth and Whittaker, 1975; Box, 1978). More recently, global warming models require accurate data on land cover and its heterogeneity (Turner et al., 2001). Studying this spatial heterogeneity and vegetation complexity involves consideration of both the structural complexity of the vegetation, as well as its spatial-temporal variability (Li and Reynolds, 1994).

Ecologists have embraced the view that the world is heterogeneous and complex (Chesson and Case, 1986). Landscapes exhibit various degrees of spatial heterogeneity due to the interactions of natural and anthropogenic processes. Certain mosaics of land use and land cover appear with boundaries and edges between them when seen at a specific scale. Within the theory of landscape ecology, boundaries are equated with transitional areas (Kent et al., 1997), of which in theory two extremes occur (Figure 3.1), referred to as ecotones and ecoclines (Whittaker, 1960; van der Maarel and Westhoff, 1964; van Leeuwen, 1966). This theory is useful when attempting to capture landscape heterogeneity and gradients. Heterogeneity is interpreted as representing various strengths of ecotones and ecoclines. Figure 1 exhibits scale through the location of map units; scale basically defines the difference between an ecotone and an ecocline.

Ecotones are important key structures of the functioning of landscape, and have a special role as indicators of climate change (Farina, 2006). Moreover, ecotone research has been linked to landscape ecology through edge effects, interior habitat, and ecological gradients (Wiens et al., 1985; Forman, 1995; Ewers and Didham, 2006). These boundaries of land mosaics may be driven by soil and vegetation discontinuities, strongly influencing species composition and distribution (Imaz *et al*., 2002). Ecotones also affect fluxes and accumulation of materials and energy (Harper et al., 2005). Studies by Fonderflick et al. (2010), and Pogue and Schnell (2001) found that reduction of ecotone areas due to agriculture intensification was one of the causes of biodiversity decline.

Spatial heterogeneity is not a static concept (Gustafson, 1998), but rather a function of spatial and temporal scales (Kent et al., 1997; Gustafson, 1998).

The spatial pattern and the intra-annual (temporal) changes within that landscape must be understood in order to quantify and study spatial heterogeneity through the analysis of imagery captured by earth observations. In other words, applying the incorrect spatial and temporal scale of remote sensing imagery to spatial analyses can lead to misinterpretation (Wiens, 1989). Therefore, careful consideration of the scale at which spatial heterogeneity is defined and measured is critical.

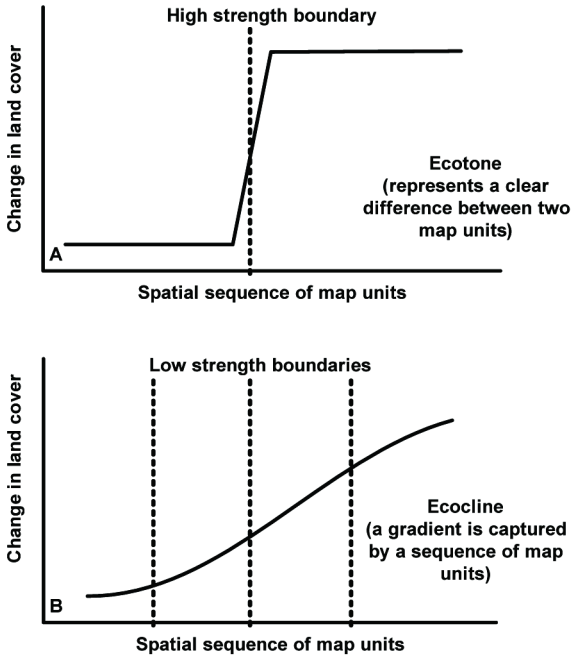

Figure 3.1: Comparing spatial sequences of map units for ecotones and ecoclines: (A) the sudden transition between two map units due to an ecotone; (B) the comparatively more gradual transition across map units as is characteristic for an ecocline (gradient)

An existing method of quantifying spatial heterogeneity is through gradient representation (Gosz, 1992). Gradient models are a human construct, allowing empirical relations between conditions, distributions and ecological community patterns to be explored. Essentially, they serve to organize environmental and biotic heterogeneity in a logical way (Keddy, 1991). Sampling heterogeneity in a statistically robust and sound manner, has proven to be a challenge, with researchers often stratifying their sampling regimes along subjectively chosen landscape features (White and Hood, 2004) or transects (Skidmore and Turner, 1992). Such sampling approaches

could be further improved if they were guided by an initial idea of the spatial heterogeneity inherent in the landscape of interest.

3.1.2 Hyper-temporal NDVI Images

Many studies have explored the use of multi-temporal image datasets, acquired intra-annually or inter-annually, for ecosystem monitoring, land cover (crop) identification, and change detection (Cayrol et al., 2000; Eerens et al., 2001; Ledwith, 2002; Souza et al., 2003; Brand and Malthus, 2004; Budde et al., 2004; Coppin et al., 2004) . Other studies have discussed and demonstrated that using hyper-temporal NDVI (Normalized Difference Vegetation Index) image datasets is particularly suitable to map (agro-) ecosystems, exploiting their ability to capture aspects of vegetation phenology and crop calendar characteristics (Gorham, 1998; Murakami et al., 2001; Uchida, 2001; Hill and Donald, 2003; de Bie, 2004; de Bie et al., 2008; Sakamoto et al., 2009a; Khan et al., 2010).

The Normalized Difference Vegetation Index (NDVI) quantifies the green vegetation cover in crops and plant species present in vegetation communities on the Earth's surface (Tucker, 1979). It is calculated from (NIR-Red)/(NIR+Red). As vegetated land cover grows, ages, and dies, the concentration of chlorophyll in its tissue fluctuates over time, a change which is detectable by NDVI (Tucker, 1979). Aside from the volume of vegetated biomass present, NDVI has been related to a variety of physical and biological parameters (e.g. Leaf Area Index (LAI), species, effects of soil/snow, etc.). It effectively provides us with information on the vigor and abundance of the Earth's vegetated land cover (Campbell, 1996), which many studies have demonstrated (Justice et al., 1985; Drenge and Tucker, 1988; Maggi and Stroppiana, 2002; Archer, 2004; Sarkar and Kafatos, 2004) (Sellers, 1985; Unganai and Kogan, 1998; Weiss et al., 2004) though the biomass signal saturates at higher NDVI values (Skidmore et al., 2010).

In addition, NDVI can provide information on the spatial distribution and temporal characteristics of the vegetated land cover, with the temporal aspect being exploited in this study. Stutheit (1991) noted that NDVI multi-temporal functionality should become a fundamental enhancement to all spatial analysis systems while Saab and Haythornthwaite (1990) described the difficulties with this enhancement: 'Time is the fourth dimension', they noted, 'it is unlike the first three dimensions in that it is asymmetrical, and

difficult to envision, much less to comprehend'. However, this fourth dimension can greatly enhance the information extracted from remote sensing imagery. To achieve this enhancement, Piwowar and LeDrew (1995) called not only for new techniques to be developed, but also existing image processing tools to be used such as unsupervised classification and principal components analysis.

In comparison to semi-natural landscapes, agricultural landscapes frequently display a higher seasonal (intra-annual) variability than a spatial one (de Bie et al., 2008). In the past, this temporal variability has been under-utilized for mapping due to the unavailability of satellite images at sufficient frequency and quality. However, since 1998 and 2000, suitable temporal dataset coverage of SPOT-Vegetation and MODIS-Terra imagery respectively has been available to study, explore, and gain in-depth insights on the use of hyper-temporal datasets for improved mapping and monitoring of agro-ecosystems. Since each dataset has its own spatial and temporal characteristics, both were explored here.

Temporal trajectory analysis, drawing on time-profile-based data originating from high observation frequency (hyper-temporal) imagery, has primarily been explored using threshold-based methods, compositing-algorithms, or Fourier series approximation (Salvatori et al., 1999; Coppin et al., 2004; Canisius et al., 2007; Lhermitte et al., 2008). This paper builds on a multivariate data-reduction methodology that does not force given functions to the data like Fourier approximation. Wavelet theory (Young, 1963) also provides a general mathematical framework for decomposition of images into components at different temporal and spatial scales (Schmidt and Skidmore, 2003; Murwira and Skidmore, 2005; Schowengerdt, 2006). It minimizes fuzzy boundaries between clusters (classes), and reduces noise effects. Use of a Fourier or wavelet transform, however, assumes that behaviour between years remains stable, averaging out changes in cropping patterns or heavy variability in weather patterns.

3.1.3 The ISODATA clustering technique and cluster separability indices

Hyper-temporal image datasets are data-rich, and through classification (clustering) their data volume must be reduced and generalized. Clustering is an unsupervised classification of patterns (observations, data items, or

feature vectors) into groups, clusters or classes (Jain et al., 1999). All existing clustering algorithms (deterministic, statistical or fuzzy) share the difficulty of not knowing *a-priori* the number of clusters (Boudraa, 1999). Visual identification of clusters as input for supervised classification is hardly feasible when using hyper-temporal datasets; the feature space encapsulates too many bands (time-periods) for visual pattern recognition. A further concern is that clusters derived from hyper-temporal imagery will by default contain autocorrelation and collinearity, caused by (i) seasonality and (ii) the occurrence of a large number of mixed pixels ('*mixels*').

The iterative self-organizing data analysis (ISODATA) clustering technique (Ball and Hall, 1965) derived from the k-means clustering technique (MacQueen, 1967) systematically choose *k* initial cluster centers or means (Hoekstra, 1998). A drawback of the *k*-means algorithm is that the centroids of clusters are determined once; then they remain fixed. The ISODATA algorithm is 'self-organizing', minimizing the Euclidean distances to form clusters of pixels (Swain, 1973; ERDAS Inc. , 2003). It first merges clusters with a small distance between their centroids into one cluster, then divides the cluster with the largest variance into two clusters (Jain et al., 1999). The initial *k* centroids are iteratively updated in such a way that, after a number of cycles, the *k* centroids properly represent the inherent *k* clusters.

Since *a prior* knowledge is generally not available, estimation of the number of clusters from the observed data (*k*) is required (Boudraa, 1999). This problem, known as the 'cluster validation problem' (Halkidi et al., 2001), essentially remains unresolved at present. The goal is to estimate the optimum number of clusters during the clustering process. The number of clusters at which a validation index is lowest (or highest) is proposed as a value for the number of object classes present in the data (Davies and Bouldin, 1979; Bezdek and Pal, 1998; Halkidi et al., 2001).

Many functions called 'cluster validity indices' have been proposed (Bouguessa et al., 2006), measuring the distance between signatures of two clusters. Choosing an index is a subtle and difficult exercise (Dubes, 1987; Thomas et al., 1987). This research used the divergence index (Swain, 1978), which can be calculated for any combination of image bands (ERDAS Inc., 2009). The transformed divergence index was not used as (i) it does not add information to D_{ij}, and (ii) it has a saturating behaviour (Richards and Xiuping Jia, 2006), especially for TD_{ij} values above 1.9 (D_{ij} > 24)(Jensen,

1996). The generally recommended Jeffries-Matusita Distance index also suffers from saturation (Richards and Jia, 2006). TD_{ij} values below 1.9 (D_{ij} < 24) is generally considered to indicate 'poor separability' (Jensen, 1996; Tso and Mather, 2001; ERDAS Inc., 2009).

As the expected overlap of derived clusters is considerable, no guidance can be given as to what the separability values signify in absolute terms, except that D_{ij} must be > 24 (Jensen, 1996). Visual inspection of the cluster signatures (NDVI profiles) and comparison of the validity index values obtained are, as earlier stated, the only two options available. Bouguessa *et al*. (2006) stated that use of a validity index provides the only objective measurement of a clustering result, and that its best value is frequently used to choose the optimum number of clusters of the clustering algorithm.

A clustering iteration between a minimum and maximum amount of acceptable clusters (classes) is thus required (must be preset). Following the iteration, all recorded separability values are then studied by the researcher, to make an informed selection of the 'best' clustering result. Since D_{ij} has a quadratic behaviour (Richards and Xiuping Jia, 2006), deviation of individual D_{ij} values from the D_{ij} series trend provides the required guidance.

Besides use of ISODATA, Principal Components Analysis (PCA) is another method of interest that possesses the ability to successfully summarize the variability present in hyper-temporal image datasets. PCA (Jolliffe, 2005)essentially compresses the bulk of the variability into a small number of images, or 'principal components'. The algorithm can be used to compress the information content of a large number of bands (images) into a few number of principal component (PC) images (Richards and Xiuping Jia, 2006). However, the disadvantage of PCA concerns the size of areas input to a PCA. Smaller areas that exhibit unique, and interesting NDVI temporal profiles, will only be represented when its total contribution to remaining unexplained variability is substantive. ISODATA does not have this shortcoming.

3.2 Materials and Method

3.2.1 Data

3.2.1.1 The rice cropping system map of the Mekong delta

Results presented in this study are based on satellite-acquired imagery of the Mekong delta area, in Southern Vietnam. The predominant land cover type in the region is irrigated rice (*Oryza sativa),* cultivated throughout the year. Through earlier analysis of a SPOT-Vegetation dataset and interview-based fieldwork, a detailed rice cropping systems map is available (Nguyen et al., 2012b).

3.2.1.2 SPOT Vegetation

Geo-referenced SPOT-4 and SPOT-5 Vegetation 10 day composite NDVI images at 1 km^2 resolution were used. The dataset extended from April 1998 until 31 January 2008 (354 images) and was obtained from www.VGT.vito.be as the S10 product. The SPOT-Vegetation sensor measures four spectral bands, i.e.: B1 (Blue) at 0.43-0.47 μm, B2 (Red) at 0.61-0.68 μm, B3 (Near Infrared-NIR) at 0.78-0.89 μm, and Middle Infrared/Short Wave Infrared (MIR/SWIR) at 1.58-1.75 μm. The images contain DN values defined as: DN = (NDVI+0.1)/0.004, with the S10 product generated using the best quality daily image values of B2 and B3 over a 10 day period as determined by the Maximum Value Compositing (MVC) algorithm. Each month, three S10 products are composited. The downloaded images were de-clouded, removing pixel values considered as invalid as determined by the supplied quality record. Only pixels with a 'good' radiometric quality rating for B2 and B3, and not having 'shadow', 'cloud' or 'uncertain' were kept. Removed pixel values were given a value of zero. No further pre-processing was carried out on the data.

3.2.1.3 MODIS Terra

Version-5 MODIS-Terra L3-V005 250 m resolution NDVI images (MOD13Q1 product) were obtained using the NASA web facility at https://wist.echo.nasa.gov. The images were a 16 day Maximum Value Composite (MVC) cycle, with the dataset extending from the 18th February 2000 to the 27th August 2008 (196 images with 23 images per year). The dataset projection was sinusoidal on the WGS84 spheroid. Version 5 MODIS-

Terra NDVI data were Validated Stage 2, meaning that accuracy had been assessed over a widely distributed set of locations and time periods via several ground-truth and validation efforts. The red and near-infrared reflectance, centered at 0.645 µm and 0.858 µm, were used to determine the daily NDVI values. The MVC data ranged between -2000 and 10000. They were rescaled using the formula: DN = Integer of (0.021333 NDVI + 43.117) to obtain values from 0 to 256. Zeros were substituted to replace any missing data values. A DN value of 85 referred to the start of photosynthetic activity. No additional pre-processing was done.

3.2.2 Method

3.2.2.1 Mapping of land cover heterogeneity

The ISODATA algorithm self-organizes the clusters when x clusters are created, showing considerably similar results when x+1 clusters are requested. It splits the cluster with the largest variance into two clusters, whilst recalibrating all other cluster centroids. Based on the new set of centroids, all pixels are re-assigned to a cluster. Each clustering output may be represented as a land unit map containing the spatial location and distribution of generated NDVI classes (clusters). Considering this, the two generated maps (of x, and x+1 clusters) will also show considerable similarity. This research, besides making use of a cluster validity index to evaluate which cluster-map is considered best (y), presents the integration of the series of maps having x to y clusters to extract the required heterogeneity index. The highest possible index value is defined by the difference between x and y. Integration of the prepared NDVI cluster maps delivers the required heterogeneity index map reflecting variability in space and time of land cover greenness.

The frequency of boundaries between clusters occurring at the same location can be used to assess the strength of boundaries. Here, a boundary is defined by the line around a group of spatially connected pixels (equating to a map unit) that have been assigned to the same cluster (class). A landscape heterogeneity map will show (spatially) the frequency or strength (within a maximum range of y minus x) with which two adjacent pixels are classified differently. The map output, a 'Landscape Heterogeneity Map', depicts boundaries with varying strength across a landscape and shows internal

heterogeneity within map units. The method by which the 'Landscape Heterogeneity Map' is generated is termed the 'LaHMa' method.

If two clusters are spatial neighbours and are spatially highly mixed (with a random 'salt and pepper' texture), the user may consider merging them into a complex unit. When the two classes show a clear pattern within the landscape, it possibly points to an underlying spatial gradient. Landscape gradients can be expressed by two or more map units (Figure 3.1). Note however that gradients can occur across map units that are not spatially connected.

The use of a landscape heterogeneity map can be compared to the use of a feature space as used to visually support supervised Maximum Likelihood classification (Richards and Xiuping Jia, 2006). The landscape heterogeneity map supports cluster separability assessment of unsupervised classification efforts.

3.2.2.2 ISODATA clustering of image stacks

For each hyper-temporal NDVI image dataset, using the ISODATA clustering algorithm, a series of unsupervised classification runs were executed to generate from 10 to 100 classes. Each ISODATA run thus generated a classified map having a pre-defined number of classes.

Following Nguyen et al.(2012b), for each classification, divergence indices (D_{ij}) were calculated between all possible pairs of signatures to assess their separability (Swain, 1978). Only the minimum and average divergence indices were kept to represent each run. The separability data for all runs were then plotted against the number of classes generated by each run. The plot was interpreted to select the best choice in terms of the number of clusters (classes) that can be generated to represent the variability in the processed hyper-temporal NDVI image datasets. Presence of gradients in a landscape will automatically lead to cluster overlap and to the question of how classes occurring across ecoclines should be divided (Figure 3.1). Presence of ecoclines (i.e. where clusters overlap) suggests that the 'cluster validation problem' can never be solved completely; any gradient can be split into a number of user defined classes.

3.2.2.3 Preparation of a landscape heterogeneity map

This procedure concerns the generated maps from 10 classes up to the map representing the best choice in number of clusters (classes) generated from the processed dataset. The output is a 'Landscape Heterogeneity Map' - LaHMa (Figure 3.2). Processing steps are:

Extract edges: Convert the raster data (class maps) to polygon and then to polyline files.

Generate rasters of the edges: Convert the polyline files to raster format with a grid size of 10% (or 50%) of the original raster resolution. Grid cells containing a line are given a value of 1, all other cells are given a value of 0.

Sum the stack of rasters: Stack all raster files and then sum the grid cell values of the stack to a single raster layer. These 'sums' represent the required LaHMa heterogeneity values for presentation as a map; the values are measures of cluster variability in the spatial-temporal domain.

Note that the heterogeneity values can be assigned to the z-scale of 3D scenes to visualize the derived heterogeneity values in combination with available maps or imagery.

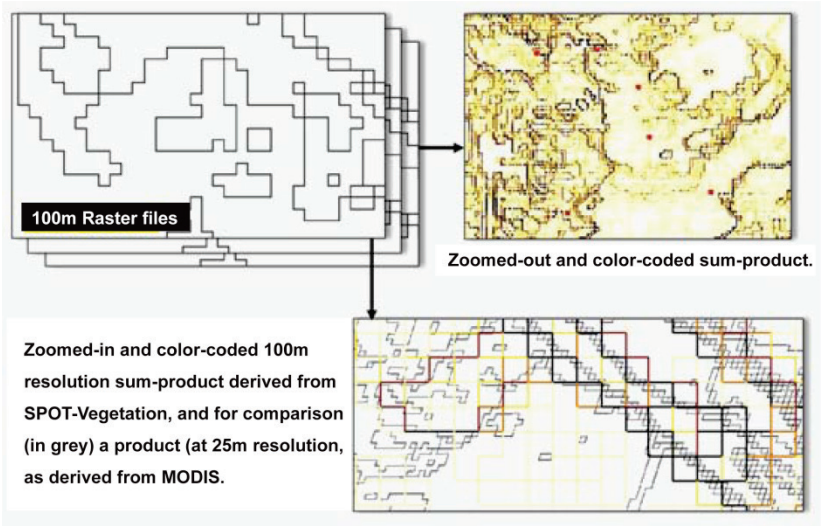

Figure 3.2: Preparation of a landscape heterogeneity map. It starts with an example of output (stacked maps) of the initial steps when a 10% grid size of the original raster resolution (1km) is used and ends with two esamples of output achieved through the final step.

3.3 Results

3.2.1 ISODATA clustering of the hyper-temporal NDVI image datasets

The minimum and average separability values, obtained for each ISODATA run, were plotted versus the number of classes generated by that run (from 10 to 100 classes) in Figure 3.3, which supports the choice about the best number of clusters to represent the variability in the hyper-temporal NDVI image dataset. Positive deviations from the trend lines indicate a relatively balanced clustering solution. A sharp peak occurs in the average separability values at 77 clusters (Figure 3.3a), which coincides with a moderate peak in minimum separability. The loss of valuable information due to under-estimation of the number of classes should be avoided, so 77 classes appear to be a reasonable compromise.

(a)

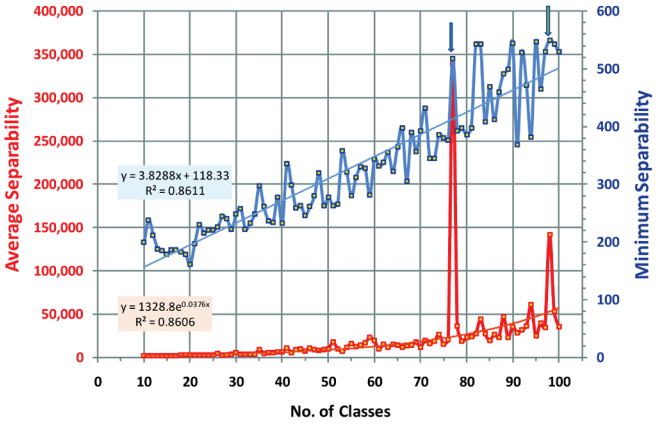

Two clear high peaks of the avg. separability were detected to select the optimum no.of classes directly; they indicate the natural no.of cluster in the dataset. The higher peaks of the min.separabi-lity do not matter in comparison; it stays on a linearly increasing track.	No.of classes	avg.	min.	comments avg.	comments min.	comments verdict	77 Classes is on the higher side, the unique jump in the avg.separability voids studying individual NDVI-profiles and spatial locations to merge them.
	77	338,814	518	high	high	**select**	
	98	142,239	549	medium	high		

(b)

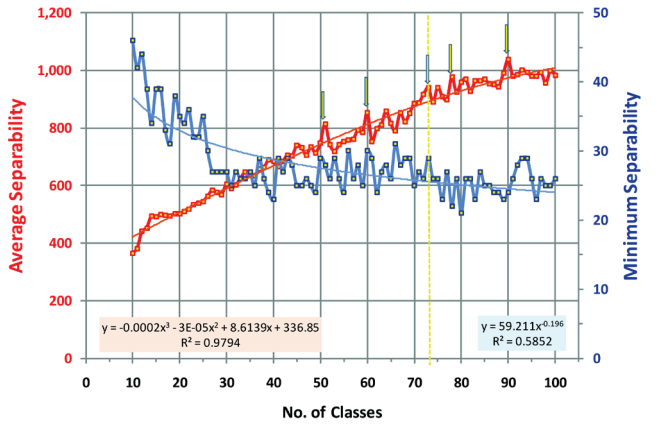

No clear high peaks were detected to select the optimum no.of classes directly. Before 40 classes, still too much gain in the avg.separability occurs, thereafter several minor peaks are found. The min.separability is generaly low and noisy.	No.of classes	avg.	min.	comments avg.	comments min.	comments verdict	73 Classes is (and should be) on the higher side, thus some classes can be merged after studying their individual NDVI-profiles and spatial locations.
	51	814	28	low	ok		
	60	854	30	still low	ok		
	73	939	29	ok	ok	**select**	
	78	977	22	ok	too low		
	90	1037	24	ok	too low		

Figure 3.3: **Estimation of the best number of classes to map the land cover of the Mekong delta. Panel (*a*) through 10-year SPOT-Vegetation NDVI images (trend-lines are added to support interpretation) (improved from Nguyen et al. (2012b)). Panel (*b*) through 8.5-year MODIS-Terra NDVI images. The red line depicts the average divergence separability values obtained per class run. The blue line represents the associated minimum divergence separability values.**

The average and minimum separability plot obtained from the MODIS-Terra NDVI image dataset is shown in Figure 3.3 (b). The identification of the best number of representative clusters is compounded by: (i) the lack of a peak divergence value, and (ii) the gradual drop of minimum divergence values below the threshold of 24 (poor separability). As stated above, the user should aim to generate the lowest possible number of classes, while not discarding valuable information caused by under-estimation of the number of clusters present in the dataset. In this case a compromise was selected with a 73 class option; this has a locally high maximum in the average divergence value which coincides with a distinctive local peak in the minimum divergence value above the threshold of 24. One might argue that the plot should be extended to incorporate more than 100 classes in order to fully explore the behaviour of the two separability statistics. However, such an action would disregard the 100 class upper limit we specified.

3.2.2 The ISODATA generated land unit maps and their NDVI profiles

The two land unit maps, derived using ISODATA, are shown in Figure 3.4. Each class is associated with a specific temporal NDVI profile. The series of NDVI profiles allow the clusters to be interpreted as classes. Fieldwork is required to interpret profile data with relevant land cover and land use descriptions.

It can be seen here that MODIS-Terra effectively discriminates linear landscape features (for the Mekong delta). In contrast, the lower spatial resolution SPOT-Vegetation product discriminates generalized landscape patterns. Both hyper-temporal dataset products represent landscape patterns at their specific pixel resolution level. If the resolution is finer, more complex patterns may occur at the cost of generalization. Colours assigned to classes shown in Figure 3.4 have, as yet, no direct meaning. However, their spatial patterning and distributions are recognizable. The spatial cluster distribution outputs are accompanied by mean cluster signature outputs that show the 10 year mean NDVI profiles by cluster. From the profiles, past temporal land cover (NDVI) behaviour, including changes made in cropping systems, can be examined and interpreted.

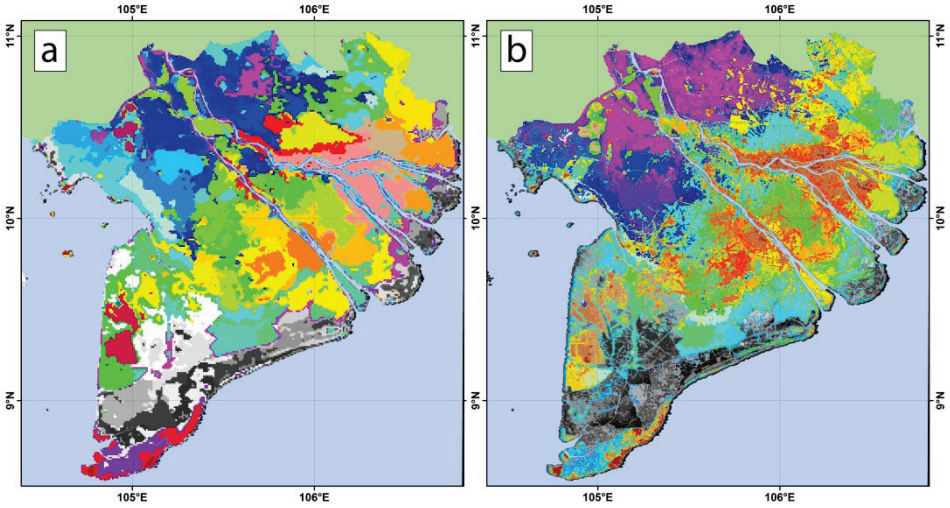

Figure 3.4: Comparing cluster distributions of the Mekong delta, Vietnam, derived using the modified ISODATA algorithm :(*a*) the 77 clusters derived from the SPOT Vegetation dataset at 1km resolution, and (*b*) the 73 clusters derived from the MODIS Terra dataset at 250m resolution. Cluster composed of pixels representing rice growing areas are shown in colours, while those covering non-rice areas are shown in grey scale.

3.2.3 The landscape heterogeneity maps

The landscape heterogeneity map obtained from the SPOT-Vegetation dataset is shown in Figure 3.5, alongside an existing 2005 rice systems map (NIAPP, 2008).

Note that for many areas, clear spatial similarities exist. A closer inspection of the landscape heterogeneity maps, derived from the SPOT-Vegetation and MODIS-Terra datasets for the Mekong delta (Figure 3.6), reveals the effect of the different spatial resolution imagery used in its construction. Large homogenous patches are evident in the SPOT-Vegetation derived map. In contrast, a higher frequency of boundaries can be observed in the MODIS-Terra derived map. The main processes underlying the cover heterogeneity in the Mekong delta are almost fully related to variability in practiced rice cropping calendars. The article by Nguyen et al., (2012b) reveals the differences between areas in cropping calendars practiced and of their related flooding regimes.

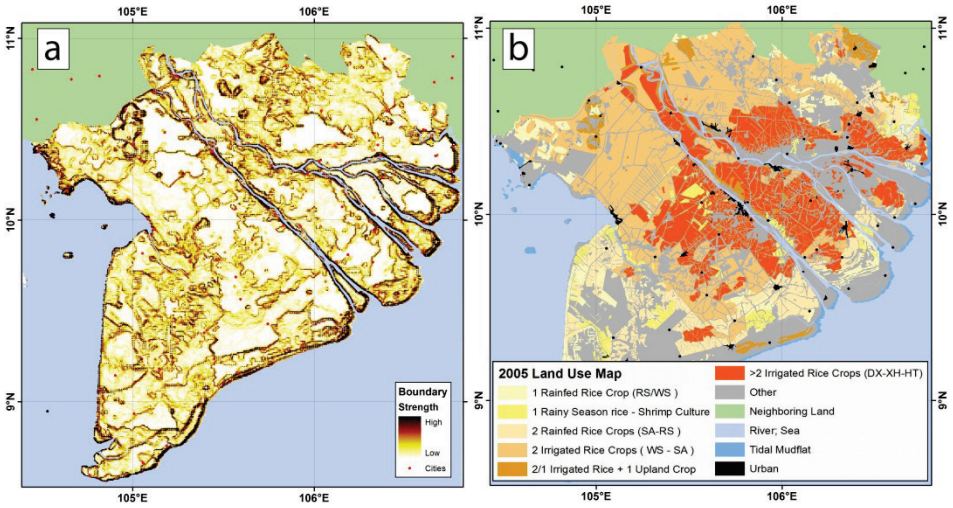

Figure 3.5: Comparison of the SPOT-Vegetation landscape heterogeneity map and the existing rice map (as of 2005). Panel (a) the landscape heterogeneity map derived from the map series of 10–77 classes, generated by the ISODATA algorithm. It depicts (i) high strength boundaries (dark brown to black), (ii) homogeneous (white) to heterogeneous areas (yellowish-brown), and (iii) low strength boundaries (light brown bands). Panel (b) rice areas as extracted from the 2005 land-use map of NIAPP (2008). They split the rice cropping systems practiced into three rainfed and three irrigated categories.

3.3 Discussion

The LaHMa method to map land cover heterogeneity at landscape level through a data-driven, unbiased approach exploits hyper-temporal remote sensing datasets. It builds on the commonly used ISODATA clustering algorithm and on data-driven guidance through the use of divergence statistics. Integration of the series of ISODATA generated land unit maps reveals units (zones) that share high strength boundaries (ecotones), and which ones do not (ecoclines) plus heterogeneity within each delineated map unit. Units that form ecocline zones jointly represent a gradient.

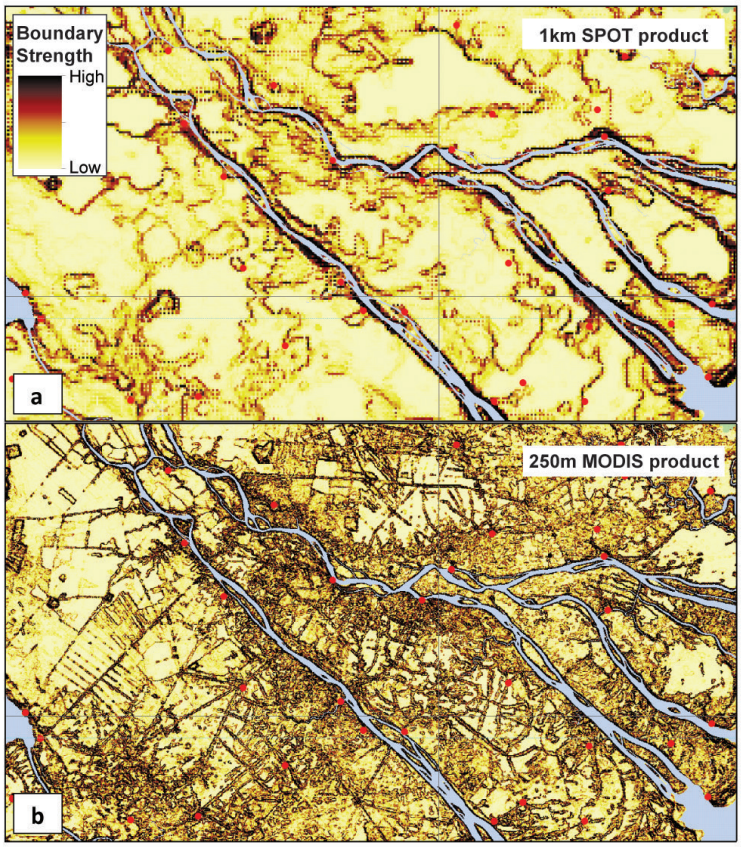

Figure 3.6: Two landscape heterogeneity maps with different resolutions compared. Panel (*a*) a map derived from the boundaries of 10–77 classes obtained from the 1-km resolution SPOT Vegetation unsupervised classification iterations (0 = low boundary strength, 77 = high boundary strength). Panel (*b*) a map derived from the boundaries of 10–73 classes obtained from the 250-m resolution MODIS Terra unsupervised classification iterations (0 = low boundary strength, 73 = high boundary strength). Larger population centers are marked in red, while the primary distributary channels of the Mekong River are marked in light blue.

The maps produced express the interaction of environmental and human created gradients on land cover variability across the landscape. The heterogeneity relates to the spatial variability of different cover types or their mosaics. High temporal landscape changes within a homogeneous area, as associated with dynamic seasonal patterns, are part of the area's characteristics; they do not contribute to heterogeneity. When the seasonal patterns differ over space, they do contribute. The map may serve to guide subsequent studies and sampling of the delineated units and zones. The

derived landscape heterogeneity map can be considered as a useful source for a landscape analyst, essentially visualizing the complexity of the landscape in question.

The method was explored using the Mekong delta, Vietnam as a case study site, and using two different hyper-temporal image datasets (1 km resolution SPOT Vegetation and 250 m resolution MODIS Terra). The SPOT Vegetation derived landscape heterogeneity map displayed potential to reflect the expression of land cover heterogeneity across the delta. In this context however, the MODIS Terra product detected many linear features representing roads/canals with houses and homestead garden aggregations. Given that landscapes exhibit distinctive spatial patterns at different scales, the scale of observation significantly influences what can be observed (Wiens, 1989; Saab, 1999). Use of finer resolution data tends to detect many more (local) changes in land cover as ecotones. Analysts should thus be mindful, that the use of finer spatial resolution data will generate more detail on local land cover variability. The influence of scale on the level of detail required must be carefully considered, and depends on research questions asked (Benson and MacKenzie, 1995). The amount and spatial uniformity of modifications made to the natural environment and the spatial cover differences within natural landscapes (patchiness) are also expected to play a role in such considerations.

The LaHMa method successfully processed spatial-temporal data of the green land cover and produced a map showing ecotones and ecoclines. In that sense, the green cover reflects in turn spatial differences (combinations) of climate, weather, landform, terrain, soils, and land use. LaHMa thus provides researchers a robust additional tool in their efforts to stratify, describe and study landscape features.

Chapter 4
Remote sensing of leaf area index for irrigated rice[5]

[5] This chapter is based on Nguyen Thi Thu Ha, Verhoef, W., de Bie, C.A.J.M., Venus, V., Suarez Urrutia, J.A., & Nieuwenhuis, W. Leaf area index of irrigated rice: a comparison of MODIS LAI product and inversion estimates by the Soil-Leaf-Canopy radiative transfer model. *Remote Sensing of Environment*. **In Revision** (after review)

Abstract

The leaf area index (LAI) is an important biophysical parameter in terrestrial ecosystem models. In this study MODIS 8-day LAI (MOD15A2) data at 1km spatial resolution were compared with field data and with LAI estimates derived from MODIS 8-day surface reflectance data (MOD09A1). Data that captured the seasonal variation in LAI of 60 irrigated rice fields located in the Mekong delta of Vietnam were used for this comparison. To estimate rice LAI, the MOD09A1 data were inverted through the Soil-Leaf-Canopy (SLC) radiative transfer model following the look-up table (LUT) approach. LAI evolution of irrigated rice during a cropping season could be much better be estimated by the SLC model (R^2=0.69, RMSE=0.9) than by the algorithm used by NASA (R^2=0.07, RMSE=2.1). By using information on background reflectance in particular of water together with rice leaf and canopy properties, SLC provided great flexibility to simulate seasonal LAI of irrigated rice.

4.1 Introduction

Remote sensing data can be exploited for the retrieval of land surface variables, such as leaf area index (LAI). These are key biophysical parameters in most ecosystem productivity models and in global models of ecology and climate (Myneni et al., 1997; Sellers et al., 1997). LAI is defined as the total one-sided area of leaf tissue per unit ground surface area (Breda, 2003), and serves as one of the most important parameters in crop growth simulation models (Bouman et al., 1996; van Ittersum et al., 2003).

LAI can be retrieved from remotely sensed data by statistical and physical approaches. While the former are mostly based on empirical relationships between *in situ* LAI and Vegetation Indices (VI) (Carlson and Ripley, 1997; Myneni et al., 1997; Turner et al., 1999; Gupta et al., 2000; Wang et al., 2005), the latter are mostly based on the inversion of a canopy radiative transfer model (RTM) (Myneni et al., 1997; Knyazikhin et al., 1998a; Kimes et al., 2000; Weiss et al., 2000; Combal et al., 2003; Schlerf and Atzberger, 2006). LAI estimations based on empirical relationships often suffer from saturation and a low sensitivity at high values of LAI (Baret and Guyot, 1991; Brown et al., 2000; Eklundh et al., 2001), and the relationships are dependent on location, vegetation type and growing stage (Baret and Guyot, 1991; Colombo et al., 2003). Empirical approaches thus lack generality and are consequently not fit to be applied for regional-scale operations.

Canopy radiative transfer models, on the other hand, describe the interaction between solar radiation and vegetation elements inside the canopy and the background surface. The models calculate , by physical laws, the Top-Of-Canopy (TOC) reflectance as a function of vegetation characteristics (Goel, 1989; Meroni et al., 2004), and are hence able to provide explicit relationships between TOC reflectance and the vegetation's physical and biochemical properties (Houborg et al., 2007).

LAI estimation by inverting RTM is a powerful approach. Inversion of canopy RTM can be sub-categorized into numerical optimization (NOP) approaches (Jacquemoud et al., 1995; Jacquemoud et al., 2000; Vohland et al., 2010), Look-Up Table (LUT) approaches (Weiss et al., 2000; Combal et al., 2003; Darvishzadeh et al., 2008), Artificial Neural Network (ANN) approaches (Weiss and Baret, 1999; Atzberger, 2004; Fang and Liang, 2005; Bacour et

al., 2006; Schlerf and Atzberger, 2006), and statistical multiple regression techniques (Durbha et al., 2007).

The NOP methods have been widely used in Bidirectional Reflectance Distribution Function (BRDF)research to retrieve LAI (Goel, 1989; Liang and Strahler, 1993; Liang and Strahler, 1994; Kimes et al., 2000; Vohland et al., 2010). Though LAI estimation by using this approach performed better than by using a simple empirical approach, the NOP methods were found to be computationally demanding, and therefore difficult to apply operationally at regional scale (Liang, 2004). The LUT and ANN methods are possible solutions to overcome the huge demand of computation time required by RTM inversion through NOP. Nevertheless, they require a large database of simulated canopy reflectance spectra for proper training (in the case of ANN) and reliable simulations (in the case of LUT) in order to achieve accurate LAI values. Although both methods appear very suitable for large-scale operation, LUT has one advantage over ANN. Conceptually, LUT is a simple method and could potentially overcome limitations of iterative optimization algorithms , namely excessive computation times and the risk of converging into local minima that are not necessarily close to the actual solution (Kimes et al., 2000; Combal et al., 2003; Schlerf and Atzberger, 2006). Hence, many have adopted it as one of the most applicable methods for their studies (Myneni et al., 1997; Knyazikhin et al., 1998a; Knyazikhin et al., 1998b). A LUT-based method is , therefore, easy to implement, whilst ANNs require a good design of the network architecture and assessment of the network's performance (Liang, 2004). LUT is also known as an advanced method to solve vegetation BRDF model inversion (Kimes et al., 2000).

A general limitation of model inversion is that this problem is often ill-posed (Combal et al., 2003; Atzberger, 2004). This happens when the inversion solutions are not unique, meaning that several combinations of canopy parameters yield similar canopy reflectance spectra (Weiss and Baret, 1999). To reduce the ill-posed problem, two methods are advised. The first method considers the use of prior knowledge to regularize the inversion process in the look-up table (LUT), and the second takes the dynamic evolution of LAI during a growing cycle into account (Atzberger, 2004).

For decades, LAI estimation by optical remote sensing for irrigated rice was mainly based on established empirical relationships between LAI and VI (Shibayama and Akiyama, 1989; Casanova et al., 1998; Xiao et al., 2002b;

Wang et al., 2007; Kushida and Yoshino, 2010). The use of RTM to estimate rice LAI is rarely seen (Wang et al., 2010), probably because of the typical background signal of irrigated rice system caused by standing water. To improve this knowledge gap, our research aimed to investigate the inversion of a coupled soil BRDF - canopy radiative transfer model to simulate seasonal LAI for irrigated rice. We also tested how the readily available MODIS LAI product (MOD15A2) performs in comparison.

4.2 Materials

4.2.1 Study area

The study area is part of the largest rice producing area of the Mekong basin, Vietnam. Rice is often cultivated in a double or triple cropping system.

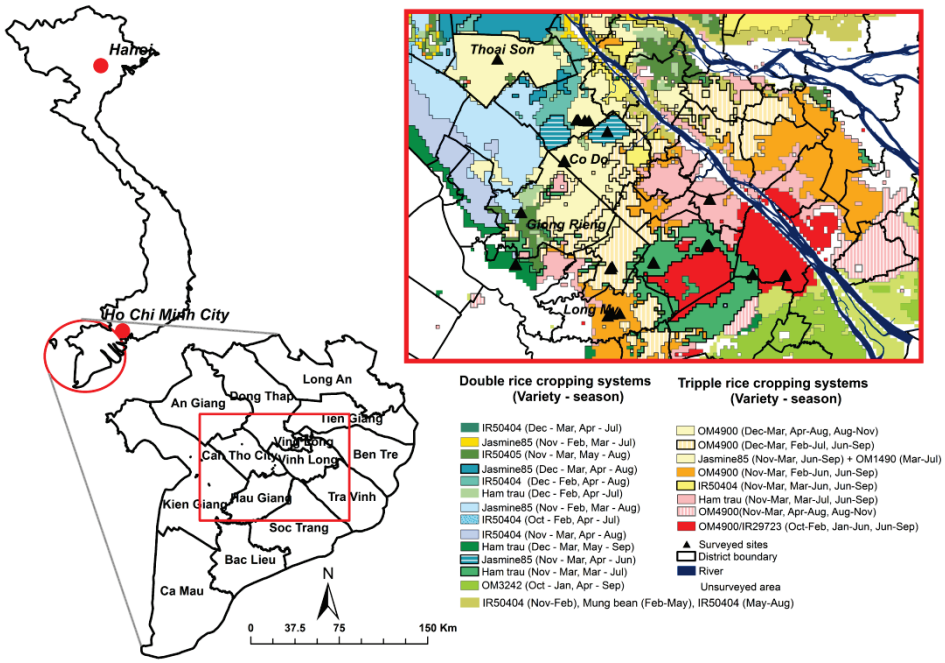

Figure 4.1: The Mekong delta, Vietnam, the surveyed rice plot locations and their rice cropping seasons

Figure 4.1 shows the location of the Mekong delta and its rice cropping patterns throughout a year. The map was derived from SPOT-NDVI 1km resolution data. More details on the mapping methodology can be found in Nguyen et al. (2012b).

To obtain *in situ* LAI, 60 rice paddies were selected based on a random stratified sampling scheme. The stratification was based on (i) type of rice cropping pattern, and (ii) type of cultivated rice variety. The 60 selected fields were all located in areas where either a double or a triple rice cropping system was practiced (Figure 4.2), and where the three most common rice varieties namely Jasmine 85, Ham Trau, and OM 4900 were grown. These are all high-yielding varieties belonging to the *Indica* rice variety group.

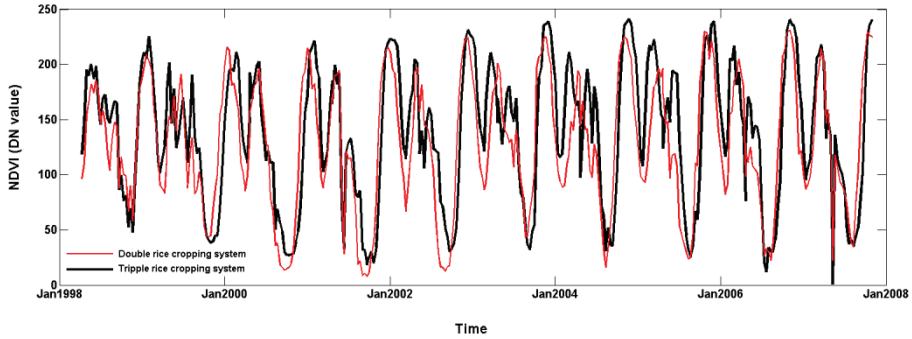

Figure 4.2: The 10-year SPOT Vegetation NDVI profiles of two typical rice cropping pattern classes in the Mekong delta

4.2.2 MODIS data

MOD15A2 is the 8-day LAI/FPAR product at 1km resolution[6]. The MOD15A2.V005 (version 5) provides LAI/FPAR retrievals for eight biomes of land cover, namely as deciduous forests, evergreen forests, grasses and cereal crops, shrubs, broadleaf crops, savannahs, broadleaf forests and needle forests. The MOD15A2.V005 algorithm refinements were targeted mainly on woody vegetation. In our study, MOD15A2.V005 data were downloaded for the period Nov 2008 – May 2009. The data cover a complete rice growing cycle for all selected paddy sites.

MOD09A1 is the 8-day surface reflectance product derived from MODIS Terra daily observations. This product is atmospherically corrected, and contains the best possible pixel-values of daily observation during an 8-day period as selected on the basis of high observation coverage, low view zenith angle,

[6]Available at: http://reverb.echo.nasa.gov/reverb/#utf8=%E2%9C%93&spatial_map=satellite&spatial_type=rectangle.

the absence of clouds or cloud shadow, and aerosol loading. These are 500m resolution data with 7 bands covering the spectral range 459 – 2155 nm. Their characteristics are provided in Table 4.1.

Table 4.1: MODIS Terra 8-day surface reflectance bands

MODIS Terra band	Spectral range (nm)	Band centre (nm)
Band 1 (Red)'	620 - 670	645
Band 2 (NIR)	841 - 876	858
Band 3 (Blue)	459 – 479	470
Band 4 (Green)	545 – 565	555
Band 5 (SWIR)	1230 – 1250	1240
Band 6 (SWIR)	1628 – 1652	1640
Band 7 (SWIR)	2105 - 2155	2130

The MOD09A1 data were downloaded for the period from Nov 2008 – May 2009 and all seven bands were used as inputs for inversion by a RTM. Cleaning MOD09A1 data was done by using the reflectance band quality (QA) values provided in the same dataset. Only pixels with "good" quality and without cloud effects were considered for analysis. Bad and fill-value pixels were assigned the "missing" value of 0.

4.2.3 In situ LAI

In situ LAI measurements were taken from December 2008 – May 2009 (winter-spring cropping season) in 60 different rice paddies (see Figure 4.1), using the LI-COR LAI 2000 Plant Canopy Analyzer. This instrument provides non-destructive measurements of canopy LAI.

Representative rice paddies were selected in the centre of relatively homogenous rice cropping pattern areas as mapped in Figure 4.1. The average field size was 1.2 ha. Every 7 to 10 days, each paddy field was revisited to take the LAI measurements of 1m by 1m plots along a diagonal transect through each field. The transect data were averaged to get date specific and field-wise LAI values (Table 4.2).

4.2.4 Leaf chlorophyll content

Leaf chlorophyll content of rice was measured at the same time as LAI measurement using a Minolta SPAD 502 instrument. Thirty SPAD readings

were taken at each 1m by 1m subplot and then averaged into one value corresponding to each LAI measurement. These were converted into leaf chlorophyll content (C_{ab}) by means of an empirical calibration equation developed by Markwell *et al.* (1995) (Table 4.2).

Table 4. 2: Summary statistics of measured biophysical and biochemical variables for rice

Variable	Min	Max	Mean	Std.
LAI (m^2. m^{-2})	0.9	7	3.7	1.3
SPAD (*unitless*)	16.6	53.7	34.1	4.7
Leaf chlorophyll content (µg.cm^{-2})	11.5	67.2	32.6	6.7

4.3 Methods

4.3.1 Comparison of in situ LAI and MOD15A2 LAI

In order to synchronize the *in situ* LAI measurements that had a time resolution of 7 to 10 days with the MOD15A2 8-day LAI data, the *in situ* LAI data were interpolated based on a dynamic LAI model shown in Equation 4.1 (Koetz et al., 2005).

$$LAI = LAI_{amp}\left\{ \frac{1}{1+\exp[-b(T-T_i)]} - \exp[-a(T-T_S)] \right\} \qquad \textbf{(4.1)}$$

where T is the accumulated daily mean air temperature above a base temperature (8^0C for rice) starting from sowing date, b is the relative growth rate at accumulated temperature T_i (the first inflection point), and a is the relative senescence rate at accumulated temperature T_s (at the time of green leaves disappearance), and LAI_{amp} describes the amplitude of maximal leaf area.

The parameters b and T_i describe the dynamics before the maximum LAI is reached, while a and T_s describe the dynamics after maximum LAI is reached.

Considering that MOD15A2 has a spatial grid of 1km x 1km, and that a surveyed rice paddy could occupy parts of several MOD15A2 pixels, a weighted sum based on the percentage of field area proportions was applied to obtain one single representative LAI value of that field. Since sites were selected in relatively homogenous areas, these corrections were marginal.

4.3.2 The SLC model

The SLC model (Verhoef and Bach, 2007) is a coupled soil-leaf-canopy radiative transfer model. It consists of three sub-models: (i) a modified Hapke soil BRDF model, (ii) the PROSPECT leaf model, and (iii) the 4SAIL2 canopy RTM.

Unlike its predecessors, such as PROSAIL, the soil reflectance model of SLC does not assume that the soil background can be treated as a Lambertian reflector. The modified Hapke model (Hapke, 1981) in SLC describes the soil's interaction with the canopy by means of two four-stream radiative transfer equations, using all combinations of hemispherical and directional radiation. For irrigated rice, since the paddies are flooded during most of the rice growing season, additional spectral reflectance information of turbid water was required. Since no such data were available for the study area, we used SLC-simulated muddy water reflectance spectra originating from the SLC spectral library.

The PROSPECT leaf optical properties model (Jacquemoud and Baret, 1990) calculates the leaf hemispherical transmittance and reflectance as a function of the leaf structural parameter (leaf mesophyll) and the leaf chemical properties. The version of PROSPECT used in SLC is version 5 regarding the chlorophyll absorption spectrum, but the refraction index from version 4 was kept. Also the brown pigment spectrum from Fourty et al. (1996) was kept to in order obtain realistic spectra for brown leaves. The input parameters of PROSPECT are leaf mesophyll structure (or number of elementary layers) N, chlorophyll concentration C_{ab} (µg.cm^{-2}), water content C_w (cm), dry matter content C_{dm} (g.cm^{-2}) and brown pigment C_s (arbitrary unit). The leaf optical properties calculated by PROSPECT are the inputs for the 4SAIL2 canopy radiative transfer model.

Table 4.3: Set of input parameters for SLC model used to estimate rice LAI

Parameter	Abbreviation	Unit	Value	Parameterization
Green leaf mesophyll parameter	N_g	-	1.5 – 1.8	Step of 0.1
Green leaf chlorophyll concentration	C_{ab_g}	µg.cm^{-2}	16.6 – 53.7	Step of 5.5
Green leaf water content	C_{w_g}	cm	0.01 – 0.02	Step of 0.005
Green leaf dry matter content	C_{dm_g}	g.cm^{-2}	0.005 – 0.01	Step of 0.0025
Green leaf brown pigment	C_{s_g}	-	0.15	Fixed
Brown leaf mesophyll parameter	N_b	-	2	fixed
Brown leaf chlorophyll concentration	C_{ab_b}	µg.cm^{-2}	0	fixed
Brown leaf water content	C_{w_b}	cm	0	fixed
Brown leaf dry matter content	C_{dm_b}	g.cm^{-2}	0.01	fixed
Brown leaf brown pigment	C_{s_b}	-	2	fixed
Leaf area index	*LAI*	m^2.m^{-2}	0 – 7	Step of 0.1 for LAI ≤ 4; 0.2 for 4 ≤LAI ≤5; and 0.5 for 5 ≤ LAI ≤ 7
Leaf inclination distribution function parameter *a*	$LIDF_a$	-	-0.65; -0.5; -0.35	
Leaf inclination distribution function parameter *b*	$LIDF_b$	-	-0.15; 0; 0.15	
Hotspot size	s_l	m.m^{-1}	0.1/*LAI*	
Fraction brown leaf area[7]	f_B	-	0.01 – 0.1	1 random value for each LUT run
Dissociation factor[8]	*D*	-	0.4 – 1	1 random value for each LUT run
Vertical crown cover fraction	C_v	-	1	
Tree shape factor	ξ	-	0	
Solar zenith angle	*sza*	deg	0 - 90	MOD09A1 data set
Viewing zenith angle	*vza*	deg	0 – 90	MOD09A1 data set
Relative azimuth angle	*raa*	deg	0 - 180	MOD09A1data set (absolute value)

[7] Parameter value range estimated through field observations and photos taken in the field

[8] Parameter value range estimated through field observations and photos taken in the field

SLC is a hybrid two-layer model which takes into account the optical interaction with a non-Lambertian soil background and the interaction between both canopy layers (Verhoef and Bach, 2003). Apart from the required input parameters related to PROSPECT for two leaf types, 4SAIL2 requires eight canopy structure parameters to produce top-of-canopy (TOC) bidirectional reflectance. These eight parameters are the total leaf area index *LAI*, mean scaled leaf slope $LIDF_a$ ([-1,1]), bimodality $LIDF_b$([-1,1]) (Verhoef, 1998), hot spot size parameter s_l (ratio of leaf width to canopy height), fraction brown leaf area f_B ([0,1]), layer dissociation factor *D* ([0,1]), vertical crown cover fraction C_v ([0,1]) and tree shape factor ξ (ratio of crown diameter to crown height). The latter two are meant for forest, and were not used in the present study; that is, C_v was set equal to 1 and the tree shape factor becomes then immaterial. In addition, the solar zenith angle *sza* (deg), the viewing zenith angle *vza* (deg) and the relative azimuth angle *raa* (deg) were required. The hot spot size parameter s_l was assumed to vary inversely proportional with *LAI*, such that the product $s_l \times LAI$ equals 0.1. Such behaviour is typical for crops like wheat and rice, which grow in height rather than by increasing their leaf size. Table 4.3 presents all input parameters for PROSPECT and 4SAIL2 in SLC used for this research.

4.3.3 LAI estimation based on the look-up table inversion

The LUT approach consists of two major steps: (i) the generation of the LUT itself, based on regular intervals or random selection from a uniform distribution of specific pre-set ranges of the respective model parameters (as shown in Table 3); and (ii) applying the LUT by selection of the optimum solutions for given referenced data (here MOD9A1).

For every 8-day composite set of MOD09A1 imagery, a LUT consisting of approximately 110,000 SLC-parameter combinations was generated. Each LUT is specific for a given date within a year through its solar zenith, viewing zenith and relative azimuth angle specifications. The generation of every LUT took approximately 15 minutes in MATLAB v7.8 on a 32-bit Windows 7 platform.

Since SLC simulations were considered for rice only during the vegetative and reproductive stages, leaf senescence was assumed minimum. The f_B was given values ranging from 0.01 - 0.1, which was estimated based on field

observations together with photos taken in the field. The other associated parameters of brown leaves (C_{ab_b} , C_{w_b}, C_{dm_b}, and C_{s_b}) in SLC, which were not measured, were fixed to nominal values due to their low contribution to the reflectance signals. Nine combinations of leaf inclination distribution function parameters were chosen with $LIDF_a$ of -0.65, -0.5, and -0.3, and $LIDF_b$ of -0.15, 0 and 0.15. This represents moderate erectophile leaf angle distributions of varying mean slope and bimodality levels, and accommodates possible differences among the three studied rice varieties.

Considering that a rice leaf is relatively thin, the leaf mesophyll parameter N was set to vary from 1.5 - 1.8, which was similar to that used for grass by Darvishzadeh et al. (2008). The green leaf water content C_{w_g} (equivalent to green leaf water thickness) was set to a nominal range of 0.01 – 0.02 cm as there was no measurement of leaf water content during the fieldwork. The green leaf dry matter content C_{dm_g} was assigned values of 0.01 – 0.02 g.cm^{-2} with a step of 0.005 based on laboratory measurements of leaf samples. Vertical crown cover fraction C_v was set to 1, since rice in the Mekong delta has no crown clumping as it is directly seeded by the broadcasting method.

Selection of the optimal LUT inversion solutions were made by minimizing the root mean square error (*RMSE*) that measures the difference between the model estimation and referenced data. *RMSE* is calculated by Equation 4.2

$$RMSE = \sqrt{\frac{\sum_{i=1}^{n_b}\left(R_{i,ref} - R_{i,j}\right)^2}{n_b}} \qquad (\mathbf{4.2})$$

where $R_{i,ref}$ is the MOD09A1 reflectance at wavelength *i* and $R_{i,j}$ is the SLC estimation at simulation *j* at wavelength *i* in the LUT; n_b is the number of wavelength bands.

Searching for the best solution for each date's LUT took about 19 minutes per image in MATLAB v7.8 on Windows 7. The LAI values of the best solution for the 60 surveyed sites were then extracted for subsequent evaluation.

Note that rice varieties were not specific considered. However, as the chosen solution is always pixel specific and the variation of the SLC input parameters, such as *LIDF* and C_{ab}, is assumed to account for the differences among the three varieties.

4.4 Results and Discussion

4.4.1 Comparison of in situ LAI and MOD15A2 product

Figure 4.3 shows the daily interpolated data of *in situ* LAI for the period from November 1, 2008 to April 30, 2009 (R^2 = 0.91; RMSE = 0.41). Since the daily temperature never dropped below the base temperature of 8^0C, the evolution of rice LAI during the growing season was presumably followed the dynamics of Equation 4.1. Interpolated LAI for rice based on *in situ* measurements rarely exceeds 6. Maximum LAI values were often reached 40 - 50 days before harvest. The different sowing and maturity dates of different rice paddies can also be recognized. Seasonal variation of LAI did not always follow the same trend even within the same variety group. For Jasmine85 and Ham trau , in the early or late sown fields, LAI behaviour was clearly dissimilar (bold curves in Figure 4.3).These varieties tended to have lower maximum LAI values. This could be caused by soil characteristics of the rice paddies (e.g. salinity or acidity), by management differences, or by sub-optimal weather conditions.

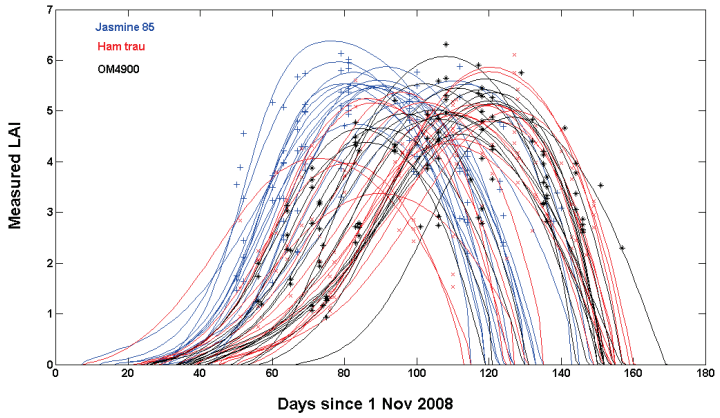

Figure 4.3: Daily interpolation of in situ LAI by site

Since *in situ* LAI measurements took place from December 18, 2008 (DOY 49) till April 30, 2009, a comparison with MODIS data was only made for the dates that LAI measurements were available. The relationship between MOD15A2 LAI and *in situ* LAI proved to be very poor (R^2 = 0.07, RMSE = 2.1) (Figure 4.4). MOD15A2 mostly underestimated rice LAI. This is likely caused by inaccurate input information of the background reflectance in the

MOD15A2 RTM, where soil reflection is assumed to have intermediate brightness for Biome 1 land cover group consisting of grass and cereal crops. This is certainly not the case for irrigated rice, of which fields are flooded during most of the growing season. Other reason might be either due to the use of incorrect land cover information as one of the input of MODIS RTM or the use of back-up algorithm when MODIS RTM failed to produce LAI.

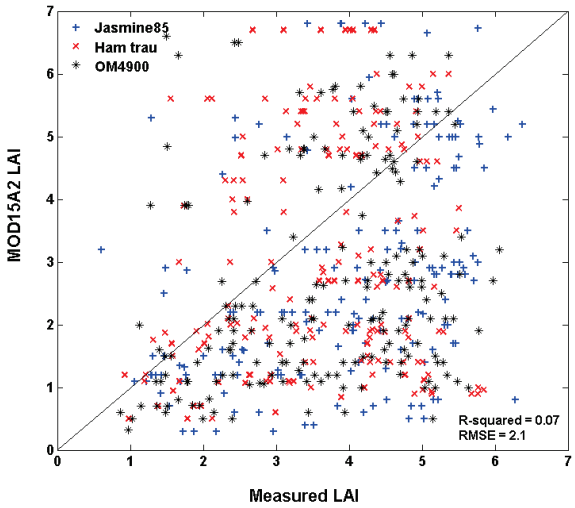

Figure 4.4: Comparison between retrieved LAI from MOD15A2 and measured LAI by site from December 18, 2008 to April 30, 2009

Another reason that can explain the poor relation between MOD15A2 LAI and *in situ* LAI is a poor inversion of the MOD15A2 RTM (Huifang et al., 2009). Figure 4.5 shows for January 17, 2009 (DOY 78) the side-by-side map comparison of MOD09A1 surface reflectance, MOD15A2 LAI and generated LAI from the SLC model. Though rice in the upper left (circle 1) of the studied area was in its mid growing season when LAI peaked (Figure 4.3), MOD15A2 LAI provided too low values that varied substantially within the circle. Similarly, in the lower right (circle 2), MOD15A2 LAI showed extreme high LAI values despite the fact that the district of Ke Sach was on the transition from late harvesting to sowing. This area is famous for non-stop rice cropping system without intermittent fallow periods.

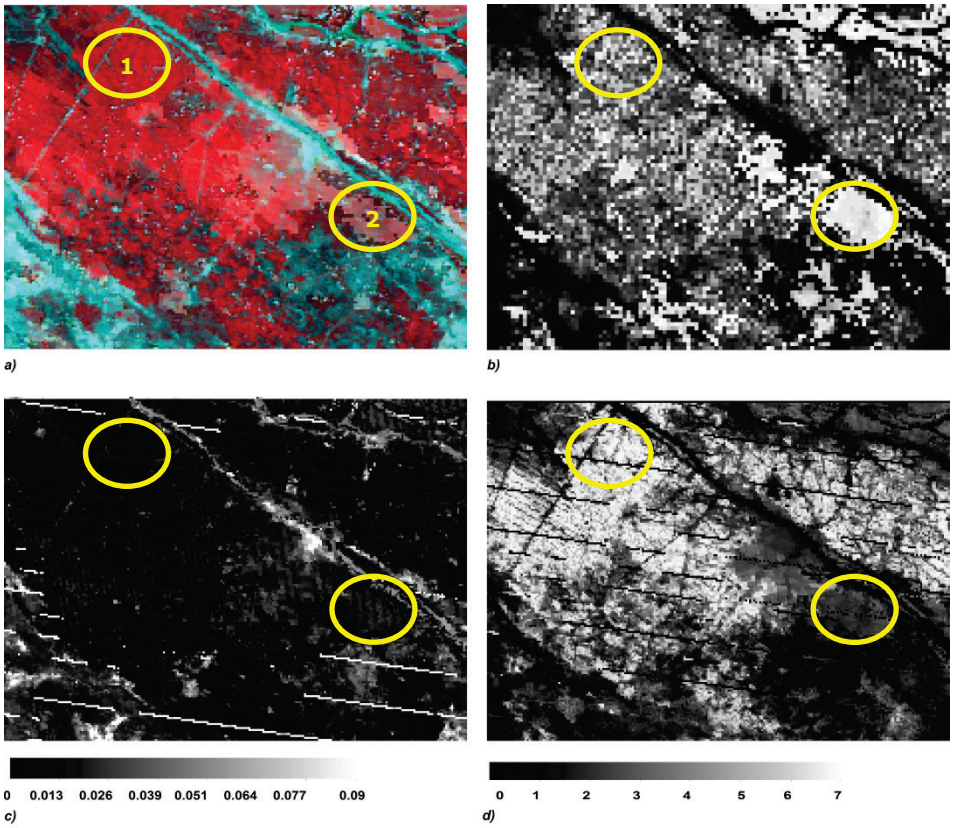

Figure 4.5: Comparison for 17 January 2009: (a) MOD09A1 false colour composite (RGB : bands 213); (b) MOD15A2 LAI; (c): simulated reflectance error (RMSE) of the SLC; (d) estimated rice LAI from SLC inversion. The stripes seen in (c) and (d) were probably caused by an inter-detector problem of MODIS band 5.

Many studies validated the MOD15A2 LAI product for different types of land cover with the emphasis on validation at a specific date and often targeted at large areas rather than on a pixel-based interest (Myneni et al., 2002; Privette et al., 2002; Tan et al., 2005). If the interest is pixel-based, the error in LAI retrieval from coarse spatial resolution data can exceed 50% (Chen et al., 2002), and hence LAI calibration based on field measurements has to be done before use (Cheng, 2008). Fig. 6b suggests that MOD15A2 LAI variability among a group of pixels is unacceptably high and thus, not a simple one pixel problem.

4.4.2 LAI estimation from LUT inversion

For each date of MODIS data, based on the RMSE evaluation, the best pixel-based solution was retrieved from the date-specific LUT, and the corresponding LAI values were extracted. The SLC simulated MODIS reflectance spectra on a pixel-by-pixel basis for the 60 rice locations have an RMSE range of 0.021 ± 0.02. Figure 4.6 shows the distribution of these RMSE grouped by DAS (days after sowing) for all surveyed sites. Relatively high RMSE values were observed in areas where the crop was either at its very early phonological stage (1-10 DAS) or at its late reproductive stage (70-80 DAS afterward). This indicates that the LAI estimation method should be used with care during the early and late crop growing stages.

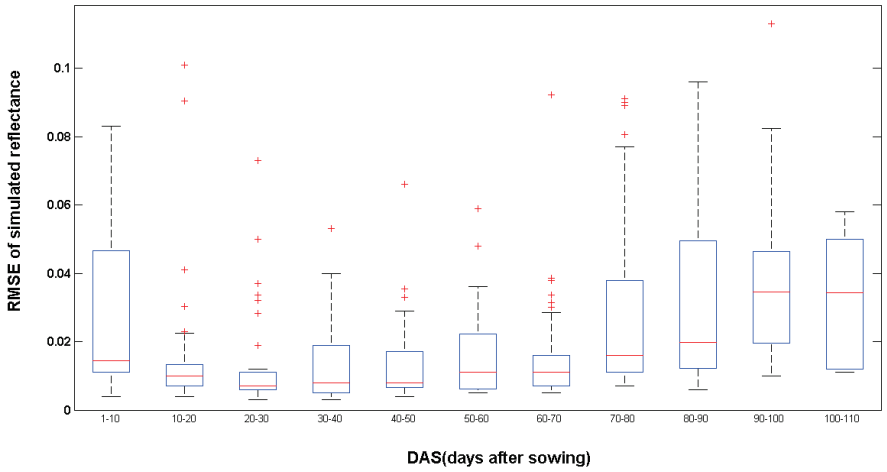

Figure 4.6: Boxplots of SLC simulated reflectance error (RMSE) for 60 surveyed sites

The highest reflectance errors around 0.12 to 0.21 were observed in non-rice areas, e.g. residential and fallow areas. This is because in the SLC simulation a water background reflectance was always considered. Thus it is important, and perhaps requires, to use the rice mask (see Figure 4.1) when using SLC to monitor rice crops. Similar error trends were found for bad-quality pixels of the MOD09A1 data that were earlier masked out (Figure 4.5 c); they were related to and appeared as stripes across the scenes.

Figure 4.7 is an example of all simulated MODIS reflectance spectra for January 17, 2009 as stored in the LUT. The points represent the actual MOD09A1 reflectance spectra of four different rice paddy pixels located in

different areas. The lines represent for these sites the simulated reflectance spectra retrieved from the SLC LUT after defining the best solution. Rice in Long My (red points) and Thoai Son (black points) was in its early tillering stage, resulting in low simulated reflectance values.

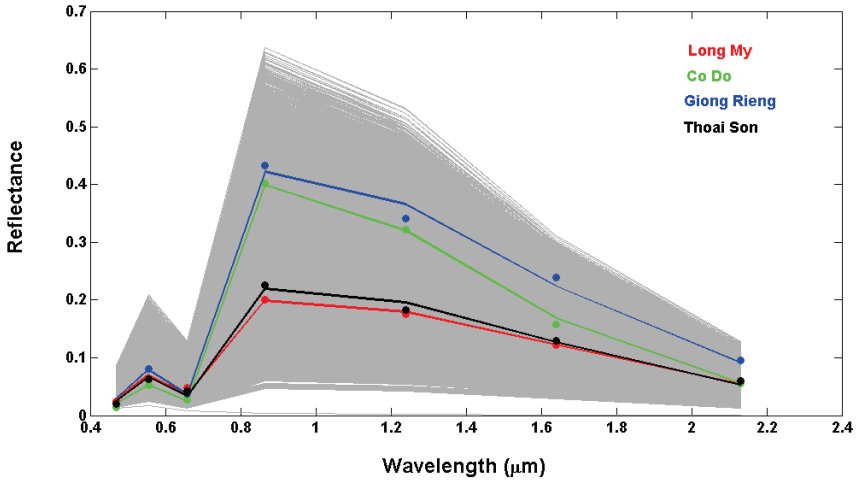

Figure 4.7: Set of 110,000 random MODIS equivalent synthesis spectra (grey lines) for LUT of January 17, 2009. The colour lines represent for 4 sites the best solution based on RMSE evaluation. The colour points show the actual MOD09A1 reflectance values for 4 rice paddy pixels located in Long My, Co Do, Giong Rieng and Thoai Son

Figure 4.5c and 4.5d show the January 17, 2009 SLC simulated MODIS reflectance error (RMSE) and the estimated LAI. The stripes seen across the studied site were caused by inter- detector gains' problem of MODIS band 5.

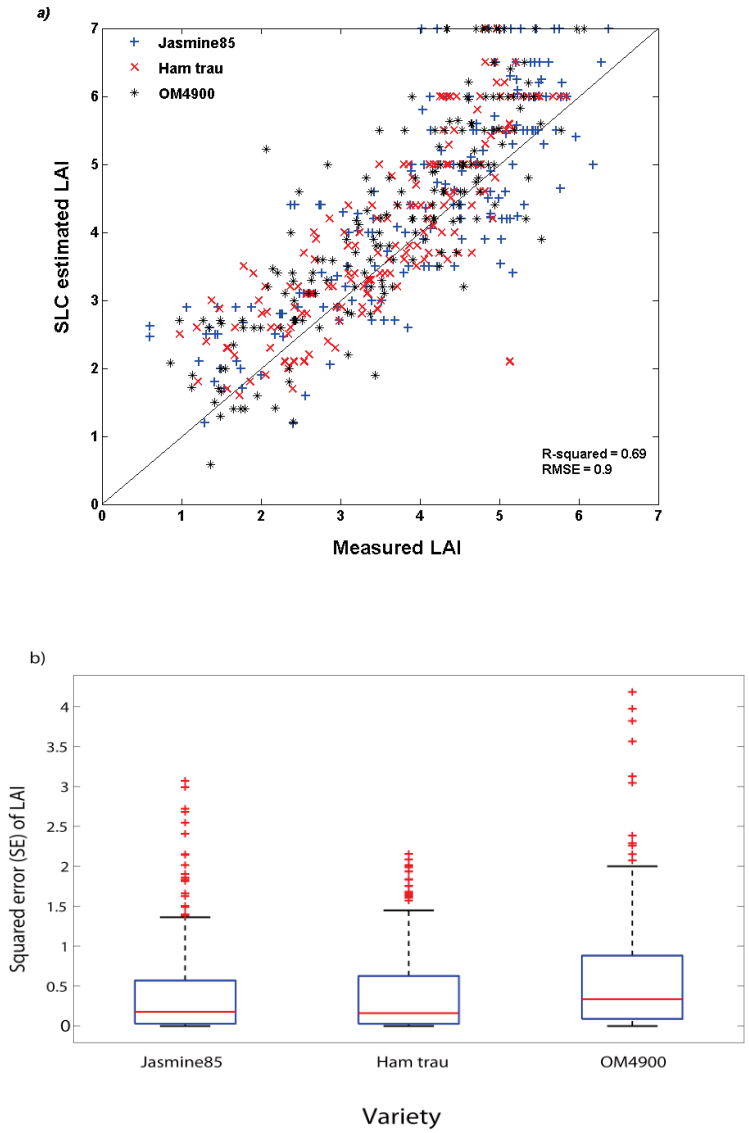

Figure 4.8: (a) Comparison between estimated LAI from the SLC inversion method and measured LAI; (b) Boxplot of squared error of LAI from December 18, 2008 to April 30, 2009 for 60 surveyed sites.

The correlation between the SLC inversion simulated LAI and the *in situ* LAI, grouped by variety (Figure 4.8a), is much better (R^2 = 0.69, RMSE = 0.9) than the one between MOD15A2 LAI and *in situ* LAI (Figure 4.4). The errors between estimated LAI and measured LAI are fairly randomly distributed on both sides of 1:1 line. However, for different varieties, the range of these errors was not the same (Figure 4.8b). Squared error of LAI for OM4900

variety was highest, followed by Ham trau and then Jasmine85. This might be due to the differences related to the site locations of cultivated varieties, which was not yet considered for the background information input used in SLC. While OM4900 was widely cultivated across the surveyed area, Jasmine85 and Ham trau were limited to the area around Can Tho city.

For LAI≥ 6, the agreement between measured and SLC estimated LAI values started to differ systematically, with higher values achieved through SLC. The reason could be, as found by He et al. (2007), the underestimates of true LAI by LAI-2000 due to saturation under high value of LAI (White et al., 1997; Wilhelm et al., 2000).

The mean difference between estimated LAI and MOD15A2 LAI for the whole growing season in this study is 1.4, which is less than what was reported by Cheng (2008) when comparing MOD15A2 LAI and *in situ* LAI at different phenological stages for hybrid rice. This is because hybrid rice has a different canopy structure with a higher effective LAI than the normal rice varieties cultivated in the Mekong delta.

The SLC estimates are at this point not yet considered the temporal dynamics of LAI over the cropping season as it has been used to interpolate *in situ* LAI by Equation 4.1. Such interpolation would compensate MODIS image to image quality variability and remove random errors in LAI estimates that do not relate to reality. Spatial knowledge on sowing dates is a prerequisite for such an improvement. The original map prepared in chapter 2 (Figure 2.4) does contain the required area specific information. Figure 4.9 shows great improvement of LAI estimated by SLC when seasonal LAI variation was taken into account.

Since SLC generated a date and pixel specific LAI estimation, the combination of input variables' values used to retrieve the best solution, automatically took care of spatial differences in LAI caused by differences in cultivated varieties, seasonal influences caused by too early or too late growing, and spatial variability in growing stages of the crops. The dataset of 60 sites contained ample variability concerning this real-life variability, and thus the SLC-based method was able to cope with that reality.

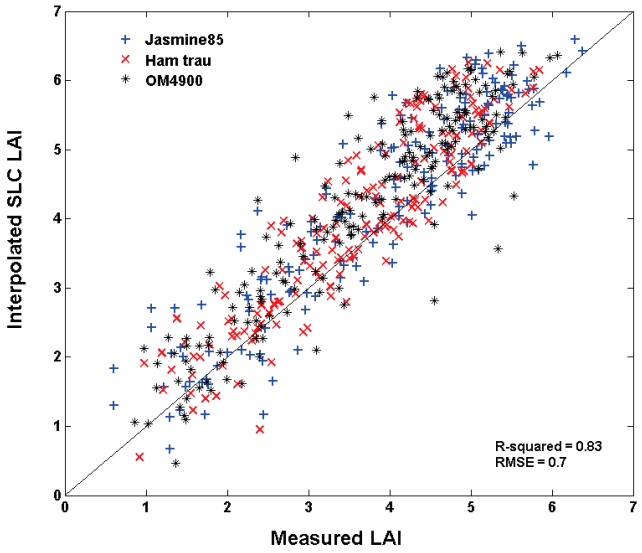

Figure 4.9: Comparison of *in situ* LAI and interpolated SLC LAI

Though SLC has significantly improved the estimation of LAI compared to MOD15A2 LAI, it still overestimated LAI. This may be due to the number of variables in SLC that can be inverted simultaneously during the inversion process. This problem has been addressed by Jacquemoud et al. (2000) when testing performances of different radiative transfer models. They suggested holding the leaf mesophyll parameter *N* at a constant value when inverting other model parameters. Another study on linking PROSPECT and SAILH to estimate the vegetation parameters C_w, C_m, *N* and LAI by Zarco-Tejada et al. (2003) used fixed values for C_{ab} during the inversion process. In our research, we only kept the PROSPECT parameters for brown leaves fixed whilst the others were allowed to vary during simulation runs. The fraction of brown leaf area was only estimated based on pictures taken on the same dates of the *in situ* LAI measurement. These could lead to a certain deviation of the SLC simulation and hence would affect the inversion results. Another issue that cannot be accommodated easily in SLC is the variation of leaf brown pigment during the end of rice flowering throughout the milking stages. This would lead to higher simulated reflectances in the visible spectral band (Verhoef and Bach, 2007).

The leaf chlorophyll content (C_{ab}) is an important parameter in SLC. In order to simulate MODIS reflectance spectra, scaling up of leaf C_{ab} measurement

values to MODIS spatial resolution of 500m needs to be handled and examined with care as this would later inherit in the simulation error. In our research, since field C_{ab} examination was carried out in several rice fields within fairly homogenous rice cropping patterns, and later was averaged before being used in SLC, this introduced error could be less severe.

The water background also plays a vital role in SLC modelling. For the irrigated rice cultivated across the Mekong delta, paddy water reflectance is anticipated to have a high variation. *In situ* measurement and calibration of the paddy water background reflectance, with the help of hyperspectral remote sensing, is expected to further improve the performance of SLC.

4.5 Conclusion

The study has demonstrated the benefit of using the model SLC for dynamic LAI estimation for irrigated rice in the Mekong delta, Vietnam. To our knowledge, this is the first study that uses SLC on temporal MODIS surface reflectance data (MOD09A1) to estimate seasonal variation of LAI for irrigated rice.

LAI estimated by inverting the SLC model was much more accurate than LAI provided by the MODIS product (MOD15A2). Look-up table inversion of the SLC model explained 69% of the variance of *in situ* LAI during the whole cropping season, with a RMSE of 0.9. A further improvement of SLC estimates was achieved when seasonal variation of rice LAI was taken into account (R^2 = 0.83, RMSE = 0.7).

The study also showed that MOD15A2 LAI has a very poor correlation with *in situ* LAI (R^2 = 0.07, RMSE = 2.1). MOD15A2 LAI often underestimated the true LAI. In order to be sufficiently useful for rice research, extensive validation and calibration have to be carried out.

As for estimating LAI by inverting SLC, further improvement can be achieved by constraining SLC input parameter values by rice variety and site specific. More paddy water reflectance samples should be added to the SLC. Further investigation of the other model input parameters (e.g. C_{ab}) would help constrain them well during the inversion process, and hence could yield better results for LAI estimates.

Acknowledgement

We sincerely thank all the farmers in Mekong delta, who kindly let us carry out the measurements in their rice paddies for such a long time. We thank J. Timmermans and Dr. C. van der Tol at ITC for providing the SLC code in MATLAB. We also thank J. Malik at ITC for valuable discussions. This work was funded by the Netherlands PhD Fellowship Program (NFP).

Chapter 5
Coupling remotely sensed LAI with a crop growth model for rice yield estimation[9]

[9] This chapter is based on: Nguyen Thi Thu Ha, de Bie, C.A.J.M., Smaling, E.M.A., & Verhoef, W. Coupling remotely sensed LAI-estimates with a modified ORYZA2000 crop growth model to estimate actual irrigated rice yields. *International Journal of Applied Earth Observation and Geoinformation.* **Submitted**

Abstract

The objective of this study was to develop and test a method to estimate actual rice yields under sub-optimal growth conditions for 0.5km^2 grids by using remotely sensed data and a Soil-Leaf-Canopy (SLC) Radiative Transfer Model (RTM), coupled with a modified version of the ORYZA 2000 Crop Growth Simulation Model (CGSM). The CGMS, set to simulate potential production, was forced to adjust its estimates using derived SLC results. Thus, growth characteristics of three rice varieties were calibrated and successively, for 58 sites in the Mekong delta, Vietnam, actual yields estimated to validate the procedure used. For that purpose series of field measurements were collected. Steps in sequence: firstly, using all 7 bands of MODIS 8-day surface reflectance data (MOD09A1), covering one crop growing season, by site, the development of the Leaf-Area-Index (LAI) was estimated using the SLC model's inversion technique; validation showed an R^2 of 0.83 and a RMSE of 0.7. Secondly, variety specific crop growth parameters were calibrated by site using the ORYZA2000 DRATE and PARAM sub-routines and by forcing the model with the earlier generated LAI-estimates. The studied varieties showed clear differences in their development rates, especially during their juvenile stages. Thirdly, the LAI values were re-used in ORYZA2000 through the forcing technique and the variety averages of the calibrated crop growth parameters. The dynamics in biomass of leaves, stems, and panicles of the 58 rice fields were accurately simulated, while, if forcing was not done, estimated biomass values were consistently over-estimated. The final grain yields estimated by ORYZA2000 using forcing LAI values and variety specific crop parameters were highly accurate (R^2=0.81; RSME= 970 kg/ha). The final average grain yield difference or overall yield-gap between forcing and non-forcing was 1727 kg/ha.

Achieved results demonstrate that forcing SLC estimated LAI into ORYZA2000 compensates for the common lack in required data and simulation routines to estimate yields under suboptimal conditions. Yield gaps result from sub-optimal rice management in combination with growth limiting and biomass reducing factors. The developed method proved able to overcome these issues and approach actual rice grain yields well, given that practiced cropping calendars and varieties sown are rather uniform across fields within the map units defined earlier through a map depicting rice cropping systems

in the Mekong area. Results hold promise for wider application of SLC models to estimate LAI from MOD09A1 and to force ORYZA2000 models to achieve cost-effective quantitative assessment of actual rice yields in the entire of the Mekong delta region and beyond.

5.1 Introduction

Use of Crop Growth Simulation Models (CGSMs) is common in agricultural research (Bouman and van Laar, 2006). Many studies that concern crop production as influenced by the environment require use of CGSMs (Maas, 1988b; Launay and Guerif, 2005; Adam et al., 2011; Li et al., 2011; Palosuo et al., 2011). The CGMSs are dynamic models and are able to simulate crop growth under different environment and management conditions and either estimate potential crop production situations that assume ample water and nutrients supply, or limited production due to water and/or nutrient deficits (Bouman et al., 1996). CGSMs are suitable to predict impacts of crop growth conditions on yields for large territories (Bouman et al., 1996; Launay and Guerif, 2005). However, their use for predicting actual yields at regional scale is complicated because of the common lack in spatial information on input variables, initial conditions, and model parameters (Guérif and Duke, 1998; Yuping et al., 2008). It is found that CGMSs lack the ability to model impacts of crop yield limiting and reducing factors since these impacts plus remedial crop management options aren't easy to include in CGMS models.

Optical remote sensing can provide extensive information on actual spatial and temporal crop characteristics. Use of remotely sensed (RS) data throughout a cropping season allows development of methods that adjust CGSM-estimates spatially and temporally (Delécolle et al., 1992; Batchelor et al., 2002). There are two possibilities to assimilate remotely sensed data in CGSMs (Delécolle et al., 1992; Moulin et al., 1998; Clevers et al., 2002; Dorigo et al., 2007). The first possibility is called forcing. In this approach a model state variable (e.g. Leaf Area Index or LAI) is replaced directly using RS estimates (Maas, 1988a; Casa et al., 2012). This approach requires ample RS datasets, preferably providing daily observations to match the interactive daily time-step of common CGSMs. The second possibility is called calibration. It uses RS data and/or actual field data that relate to CGSM estimates to adjust either model input parameters or initial conditions (i.e. sowing date). Calibration operates by minimizing the differences between actual and estimated data. A classic example of this approach was to adjust CGSM's state variable estimates through modifying used crop coefficients so that the modelled and remote sensing-inferred LAI reached agreement (Maas, 1988b). RS-LAI was derived through an established relationship between LAI and measured Normalized Difference Vegetation Index (NDVI).

The limitation of this method is that when sub-optimal conditions occur in a study area, crop coefficients are inappropriately adjusted. These coefficients must be calibrated to reflect potential and/or water-limited production situations. Subsequent monitoring with CGMSs then has the ability to reveal discrepancies between modelled estimates (potential or water-limited) versus actual field measurements. Use of the option to force these estimates downwards based on RS data, so that they properly reflect prevailing field situations, is then appropriate. Thus detected yield gaps can be caused by e.g. pests, soil limiting conditions, or suboptimal management like a too low plant density. A forcing RS-based method following calibration, is able to detect sub-optimal conditions, but without identification of underlying causes.

As stated, various authors suggested improving the RS-based assimilation approaches through coupling the CGSM with a Radiative Transfer Model (RTM) (Bouman, 1992; Guérif and Duke, 1998; Launay and Guerif, 2005; Migdall et al., 2009). The coupled method then either calibrates used CGSM input parameters or adjusts (forces) model state variable values downwards to provide the best agreement between RS-based measurements and CGSM estimates (Casa et al., 2012). The RTM can predict canopy reflectance based on CGMS-output (Verhoef, 1984) or estimates e.g. LAI from RS data for CGSM-input (Doraiswamy et al., 2003; Doraiswamy et al., 2004; Fang et al., 2011). The proposed 3-stage approach starts by making full use of all included wavelength bands of available RS-imagery, and is very suitable to capture spatially canopy LAI-variability throughout a cropping season. The only limitation of the coupling-method is the requirement of a high number of RS observations that are expected to match the CGMS daily estimates (Delécolle et al., 1992) in order to apply the successive forcing or calibration procedures. The successive stages concern calibration and finally crop yield estimation.

The aim of this study was to evaluate the use of RS-derived LAI in a CGSM to estimate irrigated rice yields through the coupled method of a soil-leaf-canopy (SLC) RTM and the ORYZA2000 CGSM, taking into account that rice field situations may be sub-optimal for rice growth and development. MODIS surface reflectance (MOD09A1) data and field crop measurements (including yields) were used in this study. We also compared yield estimates derived through the use of SLC simulated LAI values in ORYZA 2000 by means of forcing and non- forcing to derive site-specific yield-gap estimates. Rice field

measurements were conducted in 58 paddy fields located in the Mekong delta, Vietnam.

5.2 Materials and Methods

5.2.1 Data

5.2.1.1 Remote sensing data

MODIS (Moderate Resolution Imaging Spectroradiometer) surface reflectance data (MODIS Terra MOD09A1) were acquired from Dec 2008 to May 2009. The data covered a complete winter-spring rice cropping season in the studied area. MOD09A1 is the 8-day atmospherically corrected surface reflectance product. It contains the highest pixel-values of daily observations during an 8-day period subjected to zenith angle, absence of clouds or cloud shadow, and aerosol loading. MOD09A1 consists of 500m resolution data (0.25km^2 pixels) with 7 bands covering the spectral range 459 – 2155 nm.

5.2.1.2 Meteorological data

Daily meteorological data are needed as input for CGSMs. These data for the period Dec.'08 – May'09 were collected from five weather stations located in the survey area (Figure 1). Presented in Table 5.1 is a summary of total precipitation (mm), averaged minimum and maximum daily temperature (^{0}C), and averaged daily sunshine duration (h/d). The nearest meteorological station's data were used in the CGSM to simulate rice yield for each field plot.

Table 5.1: Meteorological data of the Mekong delta, Vietnam (1 Dec.'08 – 31 May'09)

Station (district)	Maximum daily T (^{0}C)	Minimum daily T (^{0}C)	Total P (mm)	Sunshine (h/d)
Soc Trang	31.2±2.1	23.5±2.2	728	6.5±3.1
Rach Gia (KienGiang)	30.6±2.0	24.2±2.1	626	7.3±2.7
Can Tho	31.4±2.3	23.8±1.9	375	7.1±2.8
Chau Doc (An Giang)	31.8±2.3	23.8±1.7	594	6.7±3.0
Bac Lieu	30.4±2.0	23.6±1.9	401	7.3±3.1

Ångström parameters were required to convert sunshine hours into radiation (required CGSM input). The Ångström parameters *a* and *b* as suggested by the Food and Agriculture Organization (FAO) for a humid tropical climatic zone being a_A: 0.29 and b_A: 0.45 were used (Frere and Popov, 1979).

5.2.1.3 Crop data

Of the 58 selected irrigated rice fields, every 7-10 days, selected crop parameters were measured during the Dec.'08 - May'09 fieldwork period. The 58 fields were all located in areas where either double or triple rice cropping systems were practiced. We recorded no significant pest and disease damages in these fields. The chosen rice varieties for crop model calibration were Jasmine85, Ham-Trau and OM4900. Measured parameters were LAI, leaf dry biomass, stem dry biomass, panicle and storage organ dry biomass, leaf nitrogen content, leaf chlorophyll content, and final grain yield at 18% moisture. All measurements were carried out for 10 to 12 plots of $1m^2$ along a diagonal transect through each rice field. These transect data were averaged to get date and field specific parameter values.

In situ LAI was measured using the LI-COR LAI 2000 Plant Canopy Analyzer. On-site measurements of leaf chlorophyll and nitrogen contents were made by portable Minolta SPAD-502. Leaf samples were also taken for laboratory analysis of nitrogen content and LAI. Leaf nitrogen content was measured by Kjeldahl's method. SPAD-502 readings were used to establish the correlations with leaf nitrogen and chlorophyll contents. Apart from harvesting grain from $1m^2$ plots, actual grain yields were also obtained from the farmers.

Crop management and phenological information on sowing date, flowering date, harvesting date, and fertilizers applications were also recorded through observation in the fields or collected through interviews from the farmers.

Crop management and phenological information on sowing date, flowering date, harvesting date, and fertilizers applications were also recorded through observation in the fields or collected through interviews from the farmers.

5.2.2 LAI estimation through soil-leaf-canopy RTM using MODIS reflectance data

The SLC model (Verhoef and Bach, 2007) is a coupled soil-leaf-canopy radiative transfer model. The model consists of three sub-models (Verhoef and Bach, 2007), which are (i) a modified Hapke soil BRDF (Bidirectional Reflectance Distribution Function) model, (ii) the PROSPECT leaf model, and (iii) the 4SAIL2 canopy RTM. In our research, SLC is employed to estimate rice LAI using 8-day MODIS reflectance data (MOD09A1). The 8-day LAI estimation was carried out through the SLC model inversion using the look-

up table (LUT) approach. SLC input parameter value ranges were selected based on actual field measurements and expert consultation. Details of the SLC input parameters are presented in Chapter 4 (see Table 4.3).

The LUT approach consists of two major steps: (i) the generation of the LUT itself, based on generating all possible combinations for the specific value-series of the respective model parameters (Table 4.3); and (ii) applying the LUT to select the optimum solutions for a given date and field to obtain the corresponding LAI values. Selection of the optimal LUT inversion solutions were made through the evaluation of the root mean square error (*RMSE*) that measures the mean difference between the model reflectance estimates and the reference reflectance data (MOD09A1) (see Equation 4.2).

Estimated LAI values from the SLC model were then interpolated and smoothed to meet the seasonal evolution of rice LAI by using an equation provided in Koetz et al. (2005) (see Equation 4.1).

5.2.3 Yield estimation using ORYZA2000 crop model

ORYZA 2000 is the product of the "School of de Wit" modelling for rice yield estimation (Bouman et al., 1996; van Ittersum et al., 2003). It calculates the daily biomass production of rice from emergence to harvest, based on gross CO_2 assimilation estimates. Biomass partitioning to the different organs varies as a function of the phenological age of the plant. ORYZA2000 simulates rice yield for potential, water limited, and nitrogen limited situations (Bouman et al., 2001). An assumption made for ORYZA2000 is that rice crop is well protected against pests, diseases, and weeds, meaning that no reduction in yield due to these effects takes place (Bouman et al., 2001; Bouman and van Laar, 2006). The model is programmed to run in the FORTRAN Simulation Environment (FSE).

To simulate yields for all surveyed rice fields, calibration of crop parameters was required since the cultivated high-yielding rice varieties in the Mekong delta were not the same as the reference varieties of the standard ORYZA2000 model. For such situations Bouman et al. (2001) suggested that the IR72.DAT file must be used to calibrate by variety the following parameters: *development rates, partitioning factors, relative leaf growth rate, specific leaf area, leaf death rate,* and *fraction of stem reserves*. Calibration of *development rates* at four crop growth stages was done

through the use of the two sub-programs DRATES and PARAM that require field observations on rice phenology; for the remaining parameters the default IR72-values were kept. In DRATES and PARAM programs, the following site-specific field observations were used: date of sowing, date of panicle initiation, date of flowering, and date of physiological maturity, plus the variety-specific parameters: green leaf weight, dead leaf weight, stem weight, panicle weight and leaf nitrogen content, which were averaged from lab measurements.

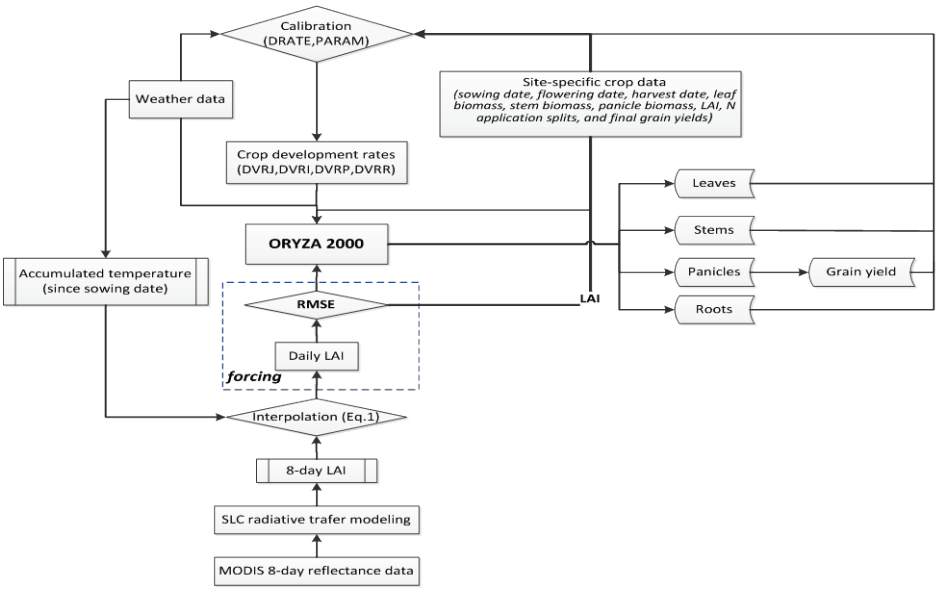

Figure 5.1: Coupling of SLC into ORYZA2000 for rice yield estimation through the use of SLC estimated LAI values

Yield estimation through ORYZA2000 model was carried out using the SLC-estimated LAI forcing and non-forcing procedures. Their difference in yield estimates quantifies the field-specific yield gap incurred. Since in general, the total amount of nitrogen fertilizer application per crop was higher than what was recommended (124 kg N/ha), N limitations were neglected, and only the potential simulation routines of ORYZA2000 were used. The ORYZA2000 simulation results from the two procedures were compared based on an assessment of the seasonal development of estimated biomass of rice leaves, stems, and panicles. In the first procedure (forcing), sub-optimal rice yields were estimated, assuming that daily interpolated remote sensing–based LAI (Equation 4.1), reflected any effects of the sub-optimal environmental conditions on rice growth and development. In the second procedure (non-

forcing), the estimated biomass of leaves, stems, and panicles, and yields were assumed under optimal growing conditions. The adapted rice yields estimation method is presented in Figure 5.1.

5.3 Results and Discussion

5.3.1 Rice LAI estimation by SLC model

For each 8-day MODIS reflectance dataset, based on the RMSE evaluation, the best pixel-based solution was retrieved from the date-specific LUT, and the corresponding LAI values extracted. The correlation between the daily interpolated SLC LAI and the *in situ* LAI, as seen in Figure 4.9, is relatively high (R^2 =0.83, RMSE=0.7). However, SLC estimated LAI values were slightly overestimated. This may be due to the number of variables in SLC that can be inverted simultaneously during the inversion process. Recent study suggested that holding some parameters, such as leaf mesophyll and leaf chlorophyll content, at constant values during the inversion process could improve LAI (Jacquemoud et al., 2000; Zarco-Tejada et al., 2003). In our research, we only kept the PROSPECT parameters for brown leaves fixed whilst the others were allowed to vary. The fraction of brown leaf area was only estimated based on pictures taken on the same dates of the *in situ* LAI measurement. These could lead to a certain deviation of the SLC simulation and hence would affect the inversion results. Another issue that cannot be accommodated easily in SLC is the variation of leaf brown pigment during the end of rice flowering throughout the milk stages. This would lead to higher simulated reflectance values in the visible spectral band (Verhoef and Bach, 2007).

For different rice variety, the agreement between SLC simulated LAI and *in situ* LAI was not the same (Figure 4.8b). The most accurate LAI estimation was found for Jasmine 85, followed by Ham-Trau and then OM 4900. This could be explained by the differences of the background reflectance that related to the site locations of cultivated varieties, which was not yet taken into account in SLC model.

5.3.2 Assimilation of SLC LAI into ORYZA200 model and rice yield estimation

For all varieties, the calibrated rice parameters (development rates) were found different in the development rates at juvenile phase (DVRJ) and the development rate at reproductive phase (DVRR) (Figure 5.2).

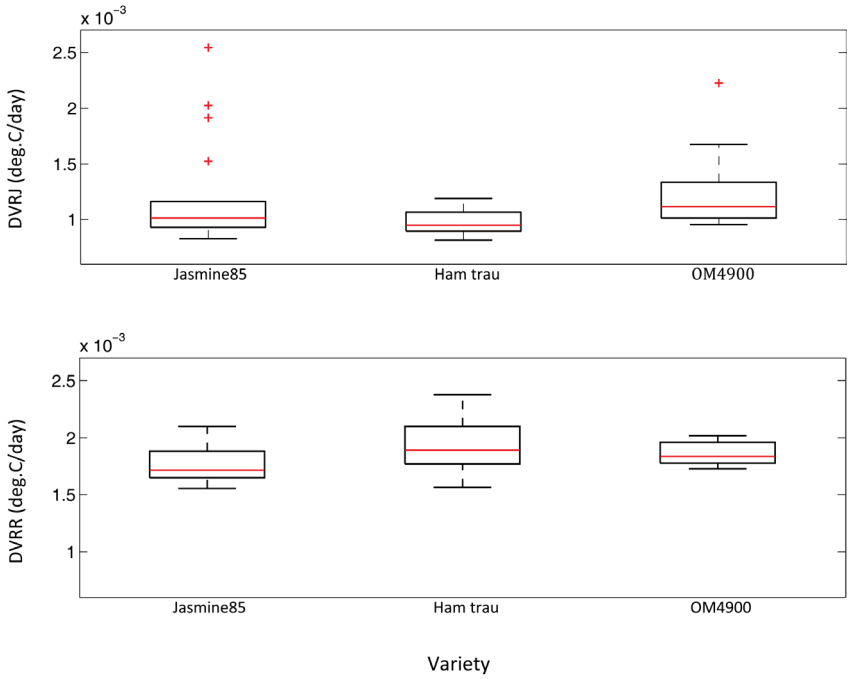

Figure 5.2: Variation of the calibrated development rate in juvenile phase (DVRJ), and development rate in reproductive phase (DVRR) for the cultivated rice varieties

The DVRJ of the studied varieties were higher compared to that of IR72, which was the model-built variety. Since the variation in temperature and irradiance in both sites were not quite different from each other, this can be explained that the cultivated IR72 at IRRI site had longer growing season (130 days) than the ones in the Mekong delta (around 90-100 days). Other factor contributing to this difference was the difference in sowing method. While IR72 was transplanted, the others were direct-seeded.

The slight difference in the development rate at reproductive phase (DVRR) of these four varieties was generally due to their growing season lengths. The

development rate in photoperiod-sensitive phase (DVRI) and development rate in panicle development (DVRP) of all four varieties were almost the same because they were genetically close to each other. For the three cultivated varieties these two parameters were found no change in all cases (Table 5.2).

Table 5.2: Calibrated ORYZA2000 parameters (means) for three varieties

Crop parameters(*) (x 10^3)	Crop growth phase	Variety			
		Jasmine 85	Ham-Trau	OM4900	IR72 (*mode*l)
DVRJ (^{0}C/day)	Juvenile	1.203	0.967	1.224	0.773
DVRI (^{0}C/day)	Photosensitive	0.758	0.758	0.758	0.758
DVRP (^{0}C/day)	Panicle dev.	0.795	0.795	0.795	0.784
DVRR (^{0}C/day)	Reproductive	1.771	1.983	1.875	1.784

(*) Parameters were averaged, with: DVRJ, development rate in juvenile phase; DVRI, development rate in photoperiod-sensitive phase; DVRP, development rate in panicle development; DVRR, development rate in reproductive phase

A first comparison of ORYZA 2000 simulation results using different approaches are shown in Figure 5.3. Grain yields simulated by using non-forcing approach were significantly higher than the others simulated using forcing approach. The largest yield gap was found in Ham-Trau (2212kg/ha), followed by Jasmine85 (1591kg/ha), and OM4900 (1366kg/ha). In average, the yield gap for all varieties was 1727 kg/ha.

Table 5.3: ORYZA simulation of grain yield using forcing for 58 sites

Variety	N	Y_{ob}	$Y_{ORYZA2000}$	α	β	R^2	RMSE
Jasmine85	18	6327 ± 350	7310 ± 480	1718	0.63	0.80	1009
Ham-Trau	20	5506 ± 811	6376 ± 801	94	0.85	0.70	983
OM4900	20	6124 ± 574	7016 ± 619	52	0.87	0.87	919
All	58	5947 ± 711	6886 ± 766	203	0.84	0.81	970

N=number of observations; Y_{ob}=mean of observed yield (kg/ha); $Y_{ORYZA2000}$=mean of ORYZA2000 simulated yield (kg/ha); α=intercept of linear relation between simulated and observed yield; β=slope of linear relation between simulated and observed yields.

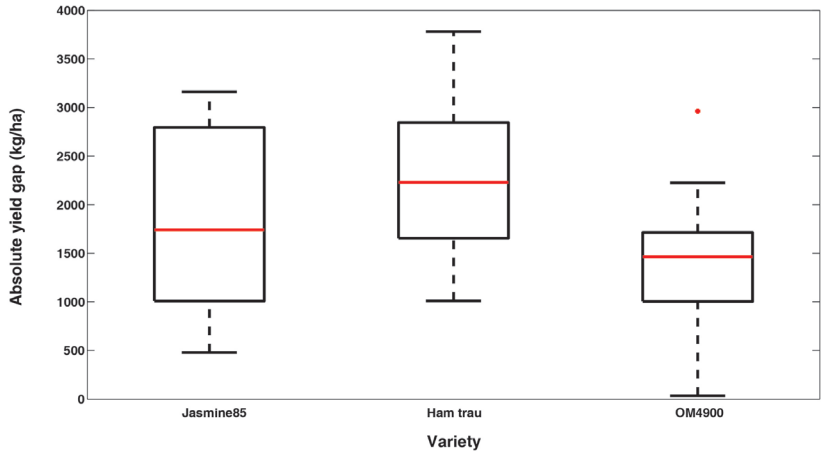

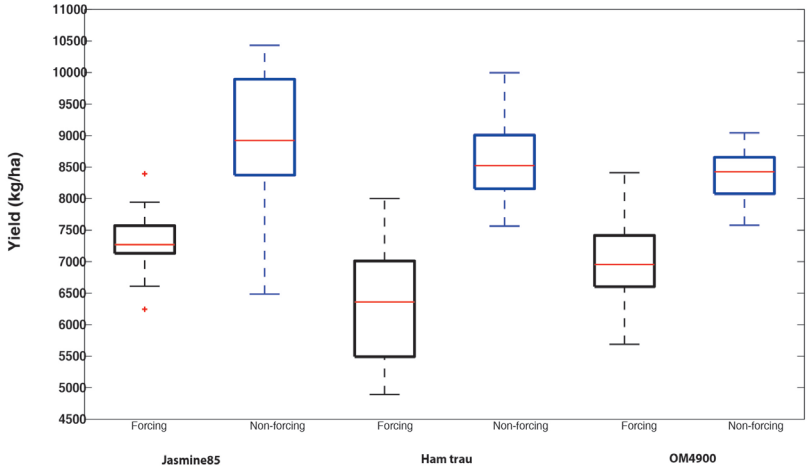

Figure 5.3: Comparison of simulated grain yield of the cultivated varieties using forcing and non-forcing SLC-LAI approaches

With forcing LAI approach, overall, for all 58 rice fields, ORYZA2000 simulation can explain for 81% variation in grain yields of all sites. However, in average, ORYZA2000 overestimated grain yields at approximately 970kg/ha (RMSE). Despite LAI estimated from SLC for Jasmine 85 was the most accurate among the three varieties, simulated Jasmine 85 yield was not as accurate as OM4900 yield (Table 5.3). This shows that rather than LAI, other ORYZA2000 crop parameters and variables might impose greatly on the

simulation results. Therefore, it was difficult to specify factors that caused the yield gap.

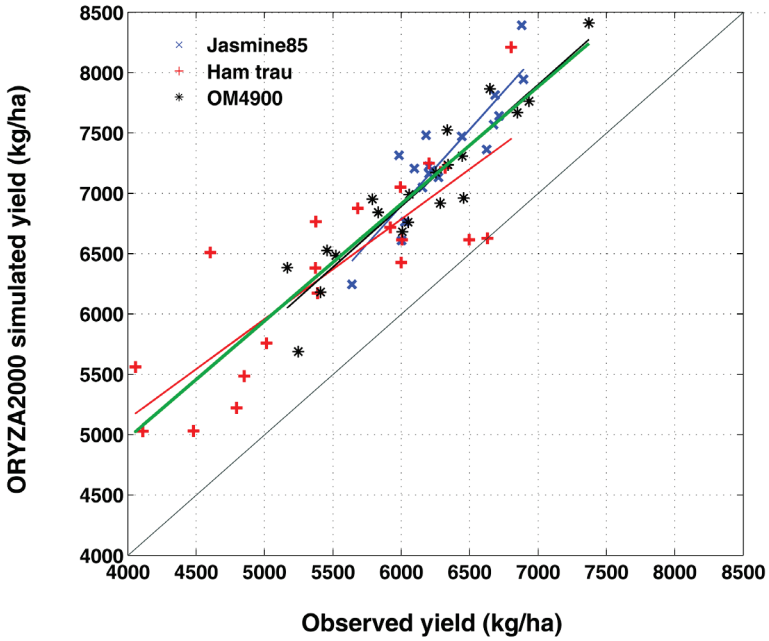

Figure 5.4: ORYZA2000 simulated rice yield vs. observed yield

The less accurate in simulating gain yields for Ham-Trau was partly due to a large variation of the observed yields. This suggests that field management, such as the management of fertilizer application, soil properties, etc., may play an important role. ORYZA2000 would yield a better simulation result if these data could be incorporated and supplied in the model. As for the Jasimine85 and OM4900, the observed and simulated grain yields were well above 6000 kg/ha with less variation (Figure 5.4). These were the high yielding varieties that often required a higher investment, and were normally cultivated in extensively rice producing areas where farmers were well-off and very experienced in skills.

5.4 Conclusion

The study has demonstrated the benefit of using the SLC model for dynamic LAI estimation for irrigated rice in the Mekong delta, Vietnam. LAI estimated by inverting the SLC model through Look-up table explained 69% of the

variance of *in situ* LAI during the whole rice cropping season. A further improvement of SLC estimates was achieved when seasonal variation of rice LAI was taken into account (R^2=0.83, RMSE=0.7). This improvement allowed to compensate MODIS image to image quality variability and to remove noises in LAI estimates.

To further improve the SLC performance in estimating LAI in the future study, two important parameters and information should be taken into account, the leaf chlorophyll content and the water background reflectance. In order to simulate as best as possible the MODIS reflectance spectra, scaling up of leaf chlorophyll content measures to MODIS spatial resolution of 500m needs to be handled and examined with care as this would inherit simulation error. In our research, since field measurement of leaf chlorophyll content was carried out in several rice fields within fairly homogenous rice cropping patterns, and was averaged before being used in SLC, this introduced error could be minor. The water background information also plays a vital role in SLC modelling, and needs to be considered too. For the irrigated rice cultivated across the Mekong delta, paddy water reflectance is anticipated to have a high variation. *In situ* measurement and calibration of the paddy water background reflectance, for example with the help of hyperspectral remote sensing, is expected to reduce SLC simulation error.

LAI estimation using SLC can be achieved better by constraining SLC input parameter values by rice variety. More paddy water reflectance samples should be added to the SLC. Further investigation of the other model input parameters (e.g. C_{ab}) would help constrain them well during the inversion process, and hence could yield better results for LAI estimates.

Forcing SLC estimated LAI from MODIS surface reflectance data in ORYZA2000 has showed its great potential in simulating rice yield under sub-optimum conditions, especially when data on nutrient balance and soil characteristic were not available. The use of forcing SLC estimated LAI allowed to re-initialize ORYZA2000 state variables and recalibrate rice crop parameters, which helped ORYZA2000 being able to explain for about 81% variation of rice yield across the Mekong delta. This use allowed to reducing the large yield gaps produced by assuming that rice grew under optimal conditions (non-forcing approach).

For regional application, this approach would work well if the most important information on cultivated rice varieties, rice cropping calendar and rice cropping patterns are well described. Since rice cultivation in Mekong is synchronized at the commune level, if there is any produced map that provides similarity as the map showed in Figure 1, the first advantage of the method can be established. This helps to set up the initial conditions to run the model. Re-initialize state variables (i.e. development stage, LAI, weight of leaves, weight of stems, etc.) will be followed, depends on the availability of remote sensed data and the environmental conditions where rice is grown. The degree of success of the method later lies in the estimation of LAI from SLC. Detailed information on rice biophysical parameter domain will have to be acquired to feed into the SLC model in order to achieve the most accurate LAI estimation. Once the acquisition of these parameters is done, standardizing them would help to build an extensive rice data library for use in SLC. Since at the regional scale, information on rice nutrient balance and soil condition are rarely available forcing SLC estimated LAI from MODIS data to re-initialize ORYZA2000 state variable LAI becomes very helpful and less time consumed.

Acknowledgement

We thank all the farmers who allowed us conducting our field measurement for a complete rice cropping season. Without their generosity this research would have never been succeeded. We also thank to the Cuu Long Delta Rice Research Institute (CLRRI) for their help in analyzing the rice samples, and great supports during our fieldwork. We thank to Willem Nieuwenhuis at ITC for his help in creating a batch file to run the model; and this really saved our time. This work was funded by the Netherlands Fellowship Programs (NFP).

Chapter 6
General Discussion: Earth observation for rice heterogeneity mapping and yield estimation

This thesis addresses the need of earth observation data for a large-scaled monitor of rice crops in the Mekong delta, Vietnam. A large set of remotely sensed data obtained from SPOT Vegetation (VGT) and MODIS Terra satellites in support of ground measurements were used in this research. Divergence statistics was applied to improve the unsupervised classification technique on the SPOT Normalized Difference Vegetation Index (NDVI) time-series imagery to map rice cropping patterns across the region. The method was further developed and expanded to map the landscape heterogeneity of the delta using both SPOT and MODIS NDVI images. Also, a radiative transfer model (RTM) was employed in monitoring and mapping the seasonal variation of leaf-area-index (LAI) for irrigated rice using an 8-day MODIS dataset. These LAI values were further used as inputs of a crop growth simulation model (CGSM) to estimate the final grain yields for the commonest rice varieties cultivated in the delta.

6.1 Hyper-temporal SPOT VGT NDVI for rice cropping pattern mapping

Time series data of NDVI have proven useful for LCLU studies thanks to their high temporal coverage and easy availability (Xin et al., 2002; Wang and Tenhunen, 2004; Xiao et al., 2005; Jiang et al., 2008). NDVI composites derived from optical remote sensors have been shown to be capable of differentiating spatial variability in vegetation productivity and greenness over time (Galford et al., 2008; Wardlow and Egbert, 2008). The use of hyper-temporal NDVI composites to map irrigated rice areas has been studied for years (Xiao et al., 2002a; Kamthonkiat et al., 2005; Xiao et al., 2005; Sakamoto et al., 2006; Xiao et al., 2006; Sakamoto et al., 2009a; Sakamoto et al., 2009b). However, since these studies majorly aimed at distinguishing rice crop from others, their methods were not been able to detect and describe all major temporal and spatial details of practiced rice cropping patterns. In this study, our specific aim was to develop a method that could differentiate and describe the spatial and temporal patterns of rice grown in the season of 2008-2009 in the Mekong delta using hyper-temporal SPOT VGT NDVI data. Our method was developed based on the ISODATA clustering routine with an additional employment of divergence statistics to evaluate the NDVI signature separabilities.

A total of 77 NDVI classes was found in the Mekong delta. With prior knowledge on the region, out of these 77 classes, 26 classes presenting rice crops were selected to design the sampling scheme for fieldwork and for rice cropping calendar characterisation. The produced map provides highly accurate information on the regional rice cropping patterns (94% overall accuracy, 0.93 Kappa coefficient). The study found that the spatial distributions of the triple and the double rice cropping systems were strongly related to the flooding regime, and the duration of flooding is highly correlated with the decision by farmers to cultivate shorter or longer duration rice varieties. The overall spatial variability of rice cropping patterns mostly coincided with administrative units, which indicated that cropping pattern choices and water control were much homogeneous within each unit. Water supply risks, soil acidity and salinity constraints, and the anticipated highly fluctuating rice market prices all strongly influenced specific farmers' choices of rice varieties. These choices vary considerably annually, and therefore grown rice varieties are difficult to map.

6.2 A comparison of SPOT VGT and MODIS Terra NDVI data for mapping agroecological heterogeneity at landscape level

Global and regional ecosystem patterns have long been recognized by biologists and ecologists (Lieth and Whittaker, 1975; Box, 1978). More recently, as scientists started monitoring of *e.g.* the global carbon cycle, and attempted to quantify sinks and sources, mapping for the modelling of these patterns has become a matter of some urgency (Turner et al., 2001). Consequently, there is a demand for more information on ecosystem vegetation patterning in space and time which presents landscape heterogeneity and gradients at various strengths of ecotones and ecoclines. This study proposes a new method to map and depict ecotones and ecocline of land cover heterogeneity using hyper-temporal remote-sensing data. The method, named LaHMa, is data-driven, unbiased, and builds on ISODATA clustering through the use of divergence separability indices.

The method was applied to 10-year NDVI-imagery time series acquired by the SPOT VGT and MODIS Terra sensors for the Mekong delta, Vietnam. Firstly, the relevant spatial-temporal variation in NDVI captured through ISODATA clustering was evaluated. Secondly, series of prepared cluster maps

were overlaid to examine and detect the frequency of spatial boundaries between clusters occur at the same location. This step defines the boundary strength between clusters and maps the spatial heterogeneity within them.

The landscape heterogeneity maps, derived from two sensors' datasets for the Mekong delta, revealed the effects of various spatial resolutions. Larger homogenous patches are evident in the SPOT VGT derived map. In contrast, a higher frequency of boundaries is observed in the MODIS Terra derived map. This indicates that the 1km resolution SPOTVGT data allows interpretation of the landscape land cover differences due to its spatial generalization, while 250m MODIS Terra data don't. Further study could investigate if the aggregated 250m or available 16-day 1km MODIS Terra product would be suitable to depict landscape heterogeneity.

6.3 Seasonal LAI estimation for irrigated rice by inversion of radiative transfer model

Radiative transfer models have been rarely applied to irrigated rice cropping systems (Jiang et al., 2010). A common approach for estimating rice LAI from optical remote sensing is based on established empirical relationships between LAI and vegetation index (VI) (Shibayama and Akiyama, 1989; Casanova et al., 1998; Xiao et al., 2002b; Wang et al., 2007; Kushida and Yoshino, 2010). Thus a potential of radiative transfer modelling to estimate LAI in a heterogeneous rice cropping system in the Mekong delta was investigated. To estimate seasonal LAIs for irrigated rice the coupled soil-leaf-canopy radiative transfer model (SLC) was inverted with MODIS Terra (MOD09A1) reflectance measurements by means of a look-up table (LUT) technique. We also tested how the readily available MODIS LAI product (MOD15A2) performs in comparison.

The study has found that in extensively rice cultivated areas like the Mekong delta, the available MODIS LAI product MOD15A2 failed to detect rice LAI evolution with time (R^2 =0.07, RMSE = 2.1). The SLC model inversion, in contrast, proved very promising to estimate the seasonal dynamic of LAI for rice. LUT inversion of the SLC model explained 69% of the variance of *in situ* LAI during the whole cropping season, with a RMSE of 0.9. However, for different rice varieties, the range of these errors was not the same due to the differences related to the site locations of cultivated varieties, which was not yet considered for the background information input used in SLC.

A further improvement of SLC estimates was achieved when seasonal trends of rice LAI were taken into account (R^2 = 0.83, RMSE = 0.7). Spatial knowledge of sowing dates is a prerequisite for this improvement. The original rice cropping pattern map (section 1) contains such required area specific information.

Though SLC significantly improved the estimation of LAI compared to MOD15A2 LAI, it still overestimated LAI due to the number of variables in SLC that can be inverted simultaneously during the inversion process. Suggestions are to hold the leaf mesophyll parameter *N* at a constant value when inverting other model parameters(Jacquemoud et al., 2000), or to use fixed values for C_{ab} during the inversion process(Zarco-Tejada et al., 2003).

Water background also plays a vital role in SLC modelling. For the irrigated rice cultivated across the Mekong delta, paddy water reflectance is anticipated to have a high variation. *In situ* measurement and calibration of the paddy water background reflectance, possibly with the help of hyperspectral remote sensing, is expected to further improve the performance of SLC, especially when rice is at its early growing stages and its canopy hasn't fully covered the background.

6.4 Forcing remotely sensed LAI into ORYZA2000 crop growth simulation model for rice yield estimation

Crop growth simulation models (CGSMs) are widely used in agricultural research for crop production estimation (Bouman and van Laar, 2006). They are dynamic models that can simulate crop growth under different environmental and management conditions. Assimilation of remote sensing into CGSMs promises to be a method to predict impacts of crop growth conditions on yields for large territories at low costs (Bouman et al., 1996; Launay and Guerif, 2005). In this study, two assimilation approaches of forcing and un-forcing seasonal LAI estimates from the SLC radiative transfer model (section 3) to ORYZA2000 CGSM to predict rice yields were both investigated.

To simulate yields of all surveyed rice fields, calibration of crop parameters in ORYZA2000 was required since cultivated high-yielding rice varieties in the Mekong delta were not the same as the model standard varieties. Using field

observations of rice crop phenology, the calibration was done for the following model parameters *development rates, partitioning factors, relative leaf growth rate, specific leaf area, leaf death rate,* and *fraction of stem reserves.*

Calibration of ORYZA2000 crop parameters for the three studied varieties showed the differences between them in development rate during the juvenile. Under sub-optimal conditions, rice yield estimates by ORYZA2000 using forcing LAI values and variety specific crop parameters assumed to reflect potential production can explain 81% variation of observed yields (R^2 = 0.81). The average difference of estimated yields between forcing and non-forcing LAI approaches was 1727 kg/ha with higher yield estimates for non-forcing. There were also significant differences in estimated yields using forcing LAI values in ORYZA2000 among three studied varieties. The less accurate in simulated gain yields for Ham trau was partly due to a large variation of the observed yields, which suggests that field management, such as fertilizer application in association with soil properties, water supply, etc., may play important roles in ORYZA2000. The model would yield a better simulation result if these data could be incorporated and supplied, instead of using the built-in model parameters. For Jasimine85 and OM4900, the simulated grain yields were well above 6000 kg/ha with more accurate and less variation compare to those of Ham trau because they were normally cultivated in extensively rice producing areas where farmers were well-off and very experienced in skills, and thus field management was anticipated not so many differences.

6.5 Conclusions

This study demonstrates the capability of earth observation to provide useful information for monitoring, better understanding, and mapping irrigated rice cropping systems and their production at landscape level. With the methods and techniques developed for hyper-temporal SPOT VEGETATION and MODIS TERRA data to investigate four successive aspects, the study is able to draw the following conclusions:

1. Hyper-temporal SPOT VEGETATION NDVI imagery and the ISODATA clustering algorithm allowed the capturing of relevant rice cropping differences in the Mekong delta, Vietnam. The choice made on the number of classes present in the NDVI data set through the use of the

divergence index is a new improvement compared to the techniques that had been used in previous studies. Despite the cloudy conditions of the Mekong delta, sufficient valid information retrieved from 10 years of decadal SPOT data with divergence statistics had overcome this problem, and proved being suitable to map irrigated rice cropping patterns. This method can be further applied and expanded to monitor and map cropping patterns of not only rice but also other annual crops that are cultivated and dominate in any farming systems around the world.

2. The new "LaHMa" method is straightforward and relatively easy to implement. The maps produced concern both the spatial and temporal dimensions of land cover variability. These landscape heterogeneity maps can be considered as useful tools for landscape analysts, essentially visualizing the complexity of the landscape heterogeneity. They indicate the homogeneity of each delineated map unit, and can be served to guide subsequent studies and sampling of the derived zones. Because the LaHMA method was built on hyper-temporal RS data, it provides ecologists possibly the best cost-effective method in identifying and delineating ecotones and ecoclines, two important structures in landscape ecology. When applying LahMa, it should be noted that, depending of the scale of the spatial resolution of the RS data, the scale of detail of landscape heterogeneity can vary. Analysts should thus be mindful that the use of higher spatial resolution data will generate more detail on local land cover variability and the influence of scale on the level of that detail must be carefully considered.
3. In extensively rice cultivated areas of the Mekong delta, while the available MODIS LAI product MOD15A2 failed to detect rice LAI evolution with time (R^2 =0.07, RMSE = 2.1), inversion of SLC RTM on temporal MODIS surface reflectance data (MOD09A1) proved a promising method. This is the first study that uses SLC on MOD09A1 to estimate seasonal variation of LAI for irrigated rice. LAI estimated by inverting the SLC model was much more accurate than the LAI provided by the MOD15A2 product. Look-up table inversion of the SLC model explained 69% of the variance of *in situ* LAI during the whole cropping season, with a RMSE of 0.9. When seasonal variation of rice LAI was taken into account, a further improvement of LAI estimates from SLC was achieved (R^2 = 0.83, RMSE = 0.7).
4. Forcing SLC estimated LAI into modified ORYZA2000 CGSM compensates for the common lack in required data and simulation routines to estimate

yields under suboptimal conditions. Yield gaps result from sub-optimal rice management in combination with growth limiting and biomass reducing factors. The developed method proved able to overcome these issues and approach actual rice grain yields well (R^2=0.81), given that practiced cropping calendars and varieties sown are rather uniform across fields within the map units defined earlier through a map depicting rice cropping systems in the Mekong area. Results hold promise for wider application of SLC models to estimate LAI from MOD09A1 and to force ORYZA2000 models to achieve cost-effective quantitative assessment of actual rice yields in the entire of the Mekong delta region and beyond.

6.6 Recommendations: future research and development

The study presented in this thesis offers ample scopes for future research. The current methods and techniques may be applied to whole lower Mekong river basin and other rice growing regions to assess their capabilities in monitoring rice growth and production under different effects of diverse environmental and field management conditions. Same methods and techniques can be further evaluated on other optical RS data.

This study illustrates some possibilities of combining the ISODATA clustering algorithm with divergence statistics for hyper-temporal remote sensing to detect temporal change of rice cropping patterns and to develop the LaHMa method to delineate agroecosystem boundaries (ecotones and ecoclines). In practical operation, apart from expanding at larger scale for a landscape dominated by intensive human activity like the one in the Mekong delta, these new method and technique should be further explored in the context of both semi-natural and natural landscapes, appraising the applicability of using either coarse or fine spatial resolution imagery in such situations. The success of this method will very much rely on the growing stage and the greenness characteristics of the dominated vegetative coverage across a landscape.

Inverting the SLC radiative transfer model with coarse spatial resolution RS data, such as MODIS TERRA, for seasonal estimates of rice LAI at larger scale could be further improved by constraining SLC input parameter values by rice variety and site characteristics. More paddy water reflectance samples, with the help of hyperspectral measurements, should be added to the SLC library

so that SLC simulation will take into account the true effect of a standing water background on retrieving canopy reflectance and LAI. It would be also interesting to investigate the effects at large scale of water and nutrient shortages, pest and disease damages on rice LAI values estimated from SLC. Future study can further investigate the use of SLC on different optical RS data or/and for different crops.

For regional applications, the integration of SLC through estimated LAI into ORYZA2000 crop growth simulation modelling should be further investigated on aspects of rice variety, soil conditions, and management factors (i.e. irrigation control, fertilizer application, etc.) at larger scales. Aggregating required data for sites that share similarly characteristics on rice cultivated variety and environmental and management conditions would be an effective way to generate a regional map of rice production. This helps to set up the initial conditions to run the ORYZA2000 model, re-initializing state variables (i.e. development stage, LAI, weight of leaves, weight of stems, etc.), and better recalibrating the model crop parameters. The degree of success of this approach, of course, lies in the accurate estimates of LAI from SLC and the availability of the required data for each region. It should be also mentioned here that at regional scale, information on rice nutrient balance and soil condition is rarely available, forcing SLC-estimated LAI from MODIS data to re-initialize the ORYZA2000 state variable LAI becomes very helpful and less time consuming.

Availability of quantitative geo-information system (GIS) based on integration of remote sensed data and rice cropping management can have a great effect on future rice production as it can be used as a decision support system (DSS) to support proper planning and correct decision making. Such quantitative information system can be set up based on all developed methods and available data in this study. It contains all spatial and temporal information that can be extracted for rice, such as cultivated area, cropping calendars, variety characteristics, greenness of coverage (NDVI), and LAI, etc. This information would help to quantify effects of these factors on rice yield and production.

Bibliography

Adam, M., Van Bussel, L.G.J., Leffelaar, P.A., Van Keulen, H., & Ewert, F. (2011). Effects of modelling detail on simulated potential crop yields under a wide range of climatic conditions. *Ecological Modelling, 222*(1), 131-143.

Archer, E.R.M. (2004). Beyond the "climate versus grazing" impasse: using remote sensing to investigate the effects of grazing system choice on vegetation cover in the eastern Karoo. *Journal of Arid Environments, 57*(3), 381-408.

Atzberger, C. (2004). Object-based retrieval of biophysical canopy variables using artificial neural nets and radiative transfer models. *Remote Sensing of Environment, 93*(1-2), 53-67.

Bacour, C., Baret, F., Béal, D., Weiss, M., & Pavageau, K. (2006). Neural network estimation of LAI, fAPAR, fCover and LAI×Cab, from top of canopy MERIS reflectance data: Principles and validation. *Remote Sensing of Environment, 105*(4), 313-325.

Baghdadi, N., Boyer, N., Todoroff, P., El Hajj, M., & Begue, A. (2009). Potential of SAR sensors TerraSAR-X, ASAR/ENVISAT and PALSAR/ALOS for monitoring sugarcane crops on Reunion Island. *Remote Sensing of Environment, 113*(8), 1724-1738.

Ball, G.H., & Hall, D.J. (1965). ISODATA, a novel method of data analysis and classification. Stanford Univerisity.

Baret, F., & Guyot, G. (1991). Potentials and limits of vegetation indices for LAI and APAR assessment. *Remote Sensing of Environment, 35*(2-3), 161-173.

Batchelor, W.D., Basso, B., & Paz, J.O. (2002). Examples of strategies to analyze spatial and temporal yield variability using crop models. *European Journal of Agronomy, 18*(1-2), 141-158.

Benedetti, R., & Rossini, P. (1993). On the use of NDVI profiles as a tool for agricultural statistics: The case study of wheat yield estimate and forecast in Emilia Romagna. *Remote Sensing of Environment, 45*(3), 311-326.

Benson, B.J., & MacKenzie, M.D. (1995). Effects of sensor spatial resolution on landscape structure parameters. *Landscape Ecology, 10*(2), 113-120.

Bezdek, J.C., & Pal, N.R. (1998). Some new indexes of cluster validity. *IEEE Transactions on Systems, Man, and Cybernetics - Part B: Cybernetics, 28*(3), 301-315.

Boudraa, A.O. (1999). Dynamic estimation of number of clusters in data sets. *Electronics Letters, 35*(19), 1606-1608.

Bouguessa, M., Wang, S., & Sun, H. (2006). An objective approach to cluster validation. *Pattern Recognition Letters, 27*(13), 1419-1430.

Bouman, B.A.M. (1992). Linking physical remote sensing models with crop growth simulation models, applied for sugar beet. *International Journal of Remote Sensing, 13*(14), 2565-2581.

Bouman, B.A.M. (1995). Crop modelling and remote sensing for yield prediction. *Netherlands Journal of Agricultural Science, 43*(2), 143 - 161.

Bouman, B.A.M., & Hoekman, D.H. (1993). MULTITEMPORAL, MULTIFREQUENCY RADAR MEASUREMENTS OF AGRICULTURAL CROPS DURING THE AGRISCATT-88 CAMPAIGN IN THE NETHERLANDS. *International Journal of Remote Sensing, 14*(8), 1595-1614.

Bouman, B.A.M., Kropff, M.J., Tuong, T.P., Wopereis, M.C.S., ten Berge, H.F.M., & van Laar, H.H. (2001). *Oryza2000: modeling lowland rice*. Los Banos, the Philippines: International Rice Research Institute.

Bouman, B.A.M., van Keulen, H., van Laar, H.H., & Rabbinge, R. (1996). The 'School of de Wit' crop growth simulation models: A pedigree and historical overview. *Agricultural Systems, 52*(2-3), 171-198.

Bouman, B.A.M., van Kraalingen, D.W.G., Stol, W., & van Leeuwen, H.J.C. (1999). An Agroecological Modeling Approach to Explain ERS SAR Radar Backscatter of Agricultural Crops. *Remote Sensing of Environment, 67*(2), 137-146.

Bouman, B.A.M., & van Laar, H.H. (2006). Description and evaluation of the rice growth model ORYZA2000 under nitrogen-limited conditions. *Agricultural Systems, 87*(3), 249-273.

Bouvet, A., & Le Toan, T. (2011). Use of ENVISAT/ASAR wide-swath data for timely rice fields mapping in the Mekong River Delta. *Remote Sensing of Environment, 115*(4), 1090-1101.

Bouvet, A., Le Toan, T., & Nguyen, L.D. (2009). Monitoring of the Rice Cropping System in the Mekong Delta Using ENVISAT/ASAR Dual

Polarization Data. *Ieee Transactions on Geoscience and Remote Sensing, 47*(2), 517-526.

Box, E. (1978). Geographical dimensions of terrestrial net and gross primary productivity. *Radiation and Environmental Biophysics, 15*(4), 305-322.

Brand, S., & Malthus, T.J. (2004). Evaluation of AVHRR NDVI for monitoring intra-annual and interannual vegetation dynamics in a cloudy environment (Scotland, UK). In, *the XXth ISPRS Congress: Geo-imagery bridging continents* (p. 6). Istanbul, Turkey.

Breda, N.J.J. (2003). Ground-based measurements of leaf area index: a review of methods, instruments and current controversies. *Journal of Experimental Botany, 54*(392), 2403-2417.

Brown, L., Chen, J.M., Leblanc, S.G., & Cihlar, J. (2000). A Shortwave Infrared Modification to the Simple Ratio for LAI Retrieval in Boreal Forests: An Image and Model Analysis. *Remote Sensing of Environment, 71*(1), 16-25.

Budde, M.E., Tappan, G., Rowland, J., Lewis, J., & Tieszen, L.L. (2004). Assessing land cover performance in Senegal, West Africa using 1-km integrated NDVI and local variance analysis. *Journal of Arid Environments, 59*(3), 481-498.

Campbell, J.B. (1996). *Introduction to remote sensing*. (2nd ed.). London: Taylor & Francis.

Canisius, F., Turral, H., & Molden, D. (2007). Fourier analysis of historical NOAA time series data to estimate bimodal agriculture. *International Journal of Remote Sensing, 28*(24), 5503 - 5522.

Carlson, T.N., & Ripley, D.A. (1997). On the relation between NDVI, fractional vegetation cover, and leaf area index. *Remote Sensing of Environment, 62*(3), 241-252.

Casa, R., Varella, H., Buis, S., GuÃ©rif, M., De Solan, B., & Baret, F. (2012). Forcing a wheat crop model with LAI data to access agronomic variables: Evaluation of the impact of model and LAI uncertainties and comparison with an empirical approach. *European Journal of Agronomy, 37*(1), 1-10.

Casanova, D., Epema, G.F., & Goudriaan, J. (1998). Monitoring rice reflectance at field level for estimating biomass and LAI. *Field Crops Research, 55*(1-2), 83-92.

Cayrol, P., Chehbouni, A., Kergoat, L., Dedieu, G., Mordelet, P., & Nouvellon, Y. (2000). Grassland modeling and monitoring with SPOT-4 VEGETATION instrument during the 1997-1999 SALSA experiment. *Agricultural and Forest Meteorology, 105*(1-3), 91-115.

Chen, J.M., Pavlic, G., Brown, L., Cihlar, J., Leblanc, S.G., White, H.P., Hall, R.J., Peddle, D.R., King, D.J., Trofymow, J.A., Swift, E., Van der Sanden, J., & Pellikka, P.K.E. (2002). Derivation and validation of Canada-wide coarse-resolution leaf area index maps using high-resolution satellite imagery and ground measurements. *Remote Sensing of Environment, 80*(1), 165-184.

Cheng, Q. (2008). Validation and Correction of MOD15-LAI using In Situ Rice LAI in Southern China. *Communications in Soil Science and Plant Analysis, 39*(11), 1658 - 1669.

Chesson, P.L., & Case, T.J. (1986). Overview: Nonequilibrium Community Theories: Chance, Variability, History and Coexistence. In J. Diamond, & T. Case (Eds.), *Community Ecology* (pp. 229-239). New York: Harper and Row.

Clevers, J.G.P.W., Vonder, O.W., Jongschaap, R.E.E., Desprats, J.-F., King, C., Prévot, L., & Bruguier, N. (2002). Using SPOT data for calibrating a wheat growth model under mediterranean conditions. *Agronomie, 22*(6), 687-694.

Colombo, R., Bellingeri, D., Fasolini, D., & Marino, C.M. (2003). Retrieval of leaf area index in different vegetation types using high resolution satellite data. *Remote Sensing of Environment, 86*(1), 120-131.

Combal, B., Baret, F., Weiss, M., Trubuil, A., Macé, D., Pragnère, A., Myneni, R., Knyazikhin, Y., & Wang, L. (2003). Retrieval of canopy biophysical variables from bidirectional reflectance: Using prior information to solve the ill-posed inverse problem. *Remote Sensing of Environment, 84*(1), 1-15.

Coppin, P., Jonckheere, I., Nackaerts, K., Muys, B., & Lambin, E. (2004). Digital change detection methods in ecosystem monitoring: a review. *International Journal of Remote Sensing, 25*(9), 1565 - 1596.

Dang, K.S., Nguyen, N.Q., Pham, Q.D., Truong, T.T.T., & Beresford, M. (2006). PART III. Policy reform and the transformation of Vietnamese agriculture. In: Rapid growth of selected Asian economies.Lessons and

implications for agriculture and food security: Republic of Korea, Thailand and Viet Nam:FAO. Online: http://www.fao.org/docrep/009/ag089e/AG089E08.htm (Accessed 10 December 2009).

Darvishzadeh, R., Skidmore, A., Schlerf, M., & Atzberger, C. (2008). Inversion of a radiative transfer model for estimating vegetation LAI and chlorophyll in a heterogeneous grassland. *Remote Sensing of Environment, 112*(5), 2592-2604.

Davies, D.L., & Bouldin, D.W. (1979). A Cluster Separation Measure. *IEEE Transactions on Pattern Analysis and Machine Intelligence, PAMI-1*(2), 224-227.

de Bie, C.A.J.M. (2000). Comparative performance analysis of agro-ecosystem. In, *ITC* (p. 232). Enschede.

de Bie, C.A.J.M. (2004). Spatial-temporal mapping of agro-ecosystems and the need to build thematic legends. In, *the XXth ISPRS Congress: Geo-imagery bridging continents* (pp. 1148-1154). Istanbul, Tukey: ISPRS.

de Bie, C.A.J.M., Khan, M.R., Toxopeus, A.G., Venus, V., & Skidmore, A. (2008). Hypertemporal image analysis for crop mapping and change detection. In, *the ISPRS XXIst Congress : Silk road for information from imagery* (pp. 803-812). Beijing, China: ISPRS.

Delécolle, R., Maas, S.J., Guérif, M., & Baret, F. (1992). Remote sensing and crop production models: present trends. *ISPRS Journal of Photogrammetry and Remote Sensing, 47*(2-3), 145-161.

Doherty, R.M., Sitch, S., Smith, B., Lewis, S.L., & Thornton, P.K. (2010). Implications of future climate and atmospheric CO2 content for regional biogeochemistry, biogeography and ecosystem services across East Africa. *Global Change Biology, 16*(2), 617-640.

Doraiswamy, P.C., Hatfield, J.L., Jackson, T.J., Akhmedov, B., Prueger, J., & Stern, A. (2004). Crop condition and yield simulations using Landsat and MODIS. *Remote Sensing of Environment, 92*(4), 548-559.

Doraiswamy, P.C., Moulin, S., Cook, P.W., & Stern, A. (2003). Crop yield assessment from remote sensing. *Photogrammetric Engineering and Remote Sensing, 69*(6), 665-674.

Dorigo, W.A., Zurita-Milla, R., de Wit, A.J.W., Brazile, J., Singh, R., & Schaepman, M.E. (2007). A review on reflective remote sensing and data assimilation techniques for enhanced agroecosystem modeling. *International Journal of Applied Earth Observation and Geoinformation, 9*(2), 165-193.

Drenge, H.E., & Tucker, C.J. (1988). Green biomass and rainfall in semi-arid sub-Saharan Africa. *Journal of Arid Environments, 15*245-252.

Dubes, R.C. (1987). How many clusters are best? - An experiment. *Pattern Recognition, 20*(6), 645-663.

Durbha, S.S., King, R.L., & Younan, N.H. (2007). Support vector machines regression for retrieval of leaf area index from multiangle imaging spectroradiometer. *Remote Sensing of Environment, 107*(1-2), 348-361.

Duveiller, G.g., Weiss, M., Baret, F.d.r., & Defourny, P. (2011). Retrieving wheat Green Area Index during the growing season from optical time series measurements based on neural network radiative transfer inversion. *Remote Sensing of Environment, 115*(3), 887-896.

Eerens, H., Kempeneers, P., Piccard, I., & Verheijen, Y. (2001). Crop monitoring and yield forecasting with NOAA-AVHRR or SPOT-VegetationOnline: http://www.geosuccess.be/geosuccess/documents/Dry_Matter_Productivity.pdf (Accessed 26 January 2011).

Eklundh, L., Harrie, L., & Kuusk, A. (2001). Investigating relationships between Landsat ETM+ sensor data and leaf area index in a boreal conifer forest. *Remote Sensing of Environment, 78*(3), 239-251.

ERDAS Inc. (2003). *ERDAS Field Guide*. (7th ed.). Atlanta, Georgia: Leica Geosystem GIS & Mapping, LCC.

ERDAS Inc. (2009). *ERDAS Field Guide™*. ERDAS Inc..

Ewers, R.M., & Didham, R.K. (2006). Continuous response functions for quantifying the strength of edge effects. *Journal of Applied Ecology, 43*(3), 527-536.

Fang, H., & Liang, S. (2005). A hybrid inversion method for mapping leaf area index from MODIS data: experiments and application to broadleaf and needleleaf canopies. *Remote Sensing of Environment, 94*(3), 405-424.

Fang, H., Liang, S., & Hoogenboom, G. (2011). Integration of MODIS LAI and vegetation index products with the CSM-CERES-Maize model for corn yield estimation. *International Journal of Remote Sensing, 32*(4), 1039-1065.

FAO (2012). FAOSTAT. Online: http://faostat3.fao.org/home/index.html#DOWNLOAD (Accessed October 8, 2012).

Farina, A. (2006). Emerging patterns in the landscape. In H. Décamps, B. Tress, & G. Tress (Eds.), *Principles and methods in landscape ecology* (pp. 179-228). Dondrecht, The Netherlands: Springer Netherlands.

Fonderflick, J., Lepart, J., Caplat, P., Debussche, M., & Marty, P. (2010). Managing agricultural change for biodiversity conservation in a Mediterranean upland. *Biological Conservation, 143*(3), 737-746.

Forman, R.T.T. (1995). Some general principles of landscape and regional ecology. *Landscape Ecology, 10*(3), 133-142.

Fourty, T., Baret, F., Jacquemoud, S., Schmuck, G., & Verdebout, J. (1996). Leaf optical properties with explicit description of its biochemical composition: Direct and inverse problems. *Remote Sensing of Environment, 56*(2), 104-117.

Frere, M., & Popov, G.F. (1979). Agrometeorological crop monitoring and forecasting. .

Fritz, S., Massart, M., Savin, I., Gallego, J., & Rembold, F. (2008). The use of MODIS data to derive acreage estimations for larger fields: A case study in the south-western Rostov region of Russia. *International Journal of Applied Earth Observation and Geoinformation, 10*(4), 453-466.

Galford, G.L., Mustard, J.F., Melillo, J., Gendrin, A., Cerri, C.C., & Cerri, C.E.P. (2008). Wavelet analysis of MODIS time series to detect expansion and intensification of row-crop agriculture in Brazil. *Remote Sensing of Environment, 112*(2), 576-587.

Goel, N.S. (1989). Inversion of canopy reflectance models for estimation of biophysical parameters from reflectance data. In G. Asrar (Ed.), *Theory and Applications of Optical Remote Sensing* (pp. 205 - 251). New York etc.: John Wiley & Sons.

Gorham, B. (1998). Mapping multi-temporal agricultural land use in Mississipi Alluvial valley of Arkansas. In, *the Spatial Technologies in Agricultural and Natural Resources: SRIEG-10 Annual Conference*. Global Hydrology and Climate Centre, Hutsville, USA. .

Gosz, J.R. (1992). Gradient Analysis of Ecological Change in Time and Space: Implications for Forest Management. *Ecological Applications, 2*(3), 248-261.

Guérif, M., & Duke, C. (1998). Calibration of the SUCROS emergence and early growth module for sugar beet using optical remote sensing data assimilation. *European Journal of Agronomy, 9*(2-3), 127-136.

Gupta, R.K., Prasad, T.S., & Vijayan, D. (2000). Relationship between LAI and NDVI for IRS LISS and Landsat TM bands. *Advances in Space Research, 26*(7), 1047-1050.

Gustafson, E.J. (1998). Quantifying Landscape Spatial Pattern: What Is the State of the Art? *Ecosystems, 1*(2), 143-156.

Hadria, R., Duchemin, B., Jarlan, L., Dedieu, G., Baup, F., Khabba, S., Olioso, A., & Le Toan, T. (2010). Potentiality of optical and radar satellite data at high spatio-temporal resolutions for the monitoring of irrigated wheat crops in Morocco. *International Journal of Applied Earth Observation and Geoinformation, 12*S32-S37.

Halkidi, M., Batistakis, Y., & Vazirgiannis, M. (2001). On Clustering Validation Techniques. *Journal of Intelligent Information Systems, 17*(2), 107-145.

Hapke, B. (1981). Bidirectional Reflectance Spectroscopy 1. Theory. *J. Geophys. Res., 86*(B4), 3039-3054.

Harper, K.A., Macdonald, S.E., Burton, P.J., Chen, J., Brosofske, K.D., Saunders, S.C., Euskirchen, E.S., Roberts, D.A.R., Jaiteh, M.S., & Esseen, P.-A. (2005). Edge Influence on Forest Structure and Composition in Fragmented Landscapes. *Conservation Biology, 19*(3), 768-782.

He, Y., Guo, X., & Wilmshurst, J.F. (2007). Comparison of different methods for measuring leaf area index in a mixed grassland. *Canadian Journal of Plant Science, 87*(4), 803-813.

Hill, M.J., & Donald, G.E. (2003). Estimating spatio-temporal patterns of agricultural productivity in fragmented landscapes using AVHRR NDVI time series. *Remote Sensing of Environment, 84*(3), 367-384.

Hoekstra, A. (1998). Generalisation in Feed Forward Neural Classifiers. In (p. 123). Delft, the Netherlands: Delft University of Technology.

Holben, B.N. (1986). Characteristics of maximum-value composite images from temporal AVHRR data. *International Journal of Remote Sensing, 7*(11), 1417-1434.

Houborg, R., Soegaard, H., & Boegh, E. (2007). Combining vegetation index and model inversion methods for the extraction of key vegetation biophysical parameters using Terra and Aqua MODIS reflectance data. *Remote Sensing of Environment, 106*(1), 39-58.

Huifang, Z., Runhe, S., Honglin, Z., Peiqing, Q., Juan, S., Wenpeng, L., & Su, L. (2009). Improvement of MODIS 8-day LAI/FPAR product with temporal filters to generate high quality time-series product. In, *Urban Remote Sensing Event, 2009 Joint* (pp. 1-7).

Imaz, A., Hernández, M.A., Ariño, A.H., Armendáriz, I., & Jordana, R. (2002). Diversity of soil nematodes across a Mediterranean ecotone. *Applied Soil Ecology, 20*(3), 191-198.

Immerzeel, W.W., Quiroz, R.A., & de Jong, S.M. (2005). Understanding precipitation patterns and land use interaction in Tibet using harmonic analysis of SPOT VGT-S10 NDVI time series. *International Journal of Remote Sensing, 26*(11), 2281 - 2296.

Jacquemoud, S., Bacour, C., Poilvé, H., & Frangi, J.P. (2000). Comparison of Four Radiative Transfer Models to Simulate Plant Canopies Reflectance: Direct and Inverse Mode. *Remote Sensing of Environment, 74*(3), 471-481.

Jacquemoud, S., & Baret, F. (1990). PROSPECT: A model of leaf optical properties spectra. *Remote Sensing of Environment, 34*(2), 75-91.

Jacquemoud, S., Baret, F., Andrieu, B., Danson, F.M., & Jaggard, K. (1995). Extraction of vegetation biophysical parameters by inversion of the PROSPECT + SAIL models on sugar beet canopy reflectance data. Application to TM and AVIRIS sensors. *Remote Sensing of Environment, 52*(3), 163-172.

Jain, A.K., Murty, M.N., & Flynn, P.J. (1999). Data clustering: a review. *ACM Computing Surveys., 31*(3), 264-323.

Jensen, J.R. (1996). *Introductory digital image processing : a remote sensing perspective*. (Second edition ed.). London etc.: Prentice-Hall.

Jiang, B., Liang, S., Wang, J., & Xiao, Z. (2010). Modeling MODIS LAI time series using three statistical methods. *Remote Sensing of Environment, 114*(7), 1432-1444.

Jiang, X., Wang, D., Tang, L., Hu, J., & Xi, X. (2008). Analysing the vegetation cover variation of China from AVHRR-NDVI data. *International Journal of Remote Sensing, 29*(17), 5301 - 5311.

Jolliffe, I. (2005). *Principal Component Analysis*. John Wiley & Sons, Ltd.

Justice, C.O., Townshend, J.R.G., Holben, B.N., & Tucker, C.J. (1985). Analysis of the phenology of global vegetation using meteorological satellite data. *International Journal of Remote Sensing, 6*(8), 1271 - 1318.

Kamthonkiat, D., Honda, K., Turral, H., Tripathi, N.K., & Wuwongse, V. (2005). Discrimination of irrigated and rainfed rice in a tropical agricultural system using SPOT VEGETATION NDVI and rainfall data. *International Journal of Remote Sensing, 26*(12), 2527 - 2547.

Keddy, P.A. (1991). Working with heterogeneity: an operator's guide to environmental gradients. In J. Kolasa, & S.T.A. Pickett (Eds.), *Ecological Heterogeneity* (pp. 181-200). New York: Springer-Verlag.

Kent, M., Gill, W.J., Weaver, R.E., & Armitage, R.P. (1997). Landscape and plant community boundaries in biogeography. *Progress in Physical Geography, 21*(3), 315-353.

Khan, M.R., de Bie, C.A.J.M., van Keulen, H., Smaling, E.M.A., & Real, R. (2010). Disaggregating and mapping crop statistics using hypertemporal remote sensing. *International Journal of Applied Earth Observation and Geoinformation, 12*(1), 36-46.

Kimes, D.S., Knyazikhin, Y., Privette, J.L., Abuelgasim, A.A., & Gao, F. (2000). Inversion methods for physically-based models. *Remote Sensing Reviews, 18*(2), 381 - 439.

Knyazikhin, Y., Martonchik, J.V., Diner, D.J., Myneni, R.B., Verstraete, M., Pinty, B., & Gobron, N. (1998a). Estimation of vegetation canopy leaf area index and fraction of absorbed photosynthetically active radiation

from atmosphere-corrected MISR data. *J. Geophys. Res., 103*(D24), 32239-32256.

Knyazikhin, Y., Martonchik, J.V., Myneni, R.B., Diner, D.J., & Running, S.W. (1998b). Synergistic algorithm for estimating vegetation canopy leaf area index and fraction of absorbed photosynthetically active radiation from MODIS and MISR data. *J. Geophys. Res., 103*(D24), 32257-32275.

Koetz, B., Baret, F., Poilvé, H., & Hill, J. (2005). Use of coupled canopy structure dynamic and radiative transfer models to estimate biophysical canopy characteristics. *Remote Sensing of Environment, 95*(1), 115-124.

Kushida, K., & Yoshino, K. (2010). Estimation of LAI and FAPAR by constraining the leaf and soil spectral characteristics in a radiative transfer model. *International Journal of Remote Sensing, 31*(9), 2351 - 2375.

Laborte, A.G., de Bie, K., Smaling, E.M.A., Moya, P.F., Boling, A.A., & Van Ittersum, M.K. (2012). Rice yields and yield gaps in Southeast Asia: Past trends and future outlook. *European Journal of Agronomy, 36*(1), 9-20.

Launay, M., & Guerif, M. (2005). Assimilating remote sensing data into a crop model to improve predictive performance for spatial applications. *Agriculture, Ecosystems & Environment, 111*(1-4), 321-339.

Le Quang Minh (2001). Environmental Governance: A Mekong Delta Case Study with Downstream Perspectives. World Resources Institute. Online: pdf.wri.org/mekong_governence_mreg_minh.pdf (Accessed June 29, 2011).

Ledwith, M. (2002). Land cover classification using SPOT-Vegetation 10-day composite images - Baltic Sea Catchment basin. In, *GLC2000 Meeting*. Ispra, Italy.

Lenney, M.P., Woodcock, C.E., Collins, J.B., & Hamdi, H. (1996). The status of agricultural lands in Egypt: The use of multitemporal NDVI features derived from landsat TM. *Remote Sensing of Environment, 56*(1), 8-20.

Lhermitte, S., Verbesselt, J., Jonckheere, I., Nackaerts, K., van Aardt, J.A.N., Verstraeten, W.W., & Coppin, P. (2008). Hierarchical image segmentation based on similarity of NDVI time series. *Remote Sensing of Environment, 112*(2), 506-521.

Li, H., & Reynolds, J.F. (1994). A Simulation Experiment to Quantify Spatial Heterogeneity in Categorical Maps. *Ecology, 75*(8), 2446-2455.

Li, R., Li, C.-j., Dong, Y.-y., Liu, F., Wang, J.-h., Yang, X.-d., & Pan, Y.-c. (2011). Assimilation of Remote Sensing and Crop Model for LAI Estimation Based on Ensemble Kaiman Filter. *Agricultural Sciences in China, 10*(10), 1595-1602.

Liang, S. (2004). *Quantitative remote sensing of land surfaces : also as e-book*. Hoboken etc.: Wiley & Sons.

Liang, S., & Strahler, A.H. (1993). An analytic BRDF model of canopy radiative transfer and its inversion. *Geoscience and Remote Sensing, IEEE Transactions on, 31*(5), 1081-1092.

Liang, S., & Strahler, A.H. (1994). Retrieval of surface BRDF from multiangle remotely sensed data. *Remote Sensing of Environment, 50*(1), 18-30.

Lieth, H., & Whittaker, R.H. (1975). *Primary productivity of the biosphere*. New York: Springer-Verlag.

Lobell, D.B., & Asner, G.P. (2004). Cropland distributions from temporal unmixing of MODIS data. *Remote Sensing of Environment, 93*(3), 412-422.

Lucas, R., Rowlands, A., Brown, A., Keyworth, S., & Bunting, P. (2007). Rule-based classification of multi-temporal satellite imagery for habitat and agricultural land cover mapping. *ISPRS Journal of Photogrammetry and Remote Sensing, 62*(3), 165-185.

Maas, S.J. (1988a). Use of remotely-sensed information in agricultural crop growth models. *Ecological Modelling, 41*(3-4), 247-268.

Maas, S.J. (1988b). Using Satellite Data to Improve Model Estimates of Crop Yield. *Agronomy Journal, 80*(4), 655-662.

MacQueen, J.B. (1967). Some Methods for Classification and Analysis of Multivariate Observations. In, *The 5th Berkeley Symposium on Mathematical Statisticsand Probability* (pp. 281-297). Los Angeles.

Maggi, M., & Stroppiana, D. (2002). Advantages and drawbacks of NOAA-AVHRR and SPOT-VGT for burnt area mapping in a tropical savanna ecosystem. *Canadian Journal of Remote Sensing, 28*(2), 231-245 .

Markwell, J., Osterman, J., & Mitchell, J. (1995). Calibration of the Minolta SPAD-502 leaf chlorophyll meter. *Photosynthesis Research, 46*(3), 467-472.

McCloy, K.R. (2006). *Resource management information systems : remote sensing, GIS and modelling*. (Second edition ed.). Boca Raton: CRC, Taylor & Francis.

McLaughlin, D. (2002). An integrated approach to hydrologic data assimilation: interpolation, smoothing, and filtering. *Advances in Water Resources, 25*(8–12), 1275-1286.

McNairn, H., Champagne, C., Shang, J., Holmstrom, D., & Reichert, G. (2009). Integration of optical and Synthetic Aperture Radar (SAR) imagery for delivering operational annual crop inventories. *ISPRS Journal of Photogrammetry and Remote Sensing, 64*(5), 434-449.

Meroni, M., Colombo, R., & Panigada, C. (2004). Inversion of a radiative transfer model with hyperspectral observations for LAI mapping in poplar plantations. *Remote Sensing of Environment, 92*(2), 195-206.

Migdall, S., Bach, H., Bobert, J., Wehrhan, M., & Mauser, W. (2009). Inversion of a canopy reflectance model using hyperspectral imagery for monitoring wheat growth and estimating yield. *Precision Agriculture, 10*(6), 508-524.

Ministry of Agriculture and Rural Development (2009). So lieu thong ke va an ninh luong thuc toan quoc giai doan 1996-2007 (in Vietnamese). In:Bo Nong nghiep va Phat trien Nong thon (MARD). Online: http://fsiu.mard.gov.vn/data/trongtrot.htm (Accessed 8 July 2009).

Mohanty, S., Wailes, E., & Chavez, E. (2010). The global rice supply and demand outlook: the need for greater productivity growth to keep rice affordable". In S. Pandey, D. Byerlee, D. Dawe, A. Dobermann, S. Mohanty, S. Rozelle, & B. Hardy (Eds.), *Rice in the Global Economy: Strategic Research and Policy Issues for Food Security* (pp. 175-187). Los Banos, the Philippines.

Moulin, S., Bondeau, A., & Delecolle, R. (1998). Combining agricultural crop models and satellite observations: From field to regional scales. *International Journal of Remote Sensing, 19*(6), 1021-1036.

Moulin, S., Zurita Milla, R., Guerif, M., & Baret, F. (2003). Characterizing the spatial and temporal variability of biophysical variables of a wheat crop

using hyper-spectral measurements. In, *Geoscience and Remote Sensing Symposium, 2003. IGARSS '03. Proceedings. 2003 IEEE International* (pp. 2206-2208 vol.2204).

Murakami, T., Ogawa, S., Ishitsuka, N., Kumagai, K., & Saito, G. (2001). Crop discrimination with multitemporal SPOT/HRV data in the Saga Plains, Japan. *International Journal of Remote Sensing, 22*(7), 1335 - 1348.

Murwira, A., & Skidmore, A.K. (2005). The response of elephants to the spatial heterogeneity of vegetation in a Southern African agricultural landscape. *Landscape Ecology, 20*(2), 217-234.

Myneni, R.B., Hoffman, S., Knyazikhin, Y., Privette, J.L., Glassy, J., Tian, Y., Wang, Y., Song, X., Zhang, Y., Smith, G.R., Lotsch, A., Friedl, M., Morisette, J.T., Votava, P., Nemani, R.R., & Running, S.W. (2002). Global products of vegetation leaf area and fraction absorbed PAR from year one of MODIS data. *Remote Sensing of Environment, 83*(1-2), 214-231.

Myneni, R.B., Ramakrishna, R., Nemani, R., & Running, S.W. (1997). Estimation of global leaf area index and absorbed par using radiative transfer models. *Geoscience and Remote Sensing, IEEE Transactions on, 35*(6), 1380-1393.

National Institute of Meteorology (2009). So lieu khi tuong In: Bo Tai nguyen va Moi truong - MONRE.

Nguyen, H.N. (2007). Flooding in Mekong River Delta, Vietnam. In: Fighting climate change: Human solidarity in a divided world. , Human Development Report 2007/2008, Human Development Report Office, UNDP,

Nguyen, L.D., Le Toan, T., & Floury, N. (2005). The Use of SAR Data for Rice Crop Monitoring: A Case study of Mekong River Delta - Vietnam In: Online: http://www.a-a-r-s.org/acrs/proceeding/ACRS2005/Papers/AGC1-4.pdf (Accessed 8 June 2009).

Nguyen, L.D., Young, F., Apan, A., Le Van, T., Le Toan, T., & Bouvet, A. (2007). Rice Monitoring Using ENVISAT ASAR Data: Preliminary Results of a Case Study in the Mekong River Delta, Vietnam. In: Online: http://www.a-a-r-s.org/acrs/proceeding/ACRS2007/Papers/TS1.3.pdf (Accessed 8 June 2009).

Nguyen, T.T.H., De Bie, C.A.J.M., Ali, A., Smaling, E.M.A., & Chu, T.H. (2012a). Mapping the irrigated rice cropping patterns of the Mekong delta, Vietnam, through hyper-temporal SPOT NDVI image analysis. *International Journal of Remote Sensing, 33*(2), 415-434.

Nguyen, T.T.H., de Bie, C.A.J.M., Amjad Ali, Smaling, E.M.A., & Chu Thai Hoanh (2012b). Mapping the irrigated rice cropping patterns of the Mekong delta, Vietnam through hyper-temporal SPOT NDVI image analysis. *International Journal of Remote Sensing, 33*(2), 415-434.

NIAPP (2008). Ban do su dung dat vung Dong bang song Cuu Long nam 2005 In. Ho Chi Minh City, Vietnam: Vien Quy hoach va Thiet ke Nong nghiep (NIAPP) - MARD.

Pal, N.R., & Bezdek, J.C. (1995). On cluster validity for the fuzzy c-means model. *Fuzzy Systems, IEEE Transactions on, 3*(3), 370-379.

Palosuo, T., Kersebaum, K.C., Angulo, C., Hlavinka, P., Moriondo, M., Olesen, J.E., Patil, R.H., Ruget, F., Rumbaur, C., Takáč, J., Trnka, M., Bindi, M., Çaldağ, B., Ewert, F., Ferrise, R., Mirschel, W., Şaylan, L., Šiška, B., & Rötter, R. (2011). Simulation of winter wheat yield and its variability in different climates of Europe: A comparison of eight crop growth models. *European Journal of Agronomy, 35*(3), 103-114.

Panigrahy, S., Manjunath, K.R., Chakraborty, M., Kundu, N., & Parihar, J.S. (1999). Evaluation of RADARSAT Standard Beam data for identification of potato and rice crops in India. *ISPRS Journal of Photogrammetry and Remote Sensing, 54*(4), 254-262.

Papademetriou, M.K., Dent, F.J., & Herath, E.M. (Eds.) (2000). *Bridging the rice yield gap in the Asia-Pacific region*: FAO.

Peng, D., Huete, A.R., Huang, J., Wang, F., & Sun, H. (2011). Detection and estimation of mixed paddy rice cropping patterns with MODIS data. *International Journal of Applied Earth Observation and Geoinformation, 13*(1), 13-23.

Peng, S., Cassman, K.G., Virmani, S.S., Sheehy, J., & Khush, G.S. (1999). Yield Potential Trends of Tropical Rice since the Release of IR8 and the Challenge of Increasing Rice Yield Potential. *Crop Sci., 39*(6), 1552-1559.

Piwowar, J.M., & LeDrew, E.F. (1995). Hypertemporal analysis of remotely sensed sea-ice data for climate change studies. *Progress in Physical Geography, 19*(2), 216-242.

Piwowar, J.M., Peddle, D.R., & LeDrew, E.F. (1998). Temporal Mixture Analysis of Arctic Sea Ice Imagery: A New Approach for Monitoring Environmental Change. *Remote Sensing of Environment, 63*(3), 195-207.

Planning Department - Ministry of Agriculture and Rural Development (2009). Chiến lược phát triển Nông nghiệp Nông thôn giai đoạn 2011-2020. (In Vietnamese). In:Ministry of Agriculture and Rural Development (MARD). Online: http://vukehoach.mard.gov.vn/chienluoc.aspx?id=37 (Accessed 11 July 2010).

Pogue, D.W., & Schnell, G.D. (2001). Effects of agriculture on habitat complexity in a prairie-forest ecotone in the Southern Great Plains of North America. *Agriculture, Ecosystems & Environment, 87*(3), 287-298.

Privette, J.L., Myneni, R.B., Knyazikhin, Y., Mukelabai, M., Roberts, G., Tian, Y., Wang, Y., & Leblanc, S.G. (2002). Early spatial and temporal validation of MODIS LAI product in the Southern Africa Kalahari. *Remote Sensing of Environment, 83*(1-2), 232-243.

Quarmby, N.A., Milnes, M., Hindle, T.L., & Silleos, N. (1993). The use of multi-temporal NDVI measurements from AVHRR data for crop yield estimation and prediction. *International Journal of Remote Sensing, 14*(2), 199-210.

Rasmussen, M.S. (1998). Developing simple, operational, consistent NDVI-vegetation models by applying environmental and climatic information. Part II: Crop yield assessment. *International Journal of Remote Sensing, 19*(1), 119-139.

Richards, J.A., & Xiuping Jia (2006). *Remote sensing digital image analysis : an introduction*. (4th ed.). Berlin etc.: Springer-Verlag.

Saab, D.A., & Haythornthwaite, T.W. (1990). Application of spatio-temporal database models to street network files. In, *the GIS for the 1990s* (pp. 1072-1085). Canadian Institute of Surveying and Mapping, Ottawa, Canada.

Saab, V. (1999). Importance of spatial scale to habitat use by breeding birds in riparian forests: A hierarchical analysis *Ecological Applications, 9*(1), 135-151.

Sakamoto, T., Cao, P.V., Nguyen, N.V., Kotera, A., & Yokozawa, M. (2009a). Agro-ecological Interpretation of Rice Cropping Systems in Flood-prone

Areas using MODIS imagery. *Photogrammetric Engineering & Remote Sensing, 75*(4), 413-424.

Sakamoto, T., Cao, V.P., Kotera, A., Nguyen, K.D., & Yokozawa, M. (2009b). Analysis of rapid expansion of inland aquaculture and triple rice-cropping areas in a coastal area of the Vietnamese Mekong Delta using MODIS time-series imagery. *Landscape and Urban Planning, 92*(1), 34-46.

Sakamoto, T., Van Nguyen, N., Ohno, H., Ishitsuka, N., & Yokozawa, M. (2006). Spatio-temporal distribution of rice phenology and cropping systems in the Mekong Delta with special reference to the seasonal water flow of the Mekong and Bassac rivers. *Remote Sensing of Environment, 100*(1), 1-16.

Salvatori, V., Skidmore, A.K., Corsi, F., & van der Meer, F. (1999). Estimating Temporal Independence of Radio-telemetry Data on Animal Activity. *Journal of Theoretical Biology, 198*(4), 567-574.

Sarkar, S., & Kafatos, M. (2004). Interannual variability of vegetation over the Indian sub-continent and its relation to the different meteorological parameters. *Remote Sensing of Environment, 90*(2), 268-280.

Schlerf, M., & Atzberger, C. (2006). Inversion of a forest reflectance model to estimate structural canopy variables from hyperspectral remote sensing data. *Remote Sensing of Environment, 100*(3), 281-294.

Schmidt, K.S., & Skidmore, A.K. (2003). Spectral discrimination of vegetation types in a coastal wetland. *Remote Sensing of Environment, 85*(1), 92-108.

Schowengerdt, R.A. (2006). *Remote sensing : models and methods for image processing : e-book*. (3rd ed.). San Diego etc.: Academic Press.

Sellers, P.J. (1985). Canopy reflectance, photosynthesis and transpiration. *International Journal of Remote Sensing, 6*(8), 1335 - 1372.

Sellers, P.J., Dickinson, R.E., Randall, D.A., Betts, A.K., Hall, F.G., Berry, J.A., Collatz, G.J., Denning, A.S., Mooney, H.A., Nobre, C.A., Sato, N., Field, C.B., & Henderson-Sellers, A. (1997). Modeling the Exchanges of Energy, Water, and Carbon Between Continents and the Atmosphere. *Science, 275*(5299), 502-509.

Shao, Y., Fan, X., Liu, H., Xiao, J., Ross, S., Brisco, B., Brown, R., & Staples, G. (2001). Rice monitoring and production estimation using

multitemporal RADARSAT. *Remote Sensing of Environment, 76*(3), 310-325.

Shibayama, M., & Akiyama, T. (1989). Seasonal visible, near-infrared and mid-infrared spectra of rice canopies in relation to LAI and above-ground dry phytomass. *Remote Sensing of Environment, 27*(2), 119-127.

Skidmore, A.K., Ferwerda, J.G., Mutanga, O., Van Wieren, S.E., Peel, M., Grant, R.C., Prins, H.H.T., Balcik, F.B., & Venus, V. (2010). Forage quality of savannas — Simultaneously mapping foliar protein and polyphenols for trees and grass using hyperspectral imagery. *Remote Sensing of Environment, 114*(1), 64-72.

Skidmore, A.K., & Turner, B.J. (1992). Map accuracy assessment using line intersect sampling. *Photogrammetric Engineering and Remote Sensing, 58*(10), 1453 - 1457.

Smith, A.M., Eddy, P.R., Bugden-Storie, J., Pattey, E., McNairn, H., Nolin, M., Perron, I., Hinther, M., Miller, J., & Haboudane, D. (2006). Multipolarized radar for delineating within-field variability in corn and wheat. *Canadian Journal of Remote Sensing, 32*(4), 300-313.

Souza, C., Firestone, L., Silva, L.M., & Roberts, D. (2003). Mapping forest degradation in the Eastern Amazon from SPOT 4 through spectral mixture models. *Remote Sensing of Environment, 87*(4), 494-506.

Stutheit, J. (1991). Temporal GIS investigates global change. *GIS World, 4*(9), 68-72.

Swain, P.H. (1973). Pattern recognition : a basis for remote sensing data analysis. .

Swain, P.H. (1978). Fundamentals of Pattern Recognition in Remote Sensing. In P.H. Swain, & S.M. Davis (Eds.), *Remote Sensing: The Quantative Approach* (pp. 136 - 185). New York: McGraw Hill Book Company.

Tan, B., Hu, J., Huang, D., Yang, W., Zhang, P., Shabanov, N.V., Knyazikhin, Y., Nemani, R.R., & Myneni, R.B. (2005). Assessment of the broadleaf crops leaf area index product from the Terra MODIS instrument. *Agricultural and Forest Meteorology, 135*(1-4), 124-134.

ten Berge, H.F.M., Thiyagarajan, T.M., Shi, Q., Wopereis, M.C.S., Drenth, H., & Jansen, M.J.W. (1997). Numerical optimization of nitrogen application

to rice. Part I. Description of MANAGE-N. *Field Crops Research, 51*(1-2), 29-42.

The Information Center - Ministry of Agriculture and Rural Development (2009). Dữ liệu ngành hàng Nông nghiệp (In Vietnamese). Online: http://www.agro.gov.vn/news/Dulieu_SMS.aspx?Nhom_DL=14&pNum=2 (Accessed).

Thomas, I.L., Ching, N.P., Benning, V.M., & D'Aguanno, J.A. (1987). Review Article A review of multi-channel indices of class separability. *International Journal of Remote Sensing, 8*(3), 331 - 350.

Tou, J.T., & Gonzalez, R.C. (1974). *Pattern recognition principles*. Massachusetts: Reading, Advance Book Program, Addison-Wesley Publishing Company.

Townshend, J.R.G., & Justice, C.O. (1986). Analysis of the dynamics of African vegetation using the normalized difference vegetation index. *International Journal of Remote Sensing, 7*(11), 1435 - 1445.

Townshend, J.R.G., Justice, C.O., & Kalb, V. (1987). Characterization and classification of South American land cover types using satellite data. *International Journal of Remote Sensing, 8*(8), 1189 - 1207.

Townshend, J.R.G., Justice, C.O., Skole, D., Malingreau, J.P., Cihlar, J., Teillet, P., Sadowski, F., & Ruttenberg, S. (1994). The 1 km resolution global data set: needs of the International Geosphere Biosphere Programme. *International Journal of Remote Sensing, 15*(17), 3417-3441.

Trade and Markets Division-Food and Agriculture Organization of the United Nation (2012). Rice Market Monitor. FAO.

Tso, B., & Mather, P.M. (2001). *Classification methods for remotely sensed data*. London etc.: Taylor & Francis.

Tucker, C.J. (1979). Red and photographic infrared linear combinations for monitoring vegetation. *Remote Sensing of Environment, 8*(2), 127-150.

Tucker, C.J., Holben, B.N., Elgin Jr, J.H., & McMurtrey Iii, J.E. (1981). Remote sensing of total dry-matter accumulation in winter wheat. *Remote Sensing of Environment, 11*(0), 171-189.

Turner, D.P., Cohen, W.B., Kennedy, R.E., Fassnacht, K.S., & Briggs, J.M. (1999). Relationships between Leaf Area Index and Landsat TM Spectral

Vegetation Indices across Three Temperate Zone Sites. *Remote Sensing of Environment, 70*(1), 52-68.

Turner, M.G., Gardner, R.H., & O'Neill, R.V. (2001). *Landscape Ecology in Theory and Practice: Pattern and Process*. New York, Berlin, Heidelberg: Springer-Verlag.

Uchida, S. (2001). Discrimination of Agricultural Land use using multi-temporal NDVI data. In, *the 22nd Asian Conference on Remote Sensing* (pp. 813-818). Centre of Remote sensing and Processing (CRISP), Singapore.

Unganai, L.S., & Kogan, F.N. (1998). Drought Monitoring and Corn Yield Estimation in Southern Africa from AVHRR Data. *Remote Sensing of Environment, 63*(3), 219-232.

van der Maarel, E., & Westhoff, V. (1964). The vegetation of dunes near Oostvoorne, Netherlands. *Wentia, 12*1-61.

van Ittersum, M.K., Leffelaar, P.A., van Keulen, H., Kropff, M.J., Bastiaans, L., & Goudriaan, J. (2003). On approaches and applications of the Wageningen crop models. *European Journal of Agronomy, 18*(3-4), 201-234.

van Leeuwen, C. (1966). A relation theoretical approach to pattern and process in vegetation. *Wentia, 15*15-32.

VEGETATION Programme (2009). 2-2 Synthesis Products. In: Vegetation Products:VEGETATION Programme. Online: www.spot-vegetation.com/vegetationprogramme/Pages/TheVegetationSystem/userguide/userguide.htm (Accessed 13 October 2009).

Verbeiren, S., Eerens, H., Piccard, I., Bauwens, I., & Van Orshoven, J. (2008). Sub-pixel classification of SPOT-VEGETATION time series for the assessment of regional crop areas in Belgium. *International Journal of Applied Earth Observation and Geoinformation, 10*(4), 486-497.

Verger, A., Baret, F.d.r., & Weiss, M. (2011). A multisensor fusion approach to improve LAI time series. *Remote Sensing of Environment, 115*(10), 2460-2470.

Verhoef, W. (1984). Light scattering by leaf layers with application to canopy reflectance modeling: The SAIL model. *Remote Sensing of Environment, 16*(2), 125-141.

Verhoef, W. (1998). Theory of radiative transfer models applied in optical remote sensing of vegetation canopies. In (p. 310). Wageningen, The Netherlands: Wageningen University.

Verhoef, W., & Bach, H. (2003). Simulation of hyperspectral and directional radiance images using coupled biophysical and atmospheric radiative transfer models. *Remote Sensing of Environment, 87*(1), 23-41.

Verhoef, W., & Bach, H. (2007). Coupled soil-leaf-canopy and atmosphere radiative transfer modeling to simulate hyperspectral multi-angular surface reflectance and TOA radiance data. *Remote Sensing of Environment, 109*(2), 166-182.

Vintrou, E., Desbrosse, A., BÃ©guÃ©, A.s., TraorÃ©, S., Baron, C., & Lo Seen, D. (2012). Crop area mapping in West Africa using landscape stratification of MODIS time series and comparison with existing global land products. *International Journal of Applied Earth Observation and Geoinformation, 14*(1), 83-93.

VITO (2008). Free Vegetation Product. In:The image processing and archiving centre, VITO, Belgium

Online: http://free.vgt.vito.be/ (Accessed 30 June 2008).

Vohland, M., Mader, S., & Dorigo, W. (2010). Applying different inversion techniques to retrieve stand variables of summer barley with PROSPECT + SAIL. *International Journal of Applied Earth Observation and Geoinformation, 12*(2), 71-80.

Wang, D., Wang, J., & Liang, S. (2010). Retrieving crop leaf area index by assimilation of MODIS data into a crop growth model. *SCIENCE CHINA Earth Sciences, 53*(5), 721-730.

Wang, F.-m., Huang, J.-f., Tang, Y.-l., & Wang, X.-z. (2007). New Vegetation Index and Its Application in Estimating Leaf Area Index of Rice. *Rice Science, 14*(3), 195-203.

Wang, Q., Adiku, S., Tenhunen, J., & Granier, A. (2005). On the relationship of NDVI with leaf area index in a deciduous forest site. *Remote Sensing of Environment, 94*(2), 244-255.

Wang, Q., & Tenhunen, J.D. (2004). Vegetation mapping with multitemporal NDVI in North Eastern China Transect (NECT). *International Journal of Applied Earth Observation and Geoinformation, 6*(1), 17-31.

Wardlow, B.D., & Egbert, S.L. (2008). Large-area crop mapping using time-series MODIS 250 m NDVI data: An assessment for the U.S. Central Great Plains. *Remote Sensing of Environment, 112*(3), 1096-1116.

Weiss, J.L., Gutzler, D.S., Coonrod, J.E.A., & Dahm, C.N. (2004). Long-term vegetation monitoring with NDVI in a diverse semi-arid setting, central New Mexico, USA. *Journal of Arid Environments, 58*(2), 249-272.

Weiss, M., & Baret, F. (1999). Evaluation of Canopy Biophysical Variable Retrieval Performances from the Accumulation of Large Swath Satellite Data. *Remote Sensing of Environment, 70*(3), 293-306.

Weiss, M., Baret, F., Myneni, R.B., Pragnere, A., & Knyazikhin, Y. (2000). Investigation of a model inversion technique to estimate canopy biophysical variables from spectral and directional reflectance data. *Agronomie, 20*(1), 3-22.

Weiss, M., Troufleau, D., Baret, F., Chauki, H., PrÃ©vot, L., Olioso, A., Bruguier, N., & Brisson, N. (2001). Coupling canopy functioning and radiative transfer models for remote sensing data assimilation. *Agricultural and Forest Meteorology, 108*(2), 113-128.

White, D.A., & Hood, C.S. (2004). Vegetation patterns and environmental gradients in tropical dry forests of the northern Yucatan Peninsula. *Journal of Vegetation Science, 15*(2), 151-160.

White, J.D., Running, S.W., Nemani, R., Keane, R.E., & Ryan, K.C. (1997). Measurement and remote sensing of LAI in Rocky Mountain montane ecosystems. *Canadian Journal of Forest Research, 27*(11), 1714-1727.

Whittaker, R.H. (1960). Vegetation of the Siskiyou Mountains, Oregon and California. *Ecological Monographs, 30*279 - 338.

Wiens, J.A. (1989). Spatial Scaling in Ecology. *Functional Ecology, 3*(4), 385-397 .

Wiens, J.A., Crawford, C.S., & Gosz, J.R. (1985). Boundary Dynamics: A Conceptual Framework for Studying Landscape Ecosystems. *OIKOS, 45*(3), 421-427.

Wigneron, J.P., Ferrazzoli, P., Olioso, A., Bertuzzi, P., & Chanzy, A. (1999). A Simple Approach To Monitor Crop Biomass from C-Band Radar Data. *Remote Sensing of Environment, 69*(2), 179-188.

Wilhelm, W.W., Ruwe, K., & Schlemmer, M.R. (2000). Comparison of three leaf area index meters in a corn canopy. *Crop Sci., 40*(4), 1179-1183.

Wood, D., McNairn, H., Brown, R.J., & Dixon, R. (2002). Erratum to The effect of dew on the use of RADARSAT-1 for crop monitoring: Choosing between ascending and descending orbits [Remote Sensing of Environment 80/2 (2002 241–247)]. *Remote Sensing of Environment, 81*(2-3), 456.

Xiao, X., Boles, S., Frolking, S., Li, C., Babu, J.Y., Salas, W., & Moore Iii, B. (2006). Mapping paddy rice agriculture in South and Southeast Asia using multi-temporal MODIS images. *Remote Sensing of Environment, 100*(1), 95-113.

Xiao, X., Boles, S., Frolking, S., Salas, W., Moore, B., Li, C., He, L., & Zhao, R. (2002a). Observation of flooding and rice transplanting of paddy rice fields at the site to landscape scales in China using VEGETATION sensor data. *International Journal of Remote Sensing, 23*(15), 3009 - 3022.

Xiao, X., Boles, S., Liu, J., Zhuang, D., Frolking, S., Li, C., Salas, W., & Moore Iii, B. (2005). Mapping paddy rice agriculture in southern China using multi-temporal MODIS images. *Remote Sensing of Environment, 95*(4), 480-492.

Xiao, X., He, L., Salas, W., Li, C., Moore, B., Zhao, R., Frolking, S., & Boles, S. (2002b). Quantitative relationships between field-measured leaf area index and vegetation index derived from VEGETATION images for paddy rice fields. *International Journal of Remote Sensing, 23*(18), 3595 - 3604.

Xin, J., Yu, Z., van Leeuwen, L., & Driessen, P.M. (2002). Mapping crop key phenological stages in the North China Plain using NOAA time series images. *International Journal of Applied Earth Observation and Geoinformation, 4*(2), 109-117.

Yamashita, A. (2009). Geology of the Mekong Delta. In:Mekong Delta in Vietnam, Can Tho University, Vietnam. Online: http://cantho.cool.ne.jp/mekong/geo/geol_e.html (Accessed January 13 2010).

Young, R.K. (1963). *Wavelet theory and its applications*. Kluwer Academic Publishers.

Yuping, M., Shili, W., Li, Z., Yingyu, H., Liwei, Z., Yanbo, H., & Futang, W. (2008). Monitoring winter wheat growth in North China by combining a

crop model and remote sensing data. *International Journal of Applied Earth Observation and Geoinformation, 10*(4), 426-437.

Zarco-Tejada, P.J., Rueda, C.A., & Ustin, S.L. (2003). Water content estimation in vegetation with MODIS reflectance data and model inversion methods. *Remote Sensing of Environment, 85*(1), 109-124.

Summary

The scope of this study was to investigate the potential of using earth observation data for identifying and mapping irrigated rice cropping systems, estimating rice biophysical parameters, and predicting rice yields of the Mekong delta, Vietnam. The methods and techniques that were developed and evaluated in this study were based on the Iterative Self-Organizing Data Analysis Technique Algorithm (ISODATA) and the divergence statistic, the inversion of a vegetation radiative transfer model, and the integration of remote sensing data and a crop growth simulation model.

Utilizing the hyper-temporal SPOT VEGETATION Normalized Difference Vegetation Index (NDVI) imagery and the ISODATA clustering algorithm allowed the capturing of relevant rice cropping differences in the Mekong delta. The choice made on the number of classes present in the NDVI data set though the use of the divergence index worked out well. It was also found that, in spite of the cloudy conditions of the Mekong delta, 10 years of decadal SPOT data contained sufficient valid information to overcome this problem. It is therefore concluded that hyper-temporal SPOT VEGETATION NDVI data is very useful and suitable to map cropping patterns.

The use of hyper-temporal NDVI data, ISODATA clustering algorithm and divergence statistical technique was further investigated to develop a new quantitative method to extract land cover heterogeneity. The method named "LaHMa" is straightforward and relatively easy to implement to map landscape heterogeneity that is defined by soil and vegetation characteristics. The maps produced from SPOT VEGETATION and MODIS NDVI data using LaHMa concerned not only the spatial but also temporal dimensions of the Mekong delta landscape variability. LaHMa is a useful tool for a landscape analyst, essentially visualizing the complexity of the landscape in question, and indicating the homogeneity of each delineated land cover map unit. The maps produced through LaHMa can be served as valuable sources to guide subsequent studies and sampling method of ecotones. It should be noted that, depending of the scale of the spatial resolution of the remote sensing data, the scale of detail of landscape heterogeneity can vary, and thus must be carefully considered when apply for different studies.

The study has demonstrated the benefit of using the Soil-Leaf-Canopy (SLC) radiative transfer model to estimate the dynamic leaf-area-index (LAI) for

irrigated rice crops. In areas where rice is cultivated extensively, the available MODIS LAI product MOD15A2 failed to detect rice LAI evolution with time (R^2 = 0.07, RMSE = 2.1), while the use of the SLC model for dynamic LAI estimation proves promising to overcome this problem. To our knowledge, this is also the first study that uses SLC on temporal MODIS surface reflectance data (MOD09A1) to estimate seasonal variation of LAI for irrigated rice. LAI estimated by inverting the SLC model was much more accurate than the LAI provided by the MOD15A2 product. Look-up table inversion of the SLC model explained 69% of the variance of *in situ* LAI during the whole cropping season, with a RMSE of 0.9. A further improvement of SLC estimates was achieved when seasonal variation of rice LAI was taken into account (R^2 = 0.83, RMSE = 0.7).

Forcing SLC-estimated LAI from MODIS surface reflectance data in ORYZA2000 crop growth simulation model has shown its great potential in simulating rice yield under sub-optimum conditions, especially when data on nutrient balance and soil characteristics were not available. The use of forcing SLC estimated LAI allowed to re-initialize ORYZA2000 CGSM state variables and recalibrate rice crop parameters, which helped ORYZA2000 being able to explain about 81% of the variation in rice yield in 58 fields across the Mekong delta. This promising approach is recommended for future uses to estimate irrigated rice yield at a large scale, such as a region, taking into account the regional variation of rice cropping calendar and rice varieties that have been captured in the maps presented in our first study.

In summary, the study has proven the value of these new techniques for identifying and mapping both the spatial and temporal heterogeneity of a complex agroecosystem that is dominated by rice cultivation. The study also indicates that by coupling remote sensing derived crop parameter LAI with crop growth simulation modelling, highly accurate estimation of rice crop yield and production can be achieved.

Samenvatting

Deze thesis bevat studies betreffende geïrrigeerde rijst teeltsystemen in de Mekong-delta, Vietnam, om tot verbeterde interpretatie methodes te komen van beschikbare aardobservatie-gegevens voor gewas identificatie, teeltsysteem kartering, het inschatten van biofysische gewas parameters, en het modelleren van behaalde opbrengsten.

De verbeterde en geëvalueerde methoden en technieken betreffen het iteratieve zelforganiserende data-classificatie algoritme (ISODATA) met gebruik van divergentie statistieken, de inversie van vegetatie reflectie data, en de integratie van aardobservatie gegevens met een gewas groei-model.

Het bleek mogelijk om relevante verschillen tussen voorkomende rijst teeltsystemen in de Mekong-delta te onderscheiden door gebruik te maken van hyper-temporale SPOT-Vegetatie beelden van genormaliseerde vegetatie reflectie-absorptie verschillen (NDVI) en het ISODATA algoritme. Met behulp van divergentie statistieken kon een goede keuze gemaakt worden betreffende het aantal rijst teelt-systeem klassen dat onderscheiden kon worden door de gebruikte NDVI data. Bovendien bleek dat door het gebruik van 10 jaar 10-daagse SPOT-Vegetatie beelden, voldoende informatie beschikbaar was om de negatieve invloed van de frequente bewolking boven de Mekong delta te omzeilen. Als conclusie is gesteld dat hyper-temporale SPOT-Vegetatie NDVI beelden uiterst geschikt zijn om verschillen in gewas teelt-patronen in kaart te brengen.

Daarnaast werd een geheel nieuwe kwantitatieve karterings benadering onderzocht en ontwikkeld, genaamd 'LaHMa', die additioneel gebruik maakt van de hyper-temporale NDVI beelden, het ISODATA algoritme en de divergentie statistieken. LaHMa legt zowel de ruimtelijke als temporele verschillen in heterogeniteit en homogeniteit van de aanwezige vegetatie vast op landschaps niveau. De methode is overzichtelijk en relatief eenvoudig te implementeren. Van de Mekong delta zijn vegetatie heterogeniteit kaarten gemaakt op basis van zowel SPOT-Vegetatie als MODIS NDVI beelden. LaHMa is bruikbaar voor landschaps analyse en geschikt geacht om de ruimtelijk-temporele complexiteit tussen en binnen kaart-eenheden visueel te maken. LaHMa kan belangrijke informatie verschaffen voor diverse ruimtelijke studies, voor het bepalen van optimale veld bemonstering schema's, en ter interpretatie van harde en geleidelijke overgangen tussen

gekarteerde eenheden. De schaal van een LaHMa kaart en daardoor zijn functie wordt beïnvloed door de gemaakte keuze betreffende de resolutie van gebruikte NDVI beelden.

Deze thesis rapporteert dat het gebruik van een bodem-blad-bedekking (SLC) reflectie inversie model zeer geschikt is om gedurende een groeiseizoen schattingen te maken van het blad-areaal (LAI) van geïrrigeerde rijst. Direct beschikbare MODIS-LAI beelden (MOD15A2) gemeten gedurende het groeiseizoen bleken onbruikbaar voor gebieden met intensieve rijstbouw (R^2=0.07, RMSE=2.1), terwijl door gebruik te maken van het SLC-model de nodige LAI-dynamiek wel goed werd ingeschat. Zover bekend, is deze studie een succesvolle primeur die de SCL-methode met MODIS aard-reflectie data (MOD09A1) temporeel toepast. De SLC resultaten, gegenereerd met de tabulaire inversie optie, verklaarden over het gehele groeiseizoen, voor 69% de variatie in lokaal gemeten LAI-waarden met een RMSE van 0.9. Een verder verbetering werd bereikt door de temporele variatie in rijst-LAI te gebruiken (R^2=0.83, RMSE=0.7).

Bewezen is dat de logica om het ORYZA2000 gewas groei model te forceren met LAI-waarden afkomstig uit de SLC-inversie een hoge potentie heeft om direct actuele rijst opbrengsten in te schatten van teelt-systemen die plaatsvinden onder sub-optimale omstandigheden. De methode is in het bijzonder relevant als nutrient status en andere bodem gegevens ontbreken. Door het gebruik van de SLC-gegenereerde LAI waarden, konden binnen het ORYZA2000 model specifieke status-variabelen gedurende het modelleren worden ge-reinitialiseerd en vooraf de benodigde gewas parameters worden gecalibreerd. Hierdoor kon ORYZA2000 voor 81% de variabiliteit in gemeten rijst opbrengsten van 58 velden verdeeld over de gehele Mekong delta verklaren. Aangeraden is om deze veelbelovende methode voor grootschalig toekomstig gebruik in te zetten om rijst oogsten regionaal in te schatten, maar dan wel met gebruik van de eerder beschreven gekarteerde informatie betreffende gevolgde gewas kalenders en geteelde variëteiten.

De waarde van deze thesis bevindt zich in de resultaten betreffende gebruikte technieken ter identificatie en het ruimtelijk als temporeel karteren van rijst systemen en de heterogeniteit van aanwezige vegetatie, als in de bevinding dat de combinatie van een gewas groeimodel met aardobservatie data uitstekende schattingen genereert betreffende actueel behaalde rijst oogsten.

Publications

Scientific papers

de Bie, C.A.J.M., **Nguyen, T.T.H.**, Amjad Ali, Scarrot, R., & Skidmore, A.K. (2012). LaHMa: a landscape heterogeneity mapping method using hyper-temporal datasets. *International Journal of Geographical Information Science, 26(11),* pp. 2177-2192.

Nguyen, T.T.H., de Bie, C.A.J.M., Ali, A., Smaling, E.M.A., & Chu, T.H. (2012). Mapping the irrigated rice cropping patterns of the Mekong delta, Vietnam, through hyper-temporal SPOT NDVI image analysis. *International Journal of Remote Sensing, 33*(2), pp. 415-434.

Everaarts, A.P., **Ha, N.T.T**, and Hoi, P.V. (2006). Agronomy of a rice-based vegetable cultivation system in Vietnam: Constraints and recommendations for commercial market integration". *Acta Horticulturae, 699,* pp. 173-180

Leisz, S.J., **Nguyen thi Thu Ha**, Nguyen thi Bich Yen, Nguyen Thanh Lam, & Tran Duc Vien (2005). Developing a methodology for identifying, mapping and potentially monitoring the distribution of general farming system types in Vietnam's northern mountain region. *Agricultural Systems, 85*(3), pp. 340-363.

Nguyen Thi Thu Ha, Verhoef, W., de Bie, C.A.J.M., Venus, V., Suarez Urrutia, J.A., & Nieuwenhuis, W. Leaf area index of irrigated rice: a comparison of MODIS LAI product and inversion estimates by the Soil-Leaf-Canopy radiative transfer model. *Remote Sensing of Environment*. **In Revision** (after review)

Nguyen Thi Thu Ha, de Bie, C.A.J.M., Smaling, E.M.A., & Verhoef, W. Coupling remotely sensed LAI-estimates with a modified ORYZA2000 crop growth model to estimate actual irrigated rice yields. *International Journal of Applied Earth Observation and Geoinformation.* **Submitted**

Conference Proceedings papers

Nguyen Thi Thu Ha, Wout Verhoef, C.A.J.M. de Bie. (2011). Seasonal LAI estimation of irrigated rice using Soil-Leaf-Canopy (SLC) radiative transfer model. In: ACRS 2011: proceedings of the 32nd Asian Conference on Remote Sensing: Sensing for Green Asia, 3-7 October 2011, Taipei, Taiwan, pp. 327-333.

Nguyen Thi Thu Ha, C.A.J.M. de Bie, Amjad Ali, E.A.M. Smaling (2012). Remote sensing-based method to map irrigated rice cropping patterns of the Mekong delta, Vietnam. In: proceedings of the International Conference on GMS 2020: Balancing Economic Growth and Environmental Sustainability, 20-21 February 2012, Bangkok, Thailand, pp. 235-244

Curriculum vitae

Nguyen Thi Thu Ha was born on November 23, 1977 in Hanoi, Vietnam. After high school, she went to Hanoi University of Agriculture (HUA) in 1995 to major in Crop Science. She spent 6 months in Da Bac, a district located in the Northern Mountainous of Vietnam, working with Tay minority group people in seeking to improve the local irrigated rice system's production. Soon after graduating in 1999, she joined the Center for Agricultural Research and Ecological Studies (CARES) at HUA as a researcher. Two year later, in 2001, she started as a lecturer at the Department of Ecology and Environmental Science at HUA, and has been remaining her position since then. Ha's first introduction to GIS and Remote sensing was back in 2000 when she took part in a CARES's project looking at the Government Policies on Resource Management and Improvement of the Livelihood of Local People in the Ca River Basin in Vietnam. Her task in this project was to map and validate the land use and land cover change in the basin. In 2003, under the financial support of the University Support to Environmental Planning and Management in Cambodia, Laos, and Vietnam (USEAPM) project funded by Danish Development Assistance (DANIDA), she went to the International Institute of Geo-information Science and Earth Observation (ITC) to obtain her master degree on Natural Resource Management with specialization on Sustainable Agriculture. She graduated from ITC in 2005 with her thesis on the use of coarse resolution satellite data in estimating sugarcane yield. In 2007, she was awarded a Fellowship Grant from the Netherlands Organization for International Cooperation in Higher Education (NUFFIC) to carry out her PhD research under the supervision of Prof. E. Smaling, Prof. W. Verhoef and Dr. Kees de Bie at ITC, which resulted in this thesis. In 2011, she earned the "Best Student Paper Award" for her paper presented at the 32nd Asian Conference on Remote Sensing in Taiwan.

ITC Dissertation List

http://www.itc.nl/research/phd/phd_graduates.aspx